An introduction to Radio-Loud AGN

Paola Grandi (INAF-IASF Bologna)

&

Eleonora Torresi (DIFA & INAF-IASF Bologna)

Laboratorio X
30.10.2018

Outline

- RADIO-LOUD AGN IN GENERAL
    1) AGN classification
    2) Spectral energy distribution

- RADIATIVE PROCESSES
    3) Thermal emission
        - Accretion
    4) Non-thermal emission
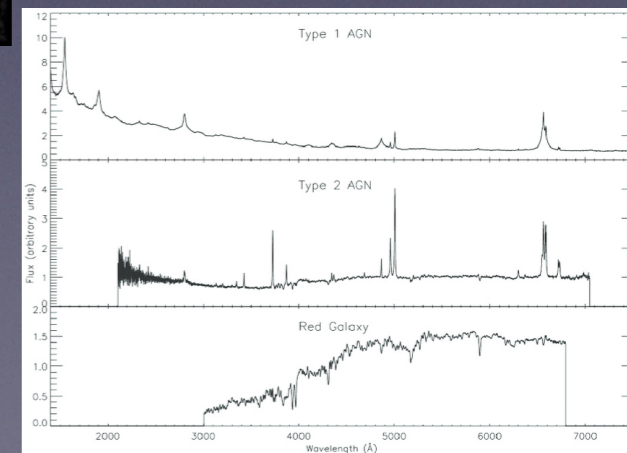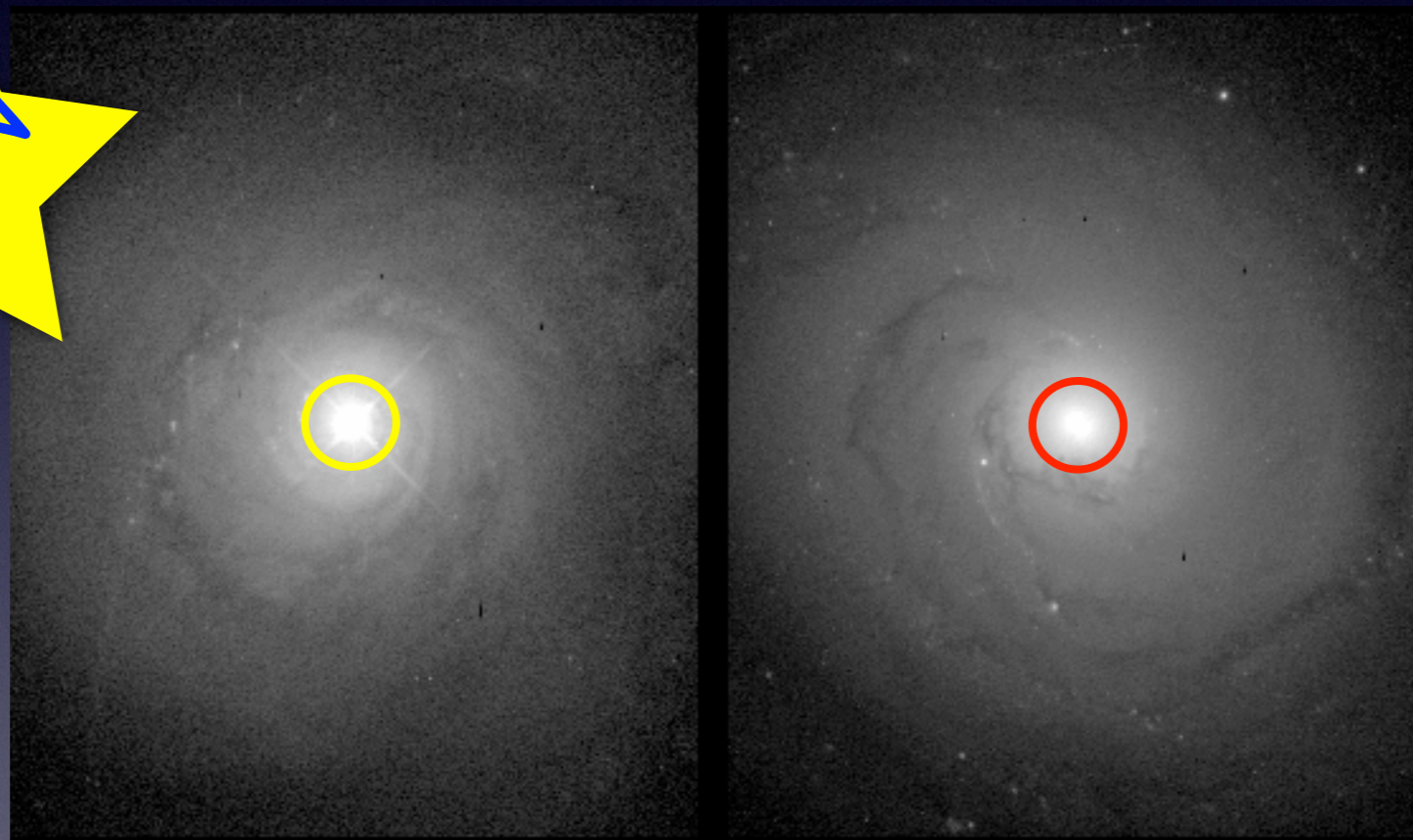   - Jets, Hot spots, Lobes

Almost every galaxy hosts a black hole from millions to billions of solar masses

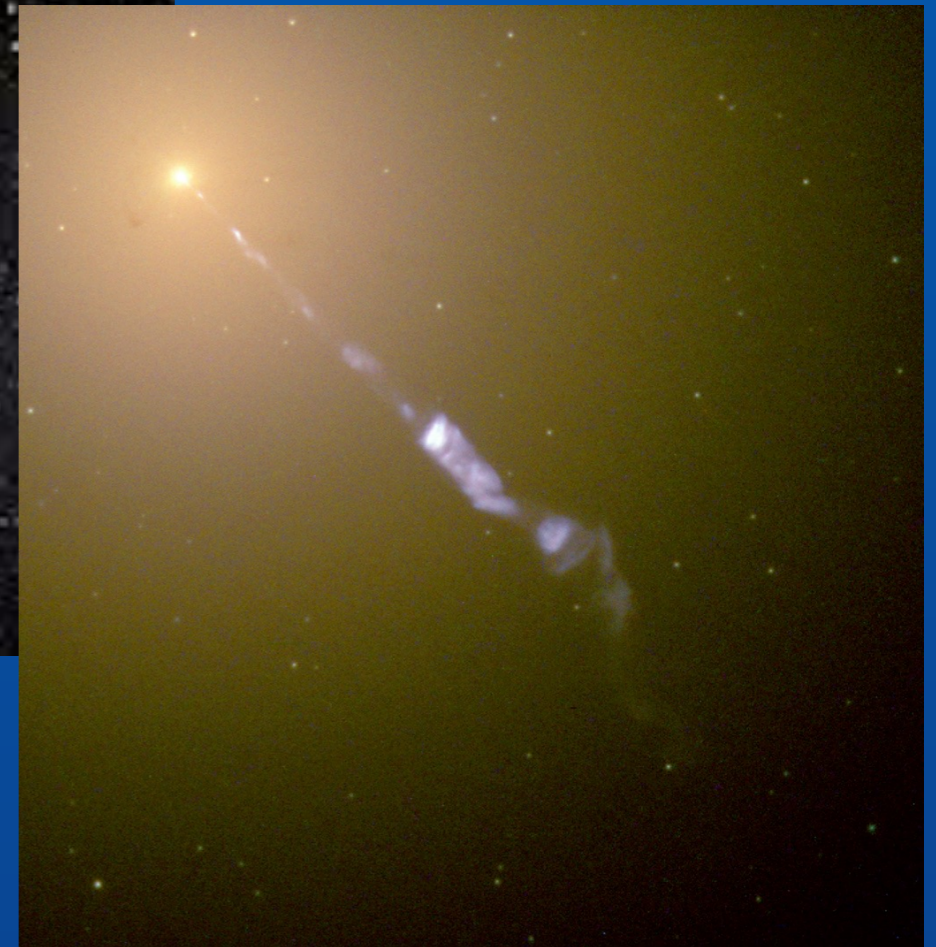(Magorrian et al. 1998, Tremaine et al. 2002, McConnell et al. 2011, Ghisellini 2011)

but...

About 10% of AGNs are Radio-Loud,
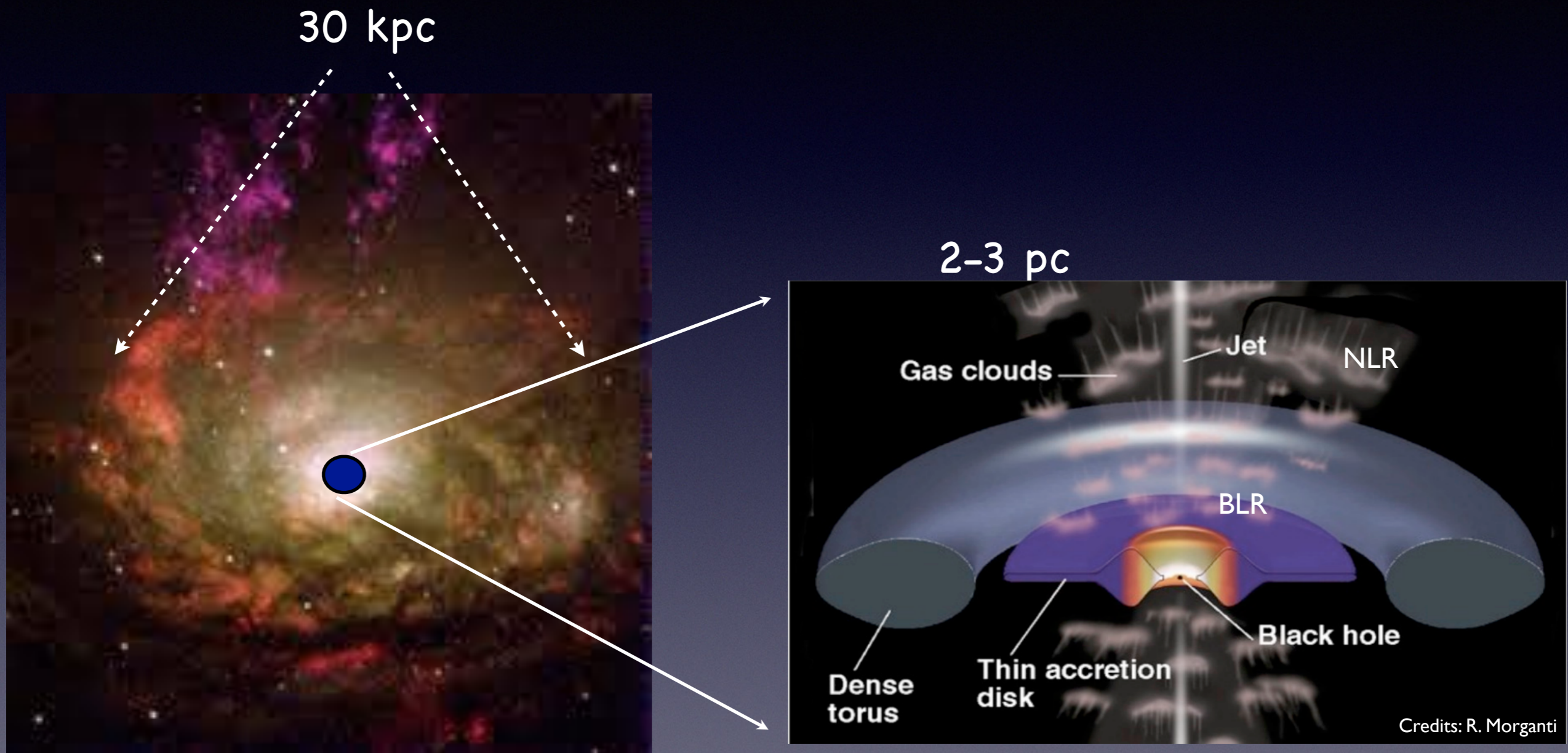## i.e. these systems are able to launch relativistic jets

RL AGN lie in elliptics
RQ AGN lie in spirals and ellipticals

Local Space Densities of Some Objects

Object		Gpc^{-3}
Spiral Galaxies	$M_V < -20$	5×10^6
	$M_V < -22$	3×10^5
	$M_V < -23$	3×10^3
Elliptical Galaxies	$M_V < -20$	1×10^6
(incl. S0)	$M_V < -22$	1×10^5
	$M_V < -23$	10^4
Rich Clusters of Galaxies		3×10^3
Radio Galaxies	$P_{1.4\,GHz} > 10^{23.5}\ W\ Hz^{-1}$	3×10^3
	$P_{1.4\,GHz} > 10^{25}\ W\ Hz^{-1}$	10
Radio Quasars	$P_{1.4\,GHz} > 10^{25}\ W\ Hz^{-1}$	3
Radio Quiet Quasars	$M_V < -23$	100
	$M_V < -25$	1
Sy 1	$M_V < -20$	4×10^4
Sy 2	$M_V < -20$	1×10^5
BL Lac	$P_{1.4\,GHz} > 10^{23.5}\ W\ Hz^{-1}$	80
Strong IRAS Galaxies	$L_{IR} > 10^{12}\ L_o$	300

The engine occupies a tiny region in the center of the galaxy
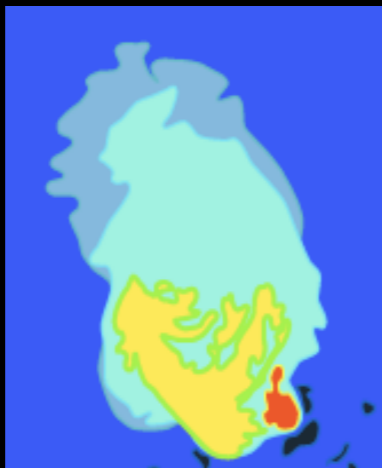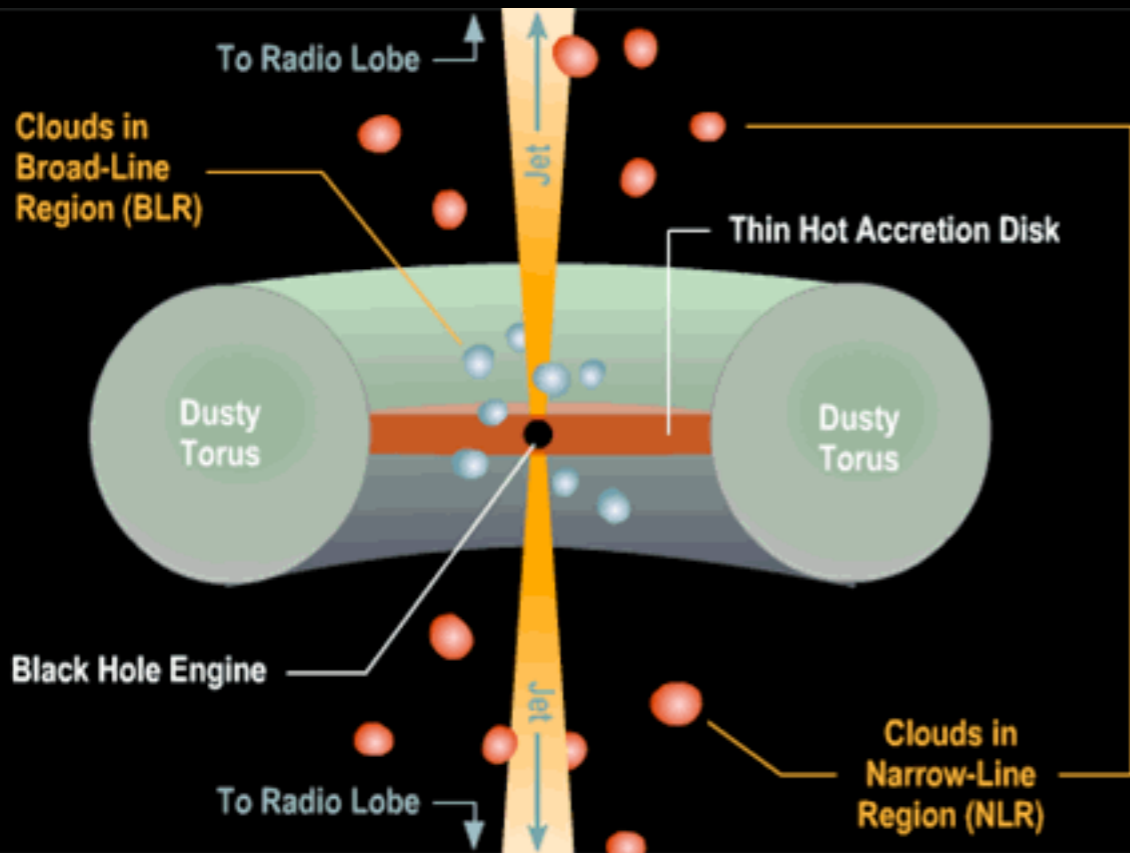
30 kpc

2–3 pc

Gas clouds

Jet   NLR

BLR

Black hole

Dense torus

Thin accretion disk

Credits: R. Morganti

The extraordinary amount of energy is produced through accretion of gas close to a SMBH

Some numbers for a typical AGN

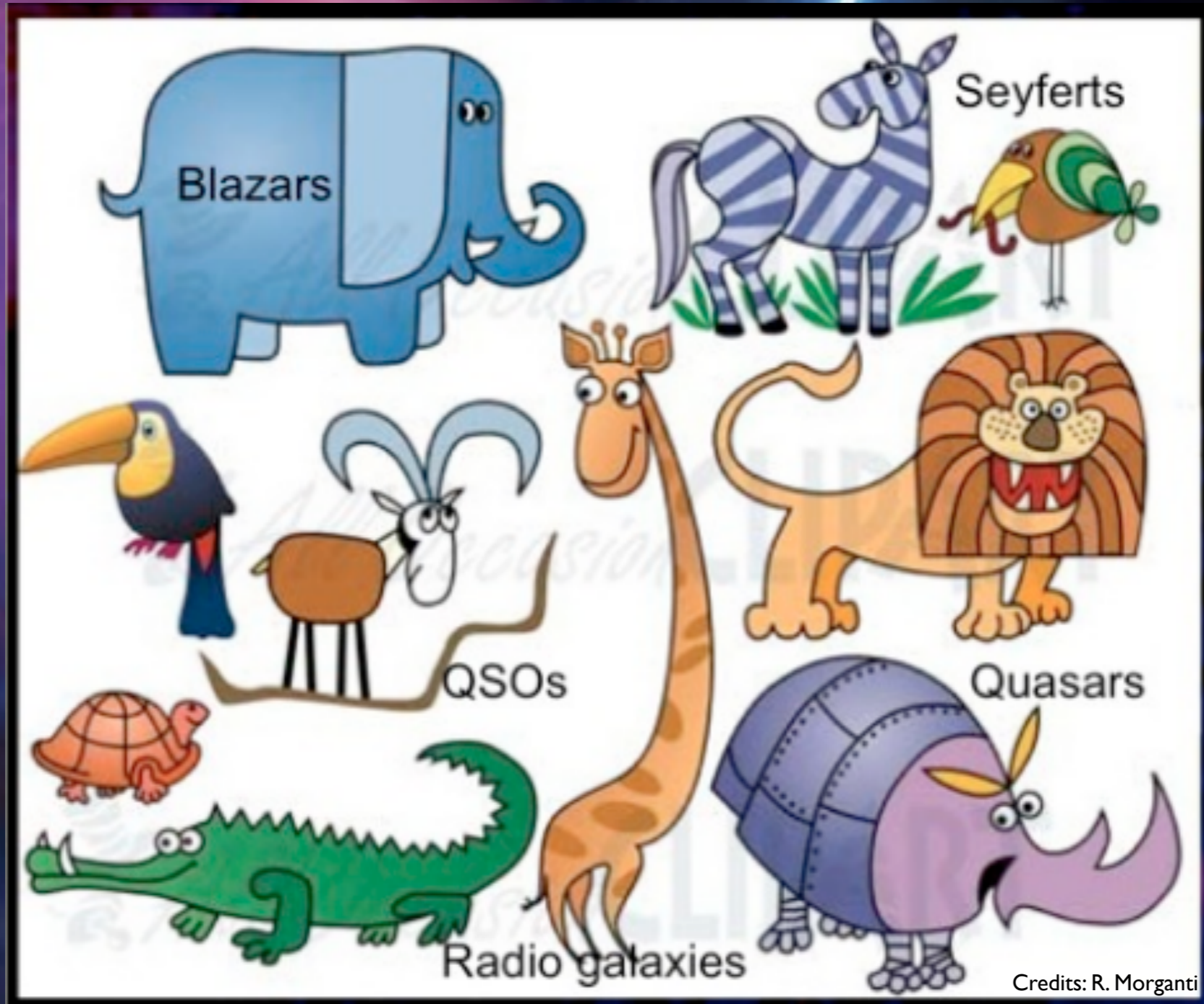|	
BH Mass	$\sim 10^8 M\odot$
Luminosity	$\sim 10^{44}\ erg\ s^{-1}$
BH radius	$\sim 3 \times 10^{13}\ cm$
BLR radius	$\sim 2 - 20 \times 10^{16}\ cm$
NLR radius	$\sim 10^{18} - 10^{20}\ cm$
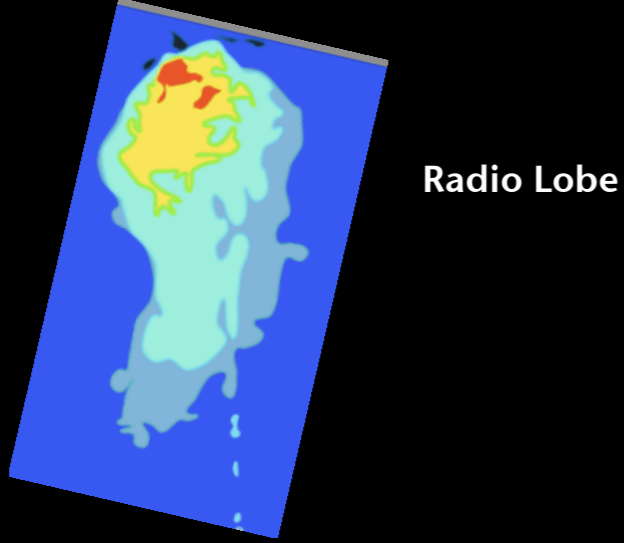
In RL AGNs

Jets end at kpc distances forming radio lobes

1. AGN classification
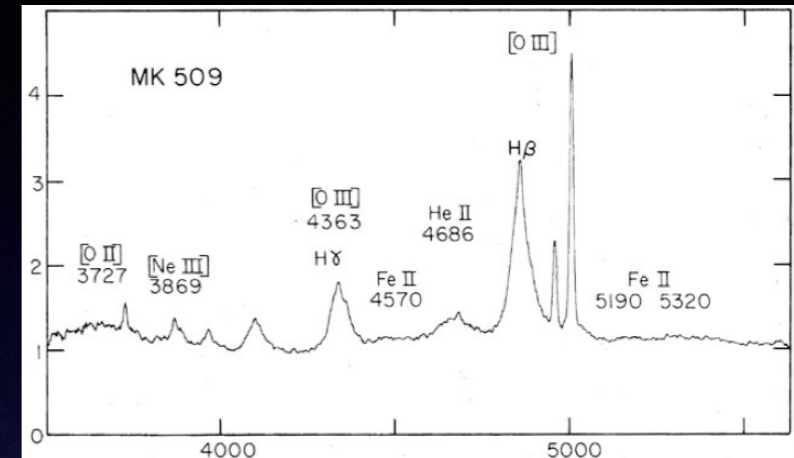

Credits: R. Morganti

OPTICAL classification

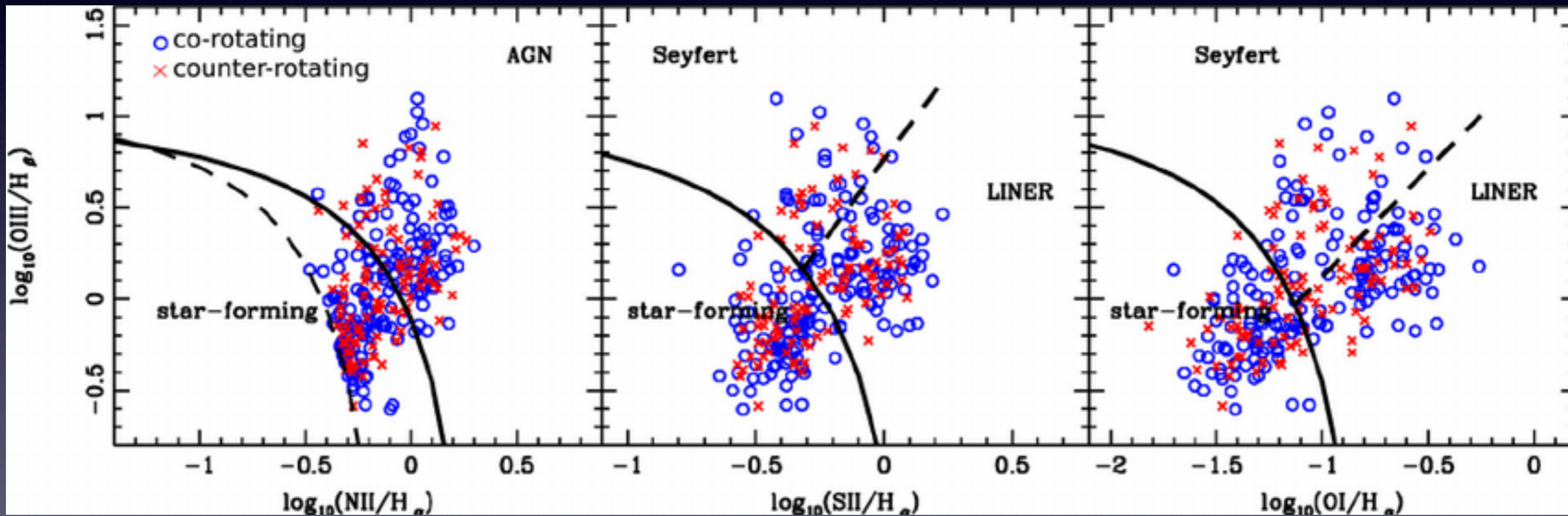|	
Type I	bright continuum and BROAD emission lines from hot high velocity gas **(FWHM~10^{3-4} km s^{-1})**
Type I	bright continuum and BROAD emission lines from hot high velocity gas **(FWHM~10^{3-4} km s^{-1})**
Type II	weak continuum and only NARROW emission lines **(FWHM~10^2 km s^{-1})**
	Low luminosity. Similar to
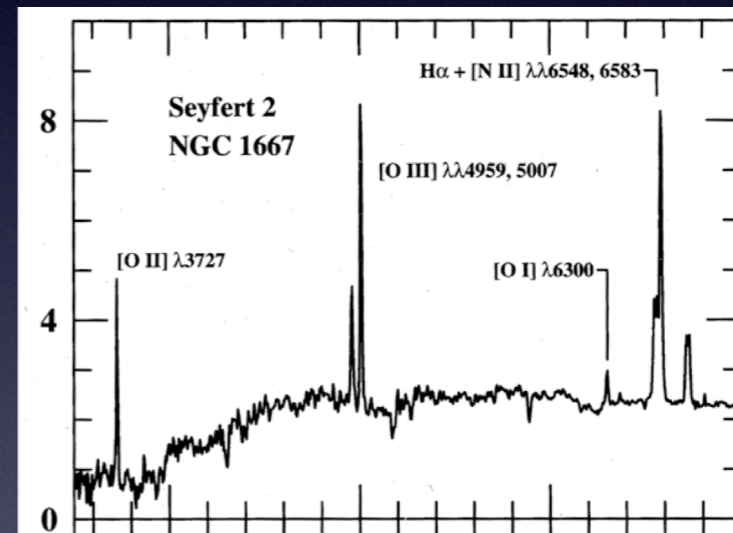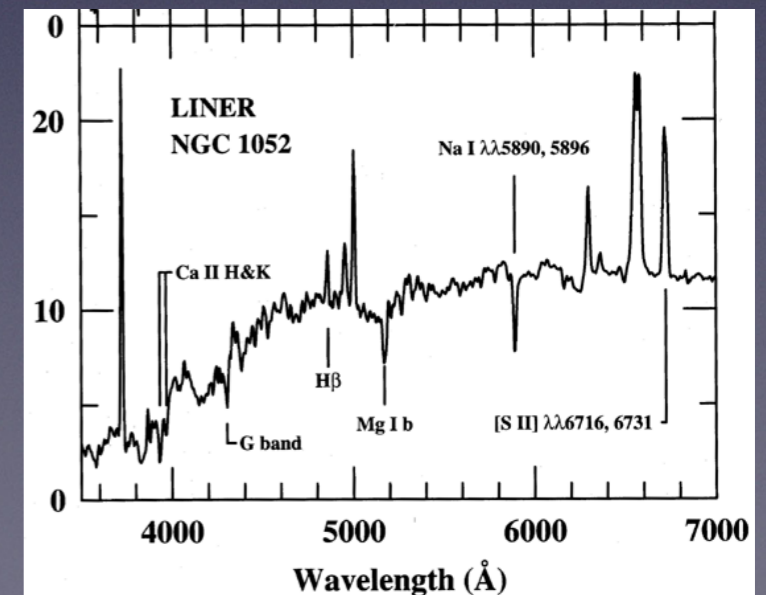
OPTICAL classification

BPT diagrams (named after
"Baldwin, Phillips & Televich")

About 10% of AGNs are Radio-Loud,
i.e. these systems are able to launch relativistic jets
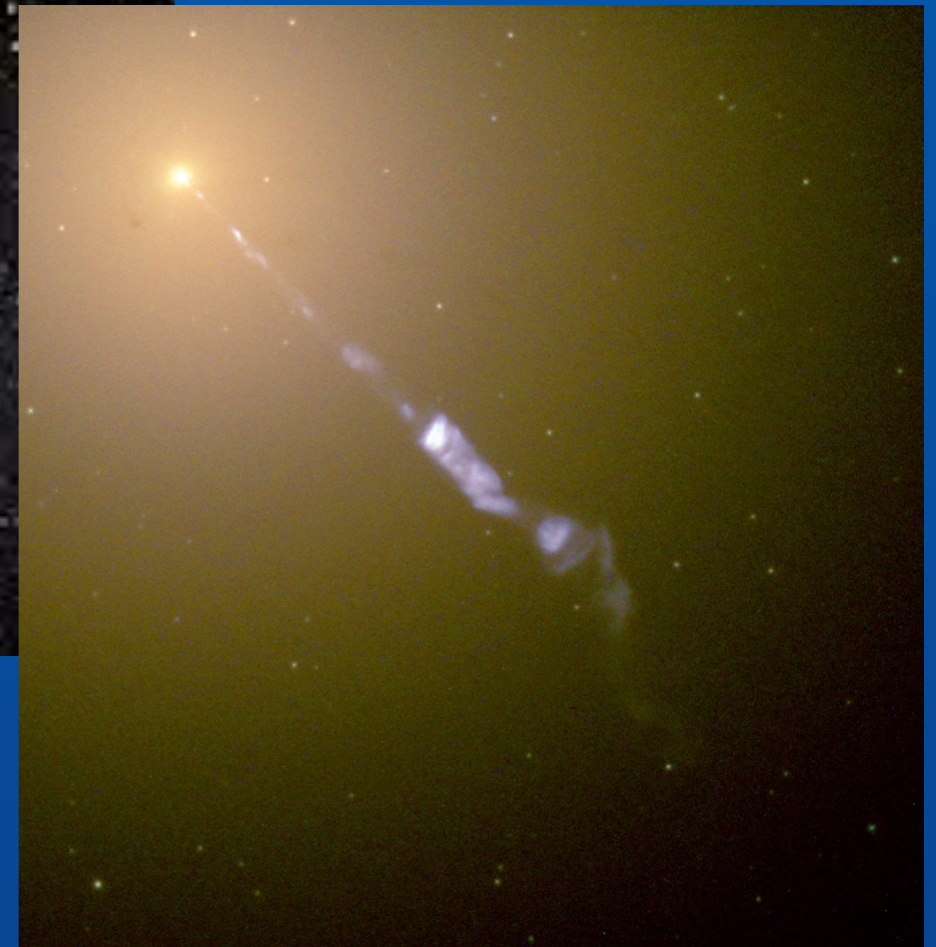
RL AGN lie in elliticals
RQ AGN lie in spirals and ellipticals

RADIO LOUDNESS PARAMETER (𝓡)

$$R = \frac{F_{GHz}}{F_B} \geq 10.$$

This definition is based on a study of quasars of the Palomar
Bright Quasar Survey with VLA (Kellermann 1989)

This is a still debated question. However recent studies seems to confirm a bimodal distribution of the radio loudness with 12% of the ojcts belonging to the radio loud component (Balokovic et al. 2012)

Optical classifications:

Brod Line Radio Galaxy (BLRG)

Quasars (large z) | bright continuum and broad emission lines from hot high velocity gas | TYPE I |
| Narrow line Radio Galaxy | weak continuum and only narrow emission lines | TYPE II |

$[OIII]$ H_α

BLRG 3C 390.3

NLRG Cygnus A

4000 5000 6000

$\lambda(\overset{\circ}{A})$
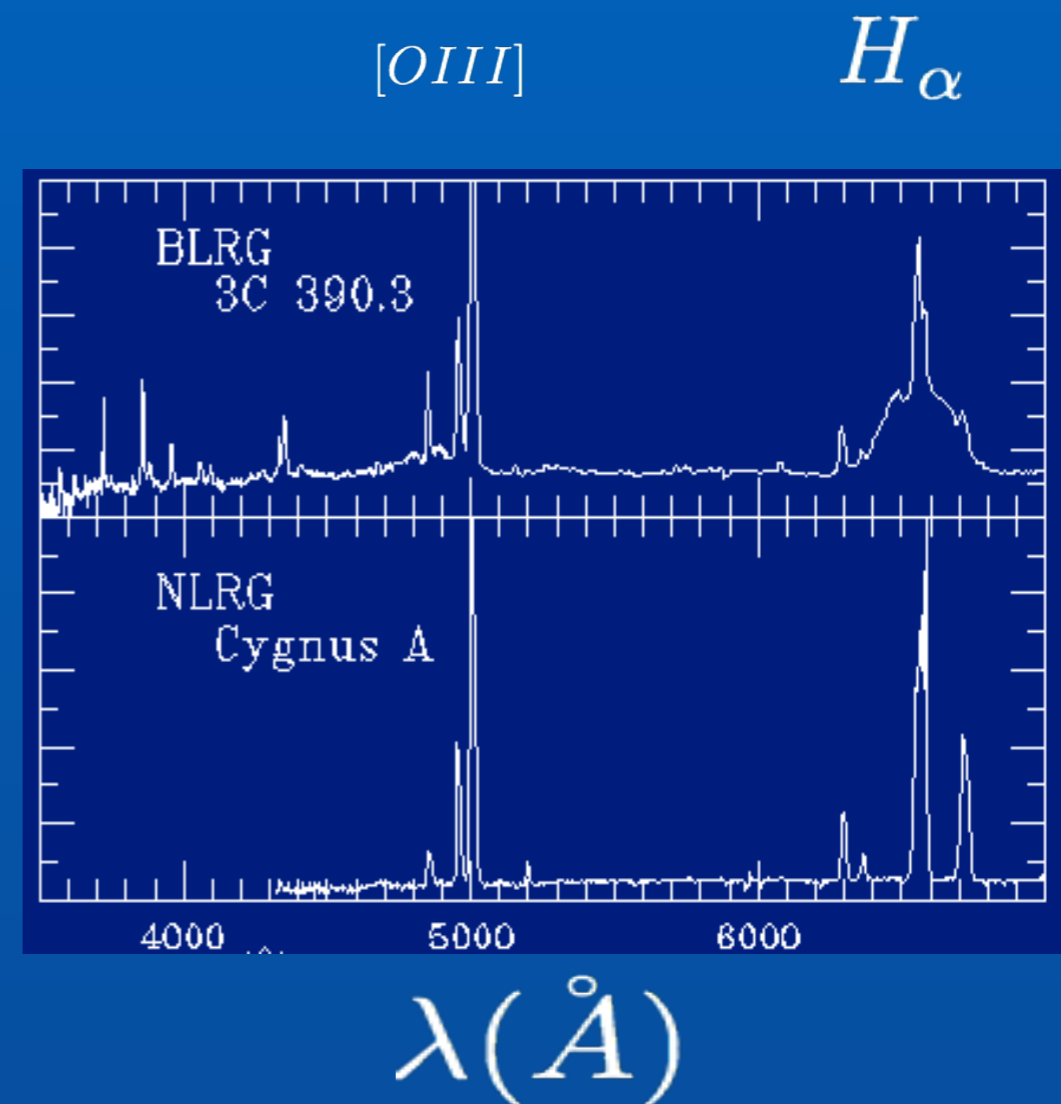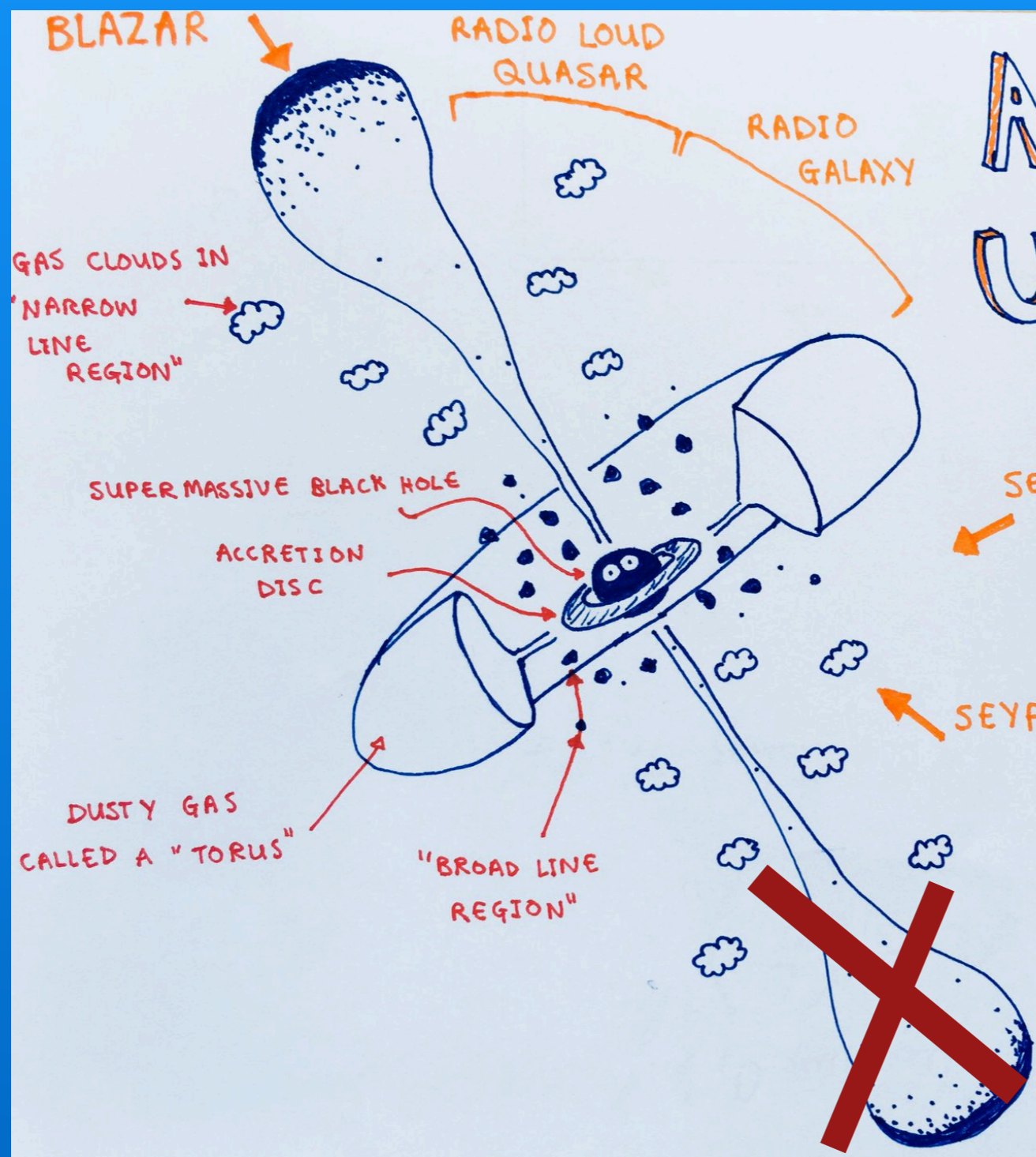
High–excitation (HERG) and low–excitation (LERG) RG ACCRETION MODE

This classification is related to the underlined excitation modes of the gas in the Narrow Line Regions: different excitation modes correspond to different accretion rates

Laing et al. (1994)
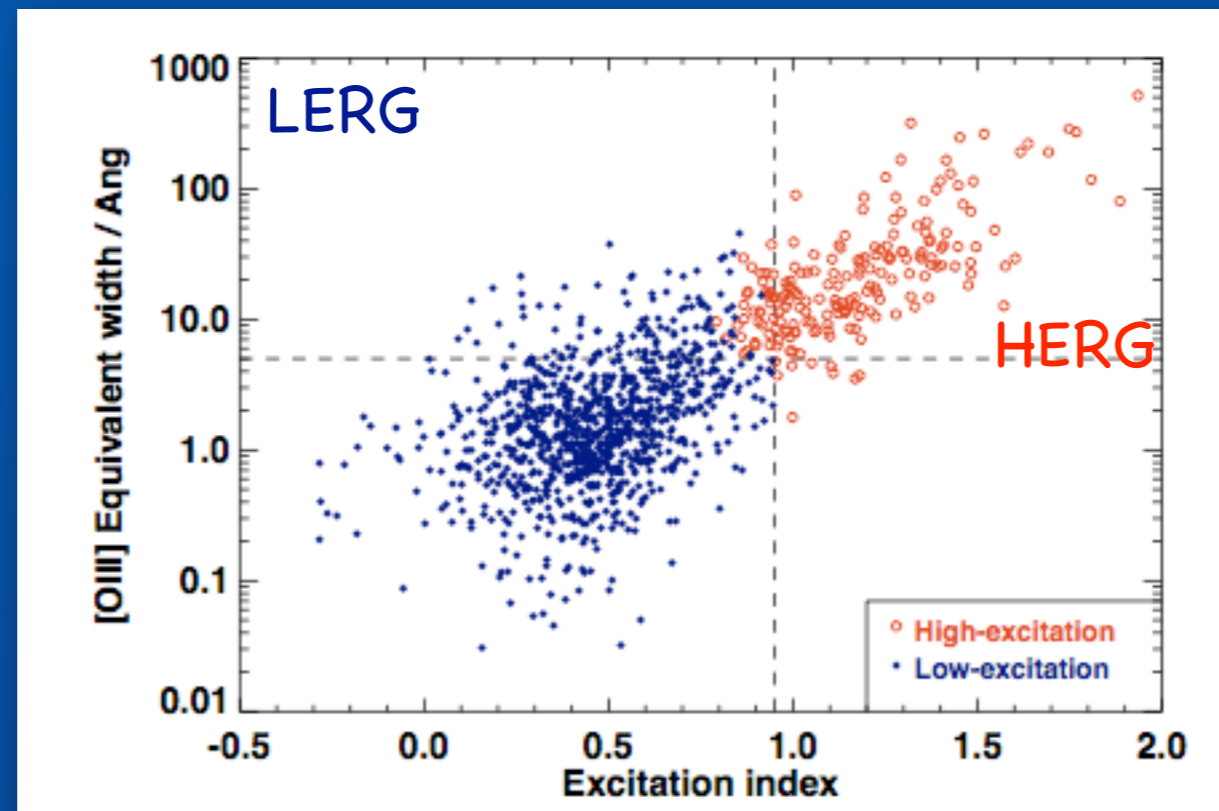HERG: $EW_{[OIII]} > 3$ Å
$[OIII]/Ha > 0.2$

Excitation Index
(Buttiglione et al. 2010)
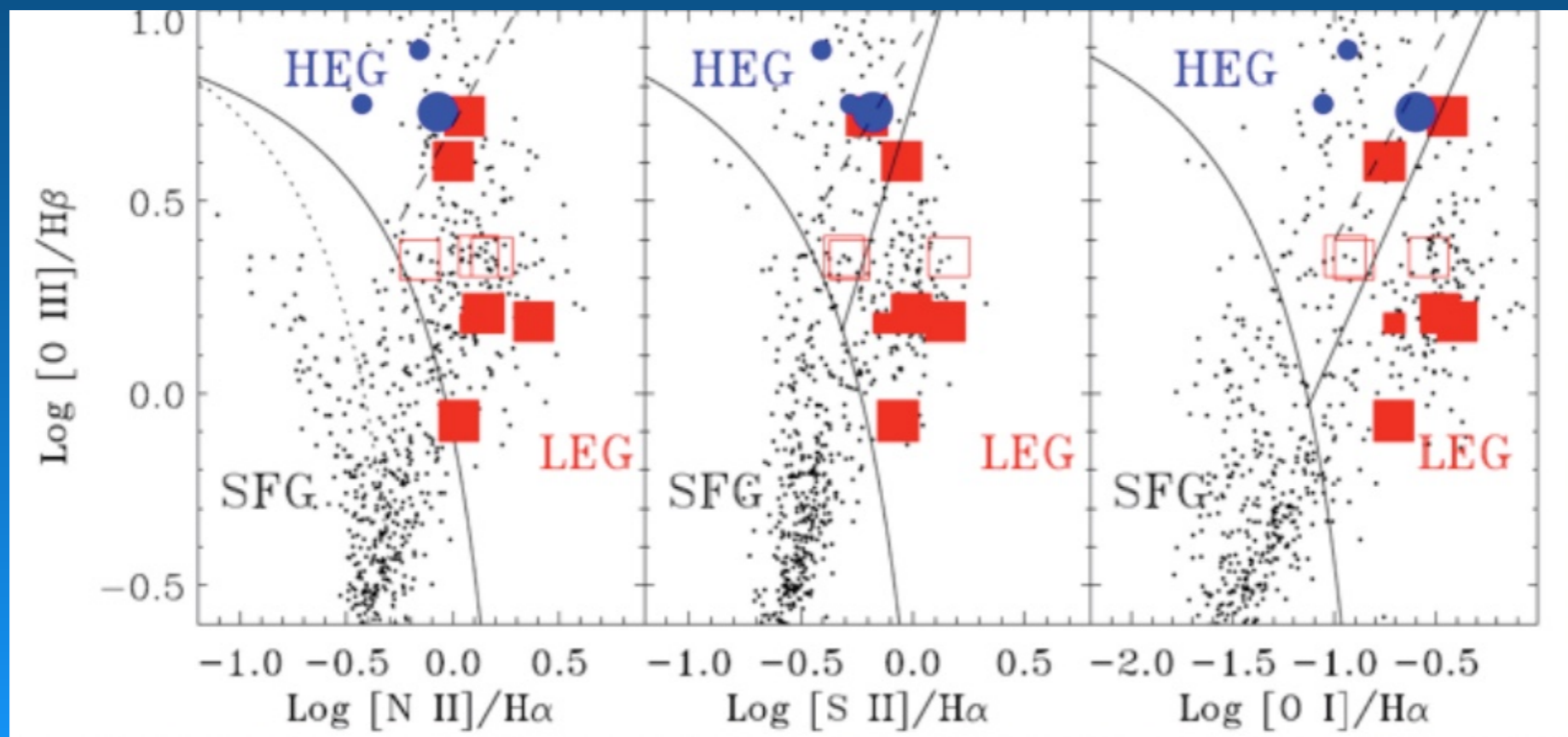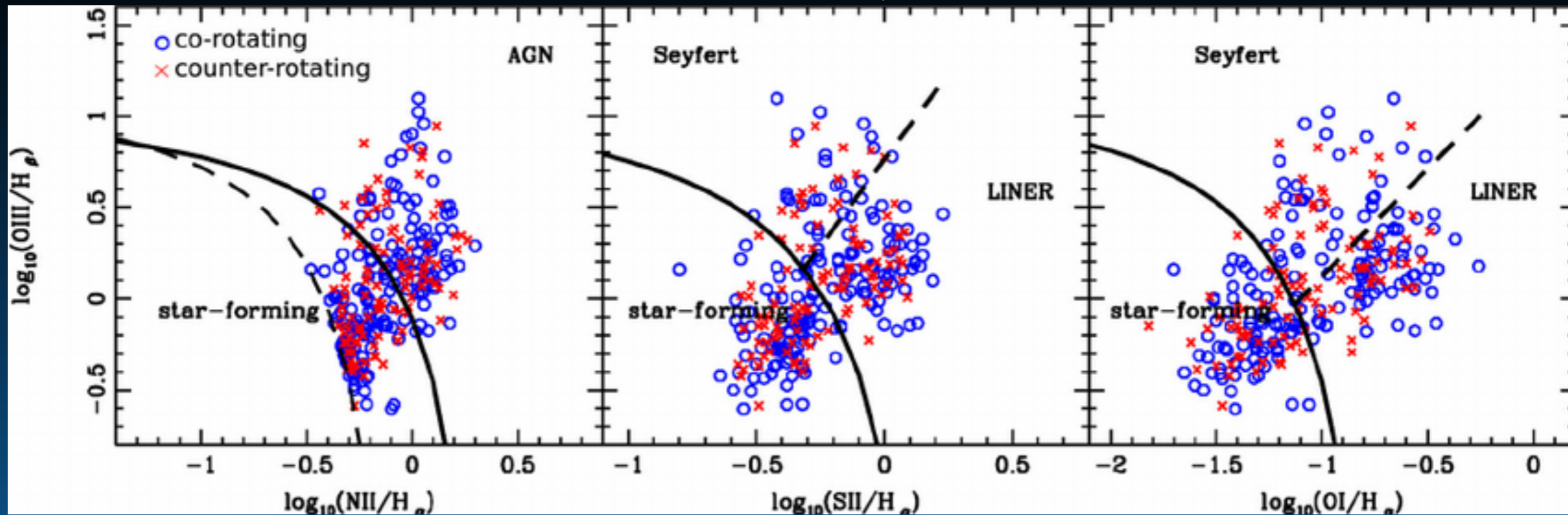$EI = \log([OIII]/Hb) - 1/3[\log([NII])/Ha) + \log([SII]/Ha) + \log([OI]/Ha)]$
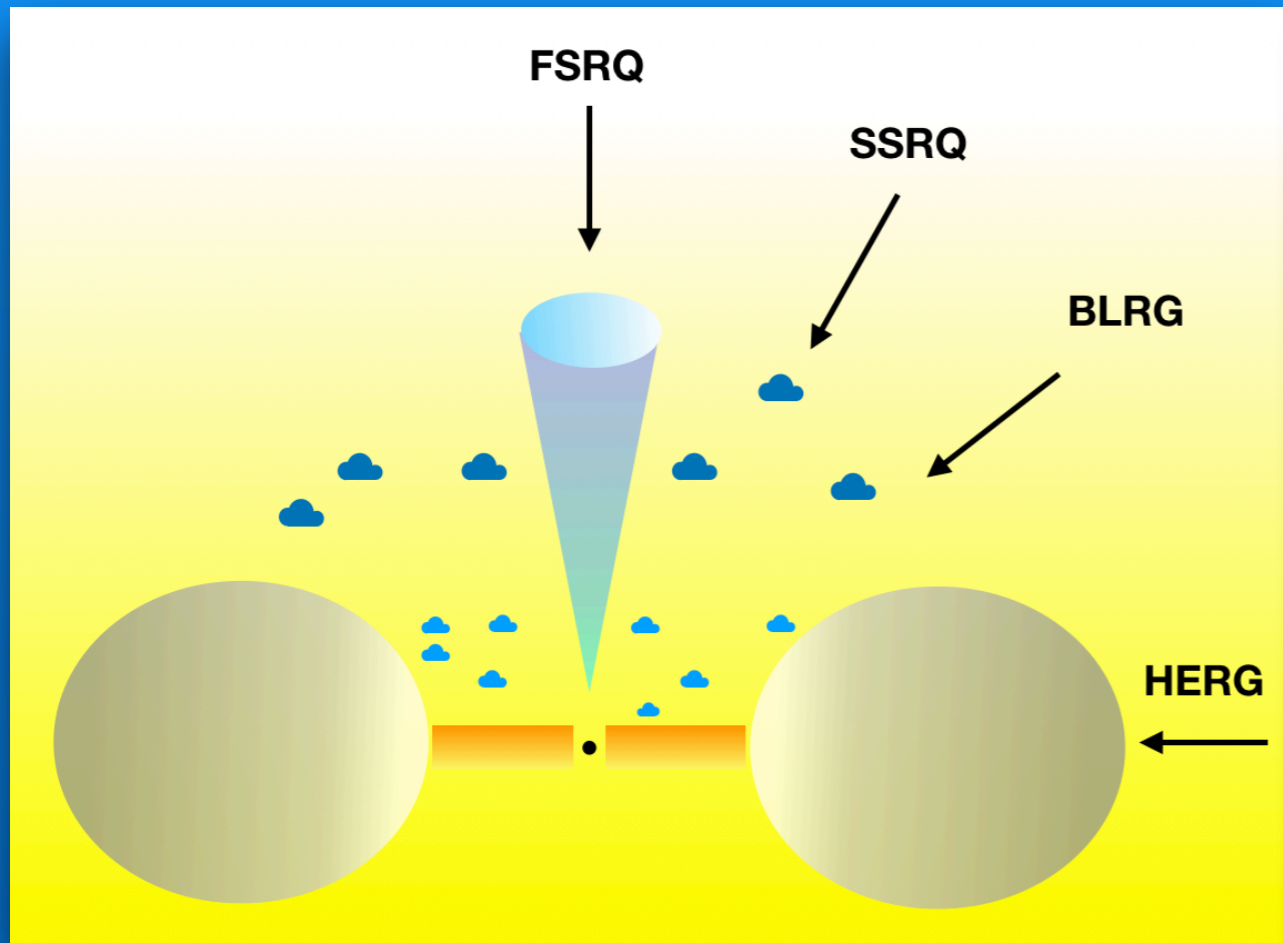

Best & Heckman 2012
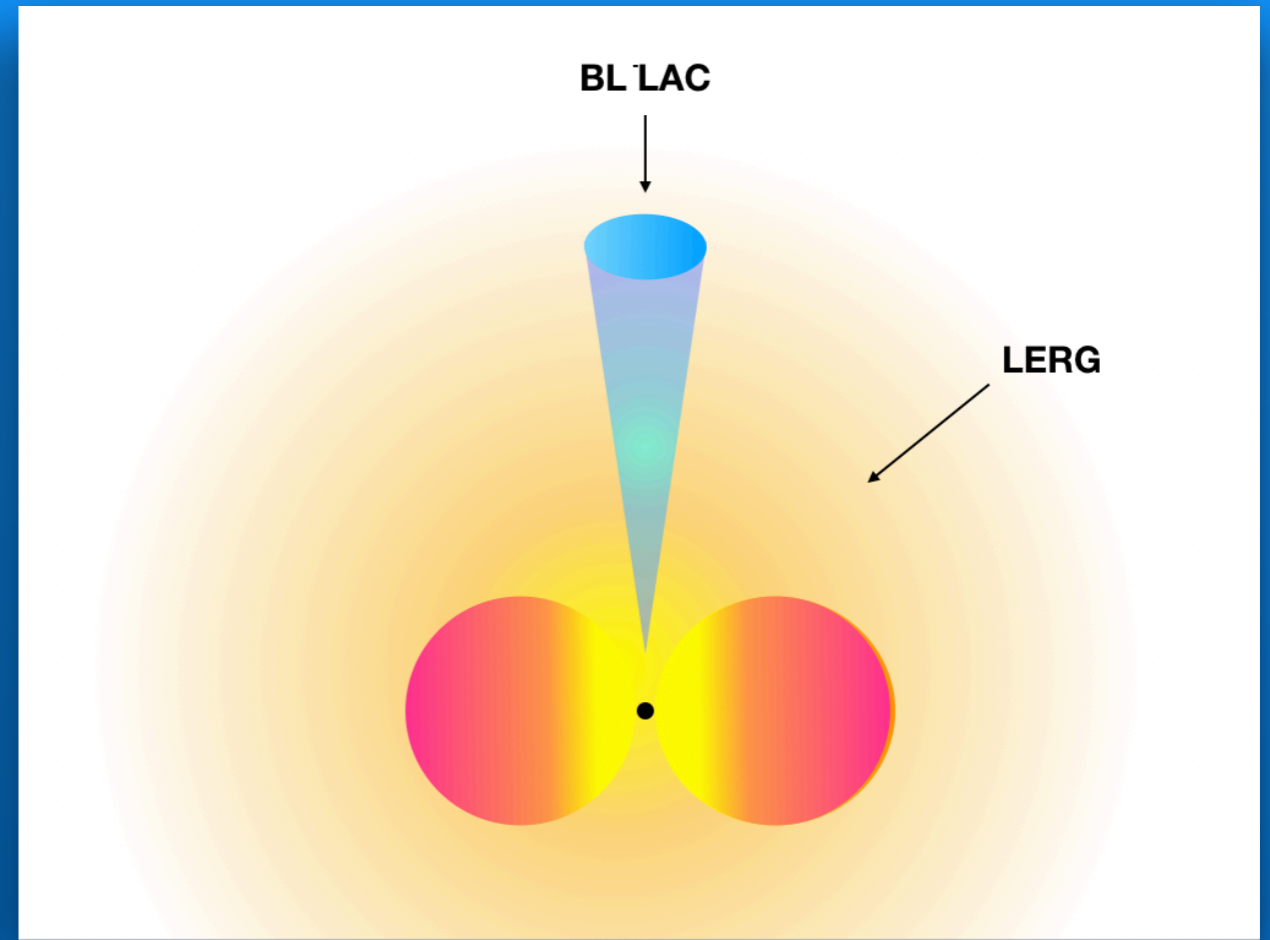
HERG: almost FRII
LERG: both FRI and FRII

Revised AGN Unified Model

Efficient Accretion
DISK

Inefficient flow
ADAF

FRI/FRII classification (Fanaroff & Riley 1974)
RADIO MORPHOLOGY

Mon. Not. R. astr. Soc. (1974) **167**, Short Communication, 31P–35P.

THE MORPHOLOGY OF EXTRAGALACTIC RADIO SOURCES OF HIGH AND LOW LUMINOSITY

B. L. Fanaroff and J. M. Riley

(Received 1974 March 6)

SUMMARY

The relative positions of the high and low brightness regions in the extragalactic sources in the 3CR complete sample are found to be correlated with the luminosity of these sources.

It has become clear from recent observations of extended extragalactic radio sources that many consist of fairly compact regions of high brightness ('hot spots') embedded in more extensive regions of much lower brightness. It is of importance to the models of the origin of the radio emission and of the energy supply to understand the relationship between these regions and other parameters of the radio emission such as luminosity, spectral index and shape. In this note we suggest that there is a definite relationship between the relative positions of the high and low brightness regions of radio sources and their luminosity.

The 199 sources in the 3CR complete sample (Mackay 1971) have been studied with high resolution using the Cambridge One-Mile telescope. All 199 sources were mapped at 1·4 GHz with a resolution of 23″ arc in RA and 23″ cosec δ in Dec. (Macdonald, Kenderdine & Neville 1968; Mackay 1969; Elsmore & Mackay 1970), and 53 of them were observed at 5 GHz with a resolution of 6″ × 6″ cosec δ (Mitton 1970a, b, c; Graham 1970; Harris 1972, 1973; Branson et al. 1972; Riley 1972, 1973; Riley & Branson 1973; Northover 1973, 1974).

In the investigation described here we have used a sub-sample of the 3CR complete sample, consisting of all those sources which were clearly resolved into two or more components in any of the series of observations mentioned above. The sources were classified using the ratio of the distance between the regions of highest brightness on opposite sides of the central galaxy or quasar, to the total extent of the source measured from the lowest contour; any compact component situated on the central galaxy was not taken into account. Those sources for which this ratio is less than 0·5 were placed in class I; those for which it is greater than 0·5 were placed in class II. In sources for which we have maps of adequate resolution, this is equivalent to having the 'hot spots' nearer to (Class I) or further away from (Class II) the central bright galaxy or quasar than the regions of diffuse radio emission. The sensitivities of most maps were sufficient for brightness temperatures a few per cent of the peak brightness to have been detected. Those sources for which the sensitivities were not good enough to detect low brightness regions, and those of two or three beamwidths in extent for which classification is impossible, are listed in Table II and have not been included in the analysis.

The results are presented in Table I whose arrangement is as follows:

(i) The luminosity at 178 MHz in W Hz^{-1} sr^{-1} (Hubble's constant = 50 km s^{-1} Mpc^{-1}); the sources are arranged in order of their luminosity.
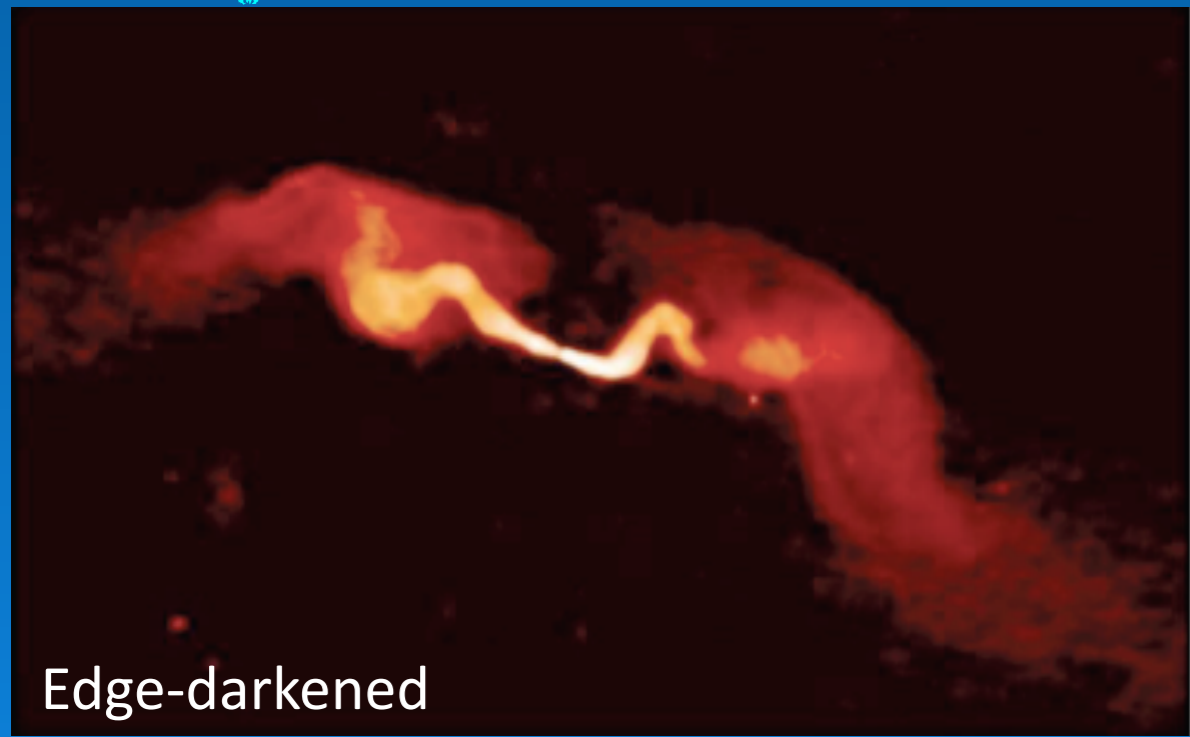
31P

FRI
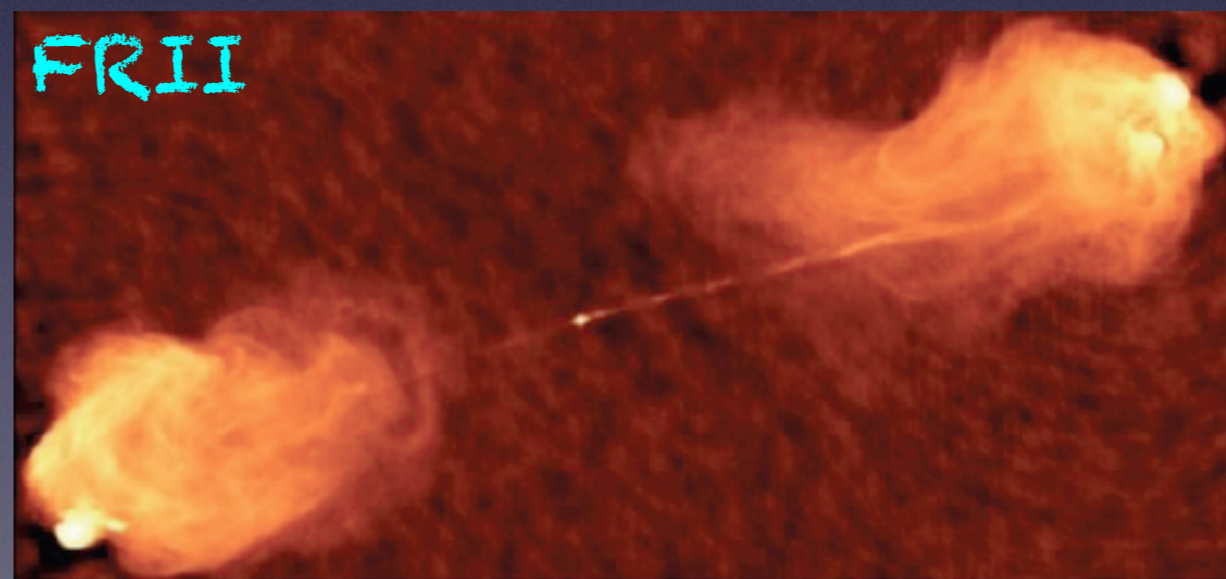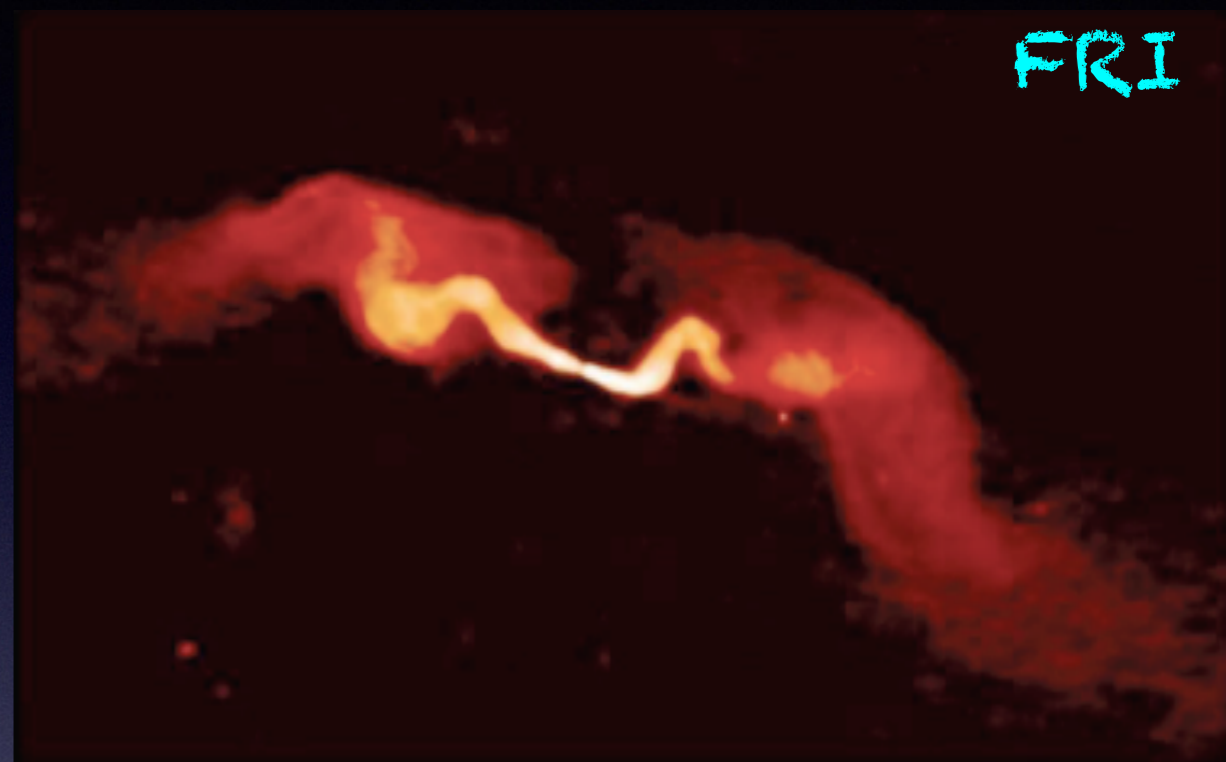
FRII

FRI – $L_{178MHz} < 2 \times 10^{25}$ W Hz^{-1} sr^{-1}
FRII – $L_{178MHz} > 2 \times 10^{25}$ W Hz^{-1} sr^{-1}

FRI/jet dominated
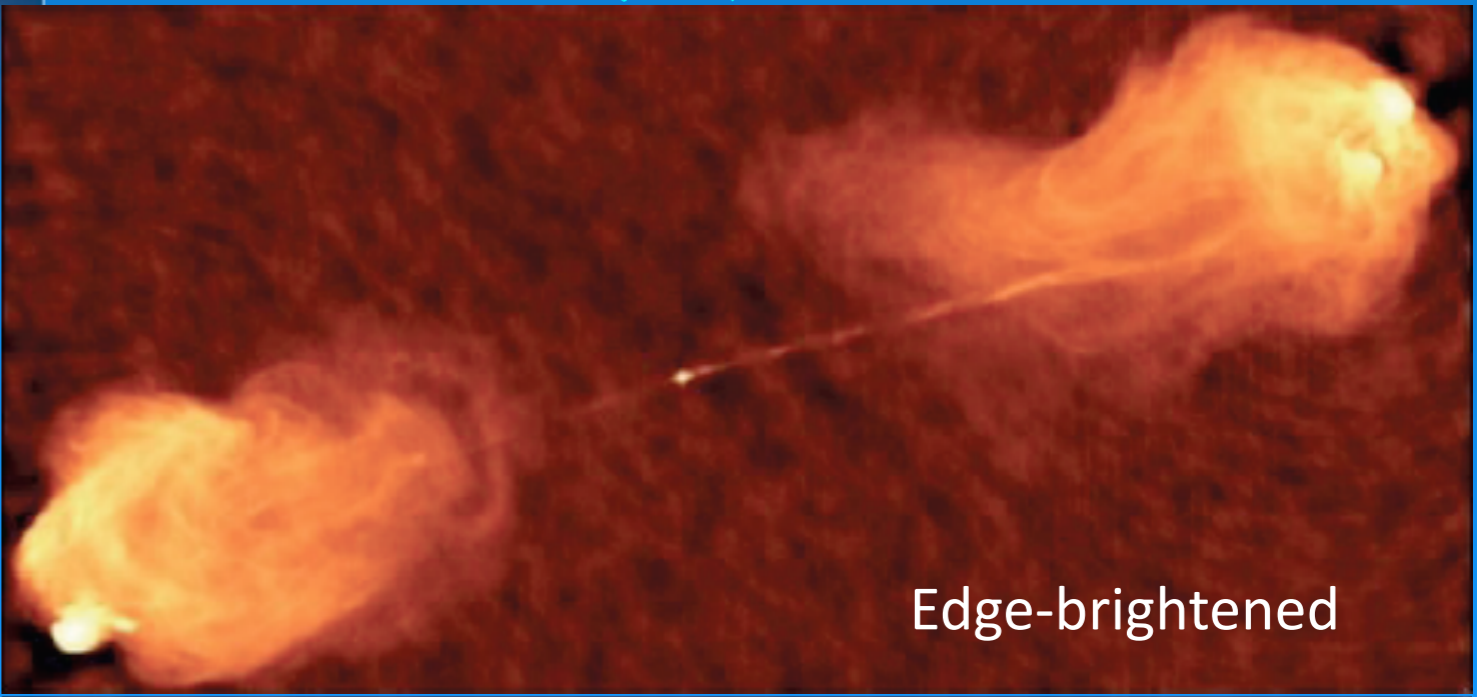
In FRI the jets are thought to decelerate and become sub-relativistic on scales of hundred of pc to kpc.

The nuclei of FRI are not generally absorbed and probably powered by inefficient accretion flows.
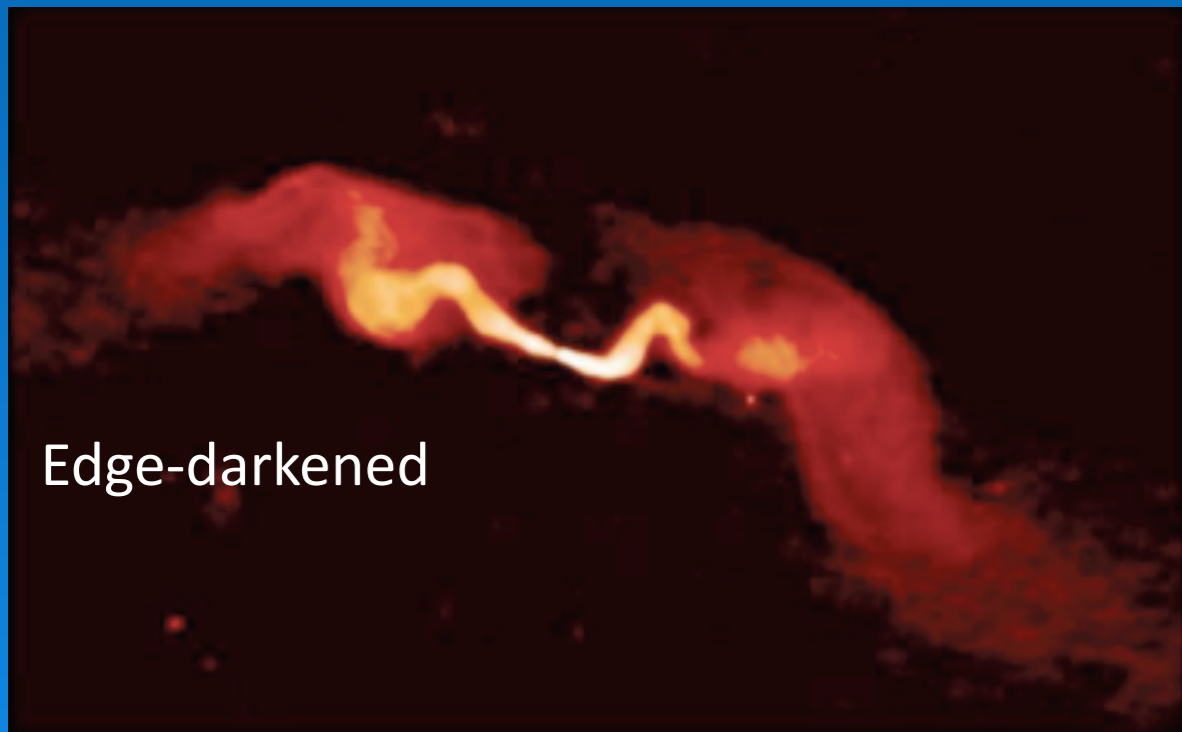
Edge-darkened

FRII/lobe dominated

The jets in FRII are at least moderately relativistic and supersonic from the core to the hot spots.

Most FRII are thought to have an efficient engine and a dusty torus.

Edge-brightened

FRI/jet dominated

FRI -> LERG

Edge-brightened

Edge-darkened

FRII/lobe dominated

FRII -> HERG

Blazars: BL Lacs (BL) and Flat Spectrum Radio Quasar (FSRQ)

Compact in radio

Extremely variable

BL are almost featureless in the optical band (FSRQ can show emission lines overimposed on a strong continuum)
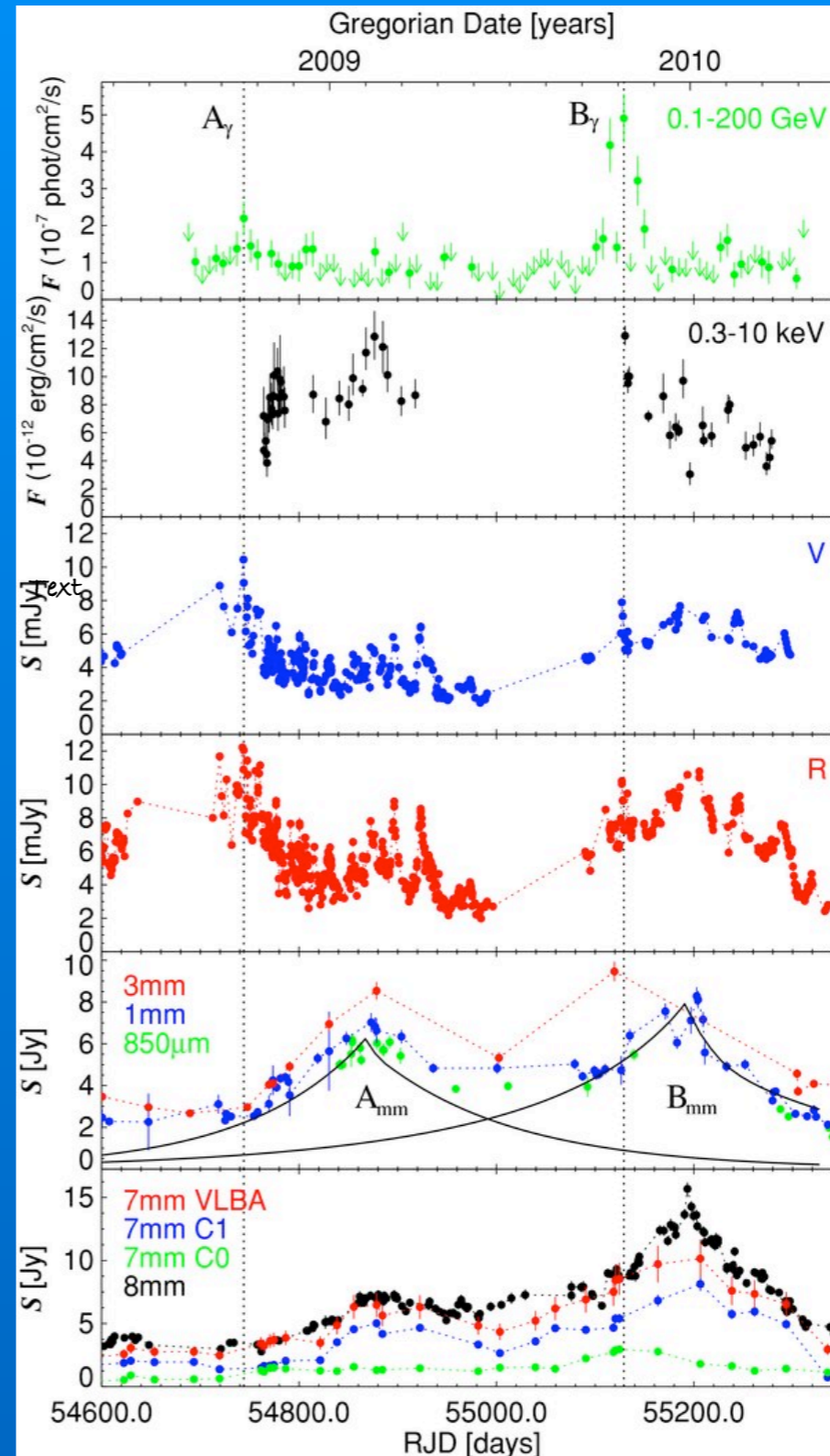
OJ 287 light curves from radio to gamma Agudo et al. 2011ApJL 726, L13

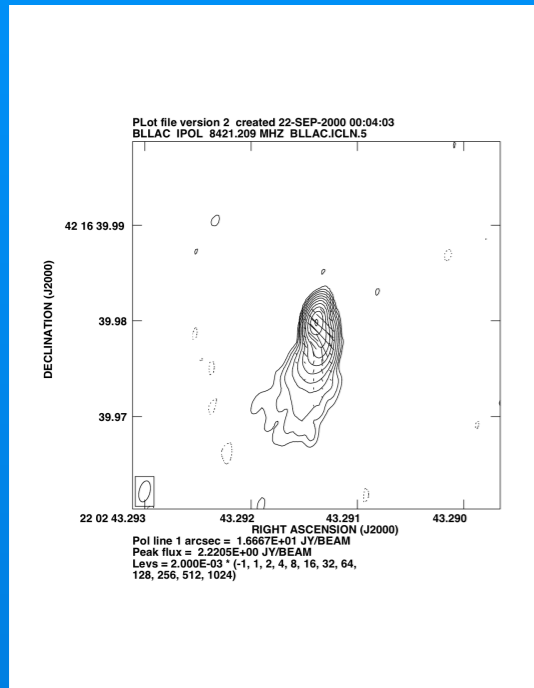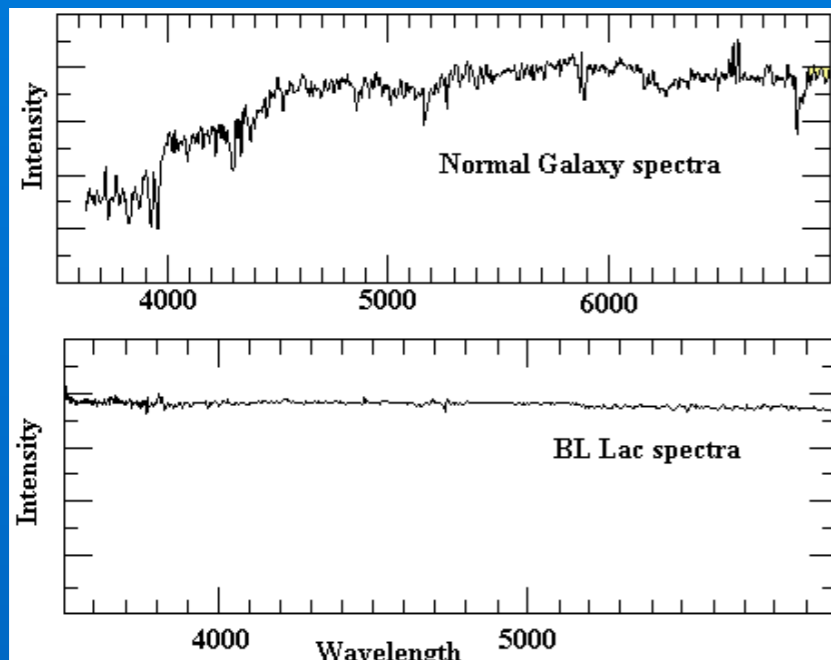# The jet emission from blazars is strongly Doppler boosted with respect to radio galaxies

The key parameter is the Doppler Factor $\delta(\beta, \theta)$

$$\delta = [\gamma(1 - \beta cos\theta)]^{-1}$$

$=\sqrt{(1 - \beta^2)}$

Lorentz factor

$=v/c$
bulk velocity

angle between
the jet axis and
the line of sight

Urry & Padovani 1995

The Doppler factor relates intrinsic and observed flux for a moving source at relativistic speed v=β c.

For an **intrinsic** power law spectrum: $F'(\nu') = K (\nu')^{-\alpha}$
the **observed** flux density is

$F_\nu(\nu) = \delta^{3+\alpha} F'_{\nu'}(\nu)$

$$\Delta t = \Delta t' / \delta$$

Blazar   Radio Galaxy/SSRQ

Doppler factor, δ

$\gamma = 15$
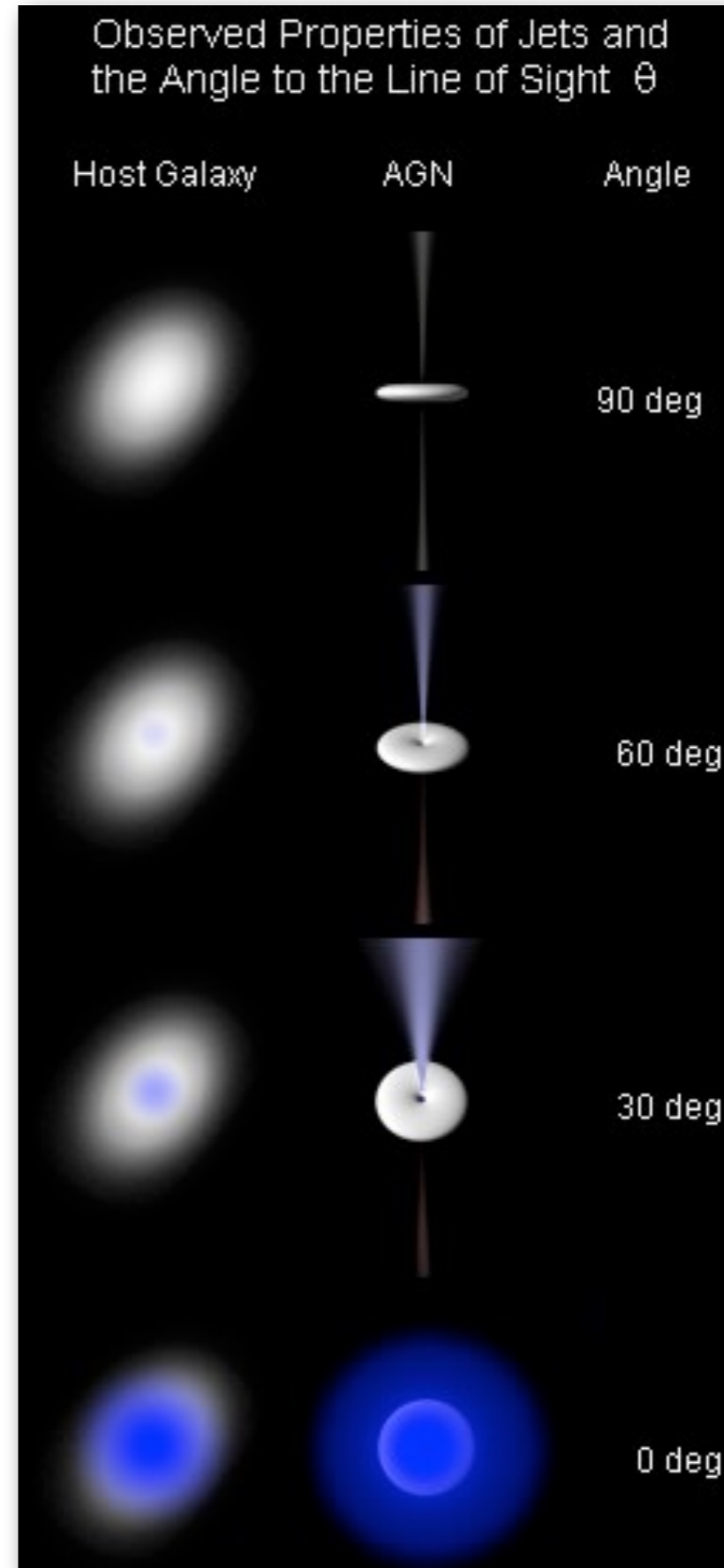$\gamma = 10$
$\gamma = 5$
$\gamma = 2$

Viewing angle, θ
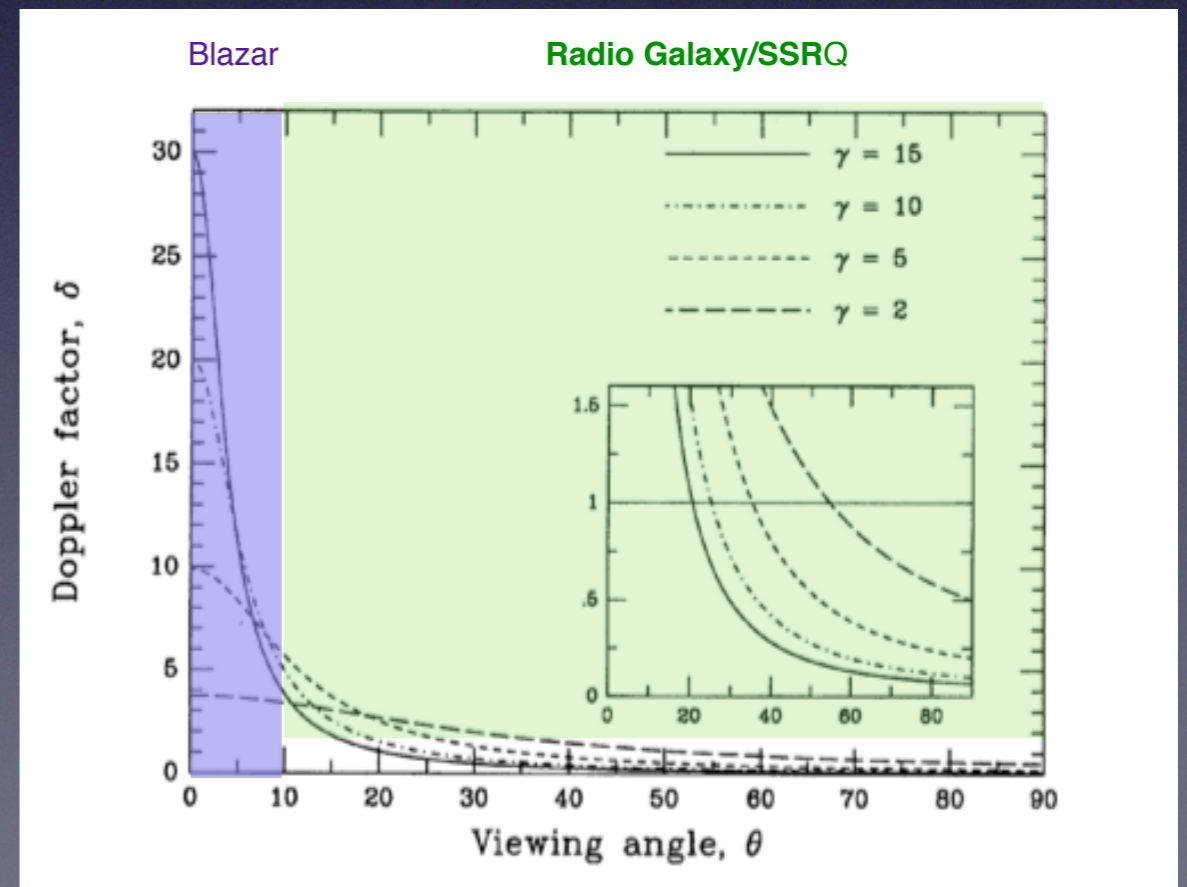
RADIO-LOUD AGN

Type 2 (Narrow Line Radio Galaxy)

Type 1 (Broad Line Radio Galaxy)

Blazar (BL Lacs, Flat Spectrum Radio Quasars)

Observed Properties of Jets and the Angle to the Line of Sight θ

Host Galaxy   AGN   Angle

90 deg

60 deg

30 deg

0 deg

FR0 radio galaxies

✳ FR0 are compact sources and lack extended radio emission

✳ From the optical point of view they share similar nuclear and host properties with FRI
  - host galaxy;
  - black hole masses ($M_{BH} > 10^8 M_\odot$)
  - spectroscopic classification (LEG)
  - X-ray spectral behavior

✳ FR0 represent the bulk of the Radio-Loud AGN population in the local Universe (the number density of the FR0Cat sources is ~5 times higher than that of FRI Baldi et al. 2017)

FRI (size > 30 kpc), sFRI (10 < size < 30 kpc) and FR0 (size < 5 kpc)
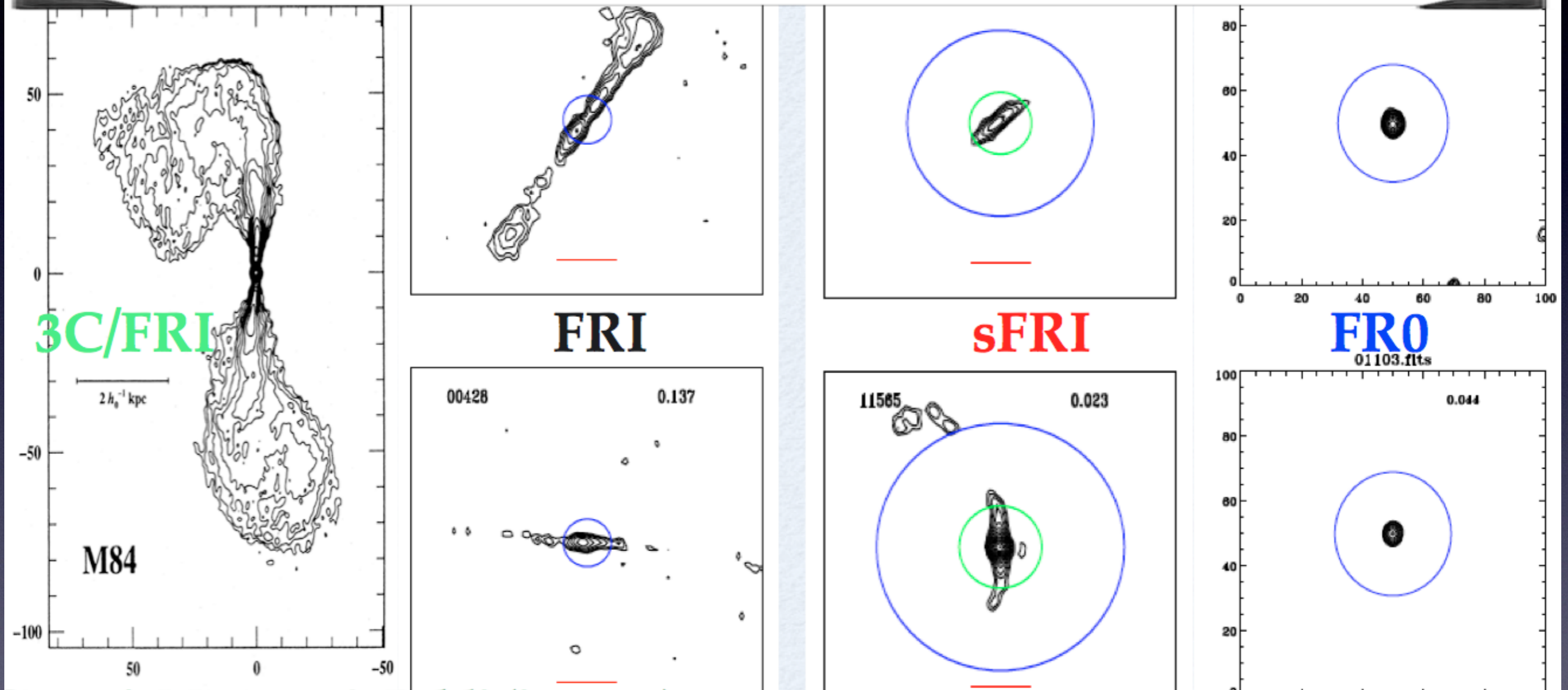
courtesy: R.D. Baldi

In the same volume 108 FR0, 21 FRI and 1 FRII

2. Spectral Energy Distribution of a RL AGN

To Radio Lobe

Clouds in Broad-Line Region (BLR)

Thin Hot Accretion Disk

Dusty Torus

Dusty Torus

Black Hole Engine

To Radio Lobe

Clouds in Narrow-Line Region (NLR)

Radio Loud

IR bump

Big Blue Bump

X-rays

log ν F(ν)

0

-1

12   14   16   18   20

log ν [Hz]

Credits: A. Marconi
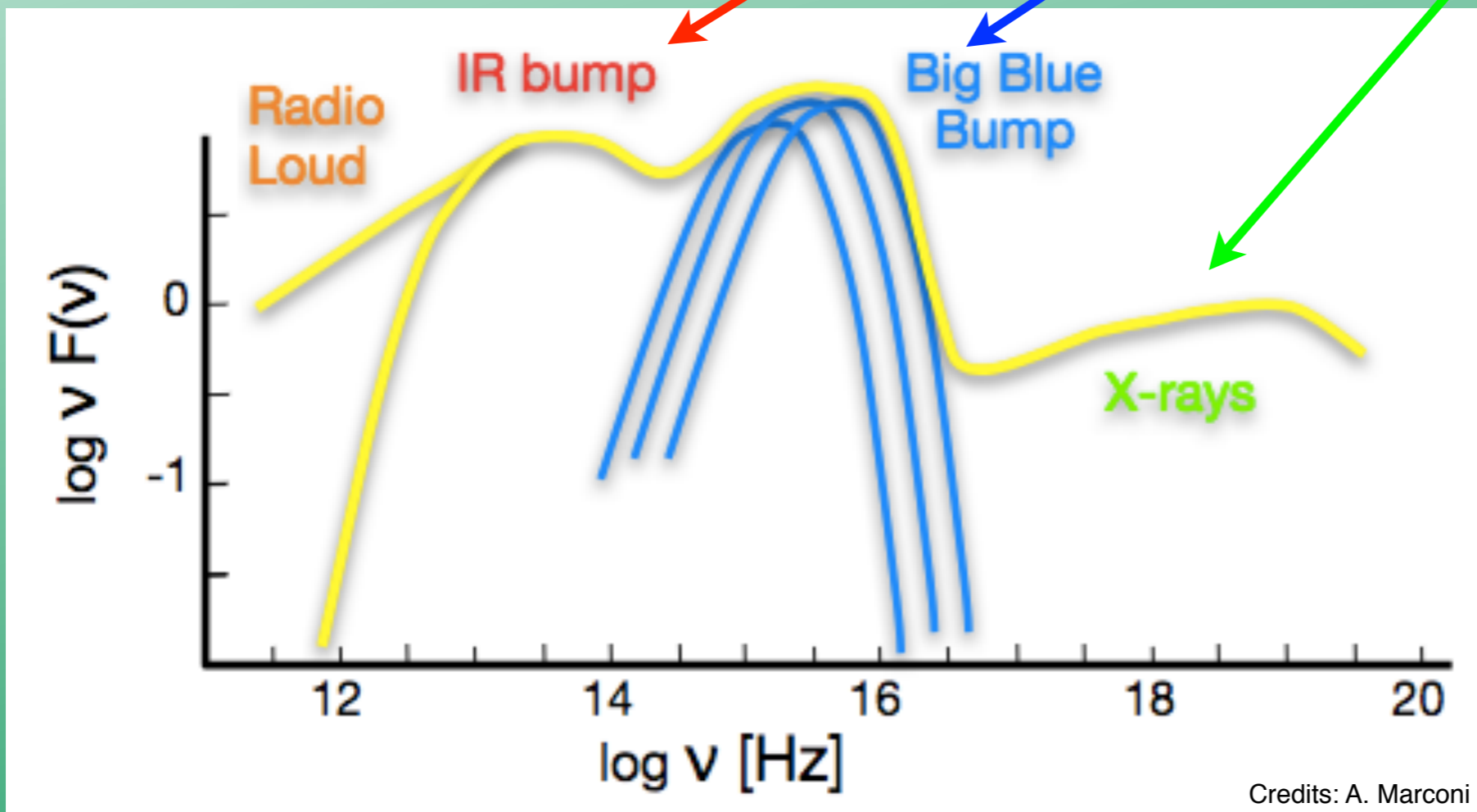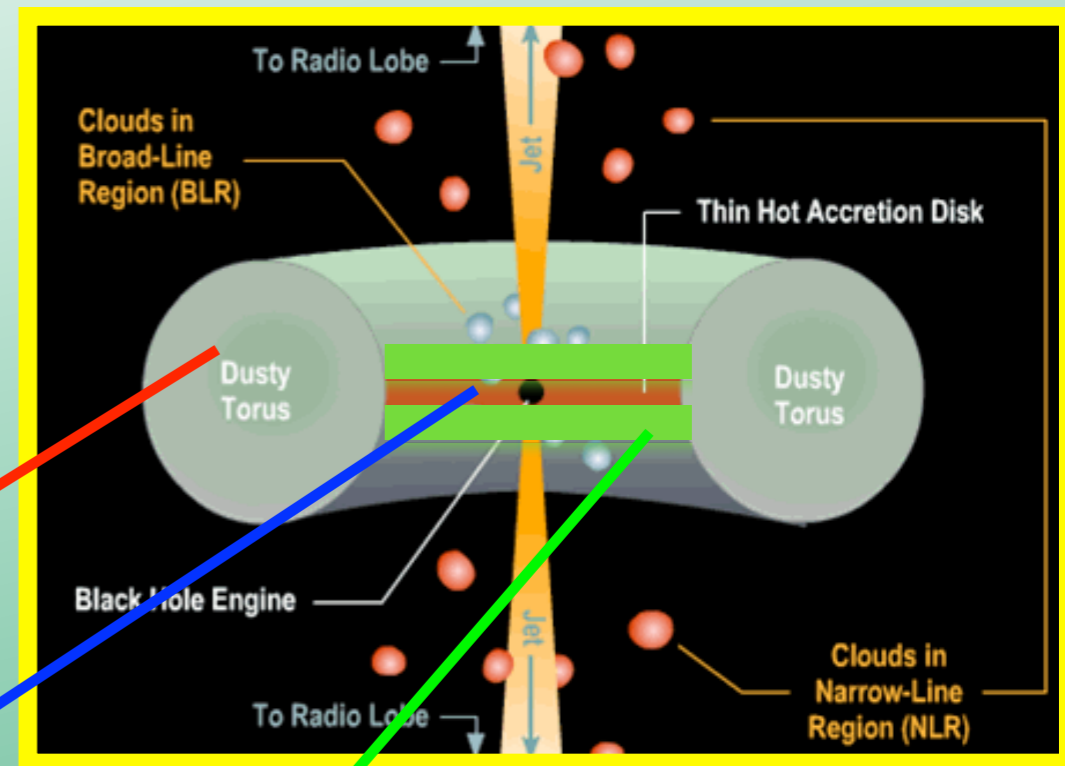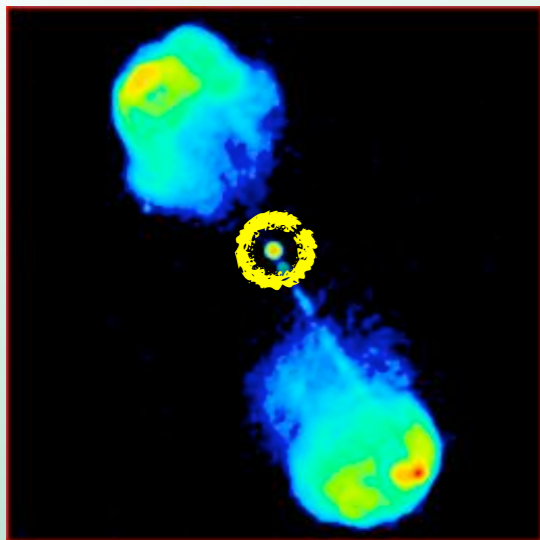
Radio Galaxies: kpc components

LOBE

Hot Spot
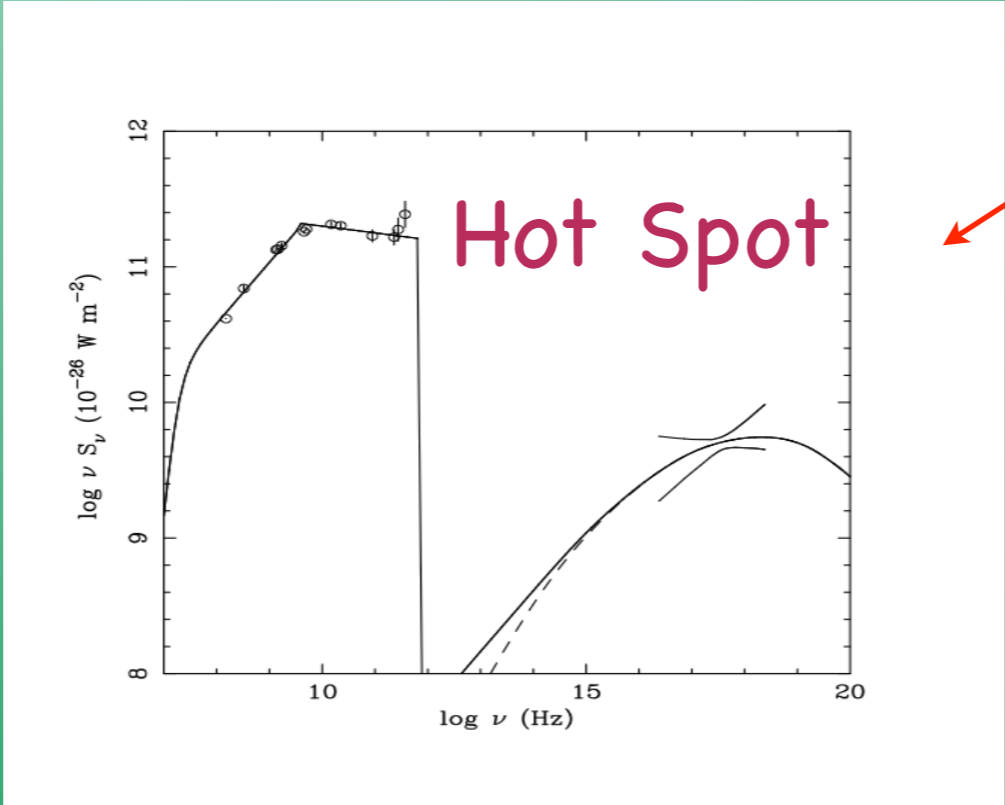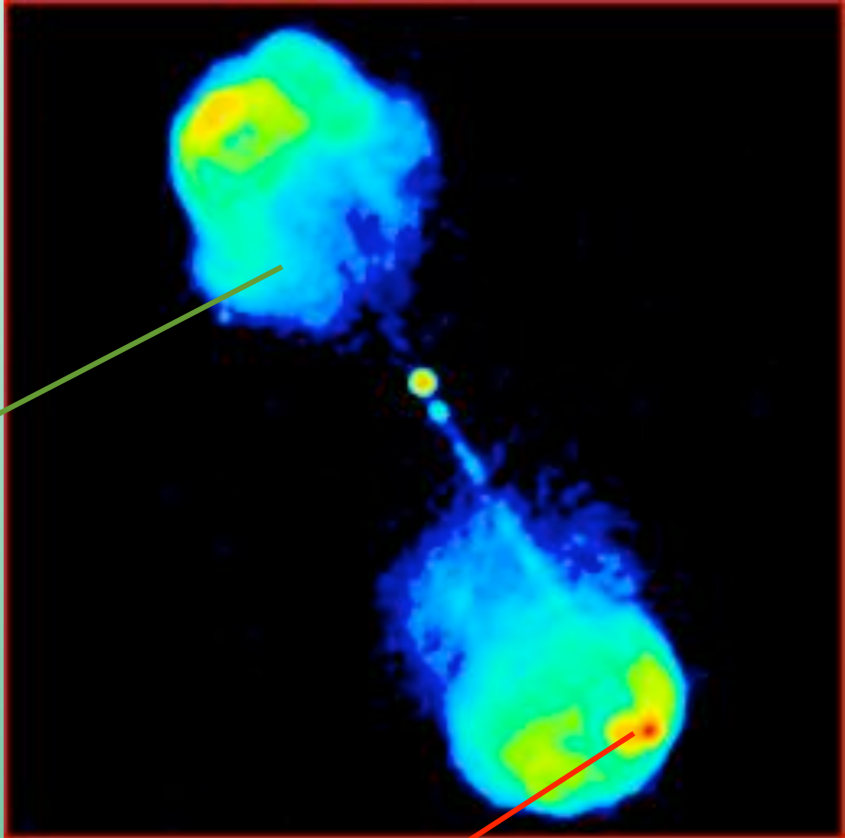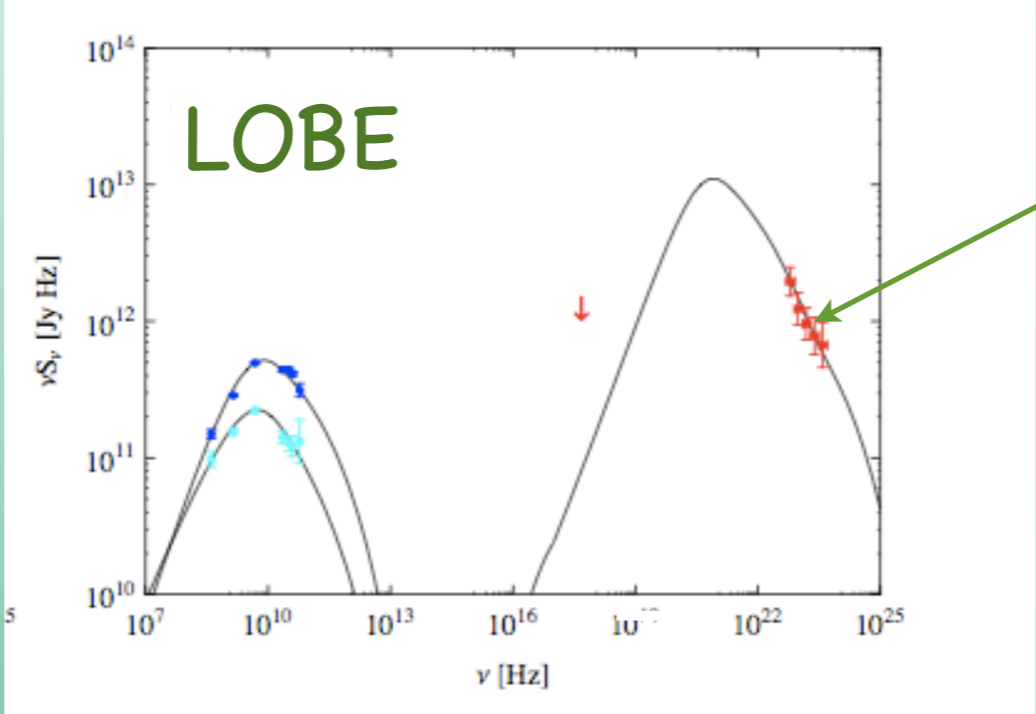
BLAZARS: double peaked SED

Synchrotron

Inverse Compton
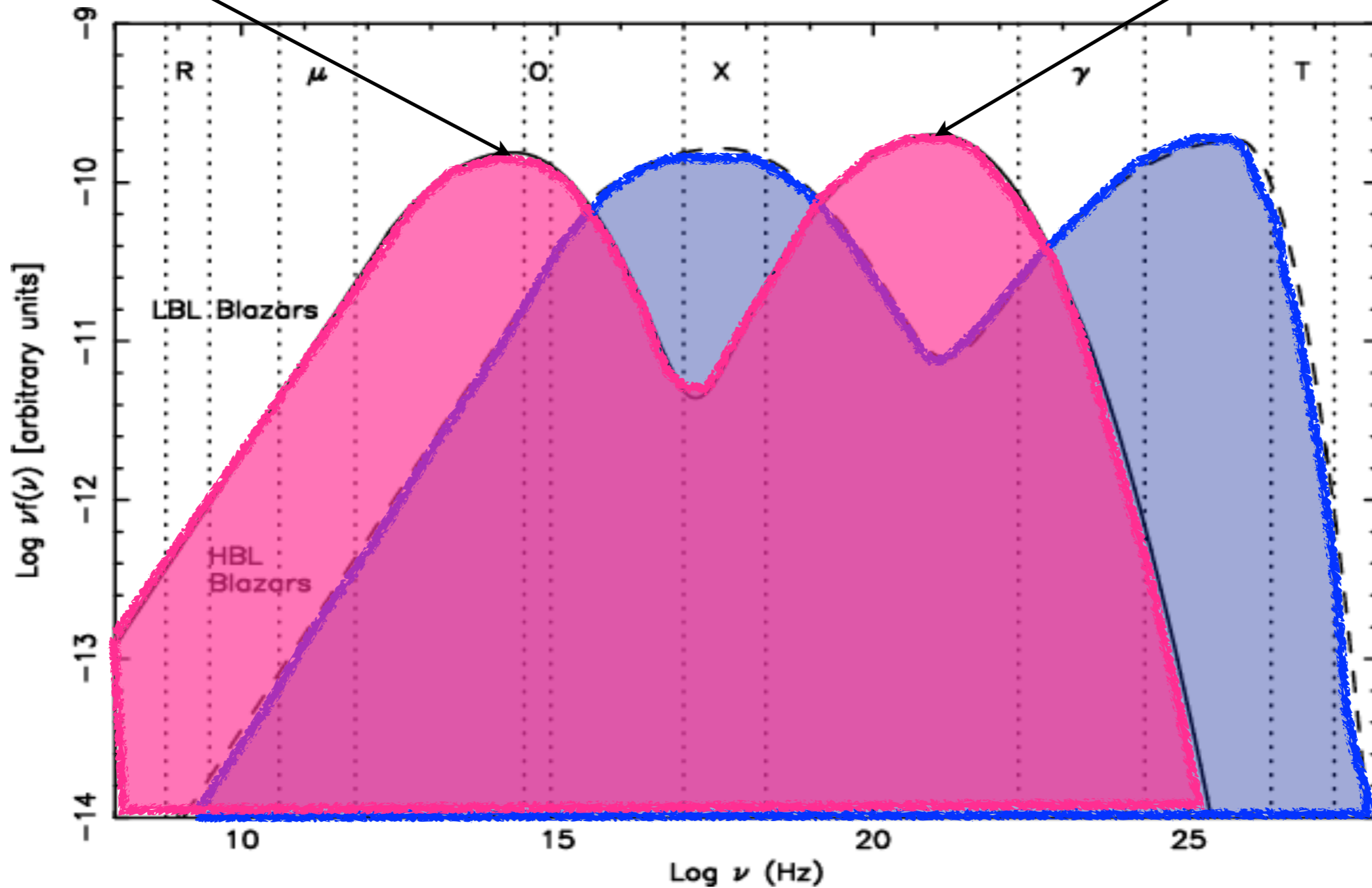
LBL= low-frequency peaked blazars

HBL= high-frequency peaked blazars

3. Radiative processes

Thermal emission
Accretion flow
Thermal Comptonization
Reprocessed features

Non-thermal emission
Synchrotron
Inverse Compton

Black Hole as engine of AGN

BH is a very efficient engine

Assuming M ~ Msun and R=10 Km

$$\Delta E_{acc} = \frac{GMm}{R} \sim 10^{20} \text{ erg/g}$$

$$\Delta E_{nuc} = 7 \times 10^{-2} mc^2 \sim 6 \times 10^{18} erg/g$$

Black Hole as engine of AGN

- **M/R is the compactness of the accretor**
  - **The more compact, the more energy can be released**

The luminosity depends on the accretion rate

$$L_{acc} = GM\dot{M}/R$$

Eddington Luminosity L_E is the luminosity at which the outward force of the radiation pressure is balanced by the inward gravitational force

$$L_{Edd} = \frac{4\pi GM m_p c}{\sigma_T} \sim 1.3 \times 10^{38} \frac{M}{M_\odot} erg/s$$

$$L_{acc} = GM\dot{M}/R$$

BH is more complex

$$L_{acc} = 2\eta GM\dot{M}/R = \eta\dot{M}c^2$$

$$R_S = \frac{2GM}{c^2}$$

Black hole radius can be derived by the escape velocity of the light

$$v_{escape} = c = \left(\frac{2GM}{R_S} \right)^{\frac{1}{2}}$$

Schwarzschild radius

$$R_S = \frac{2GM}{c^2}$$

Accretion processes around black holes involve rotating gas flow. Therefore the accretion flow structure is determined by solving simultaneously four conservation equations:

conservation of vertical momentum
conservation of mass
conservation of energy
conservation of angular momentum

Four solutions are currently known. In these solutions viscosity transports angular momentum outward, allowing the accretion gas to spiral in toward the BH. Viscosity acts a source of heat that is radiated away.

The most famous solutions are:

i) Shakura & Sunyaev thin optically thick disk model (standard model)
ii) Optically thick Advection-Dominated Accretion Flow (ADAF)

ACCRETION DISCS   ✖ 2180
IN ASTROPHYSICS

J. E. Pringle

Institute of Astronomy, University of Cambridge, Madingley Road,
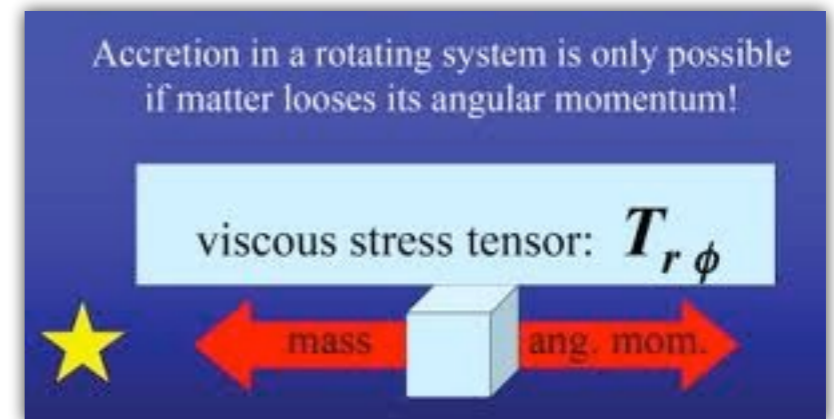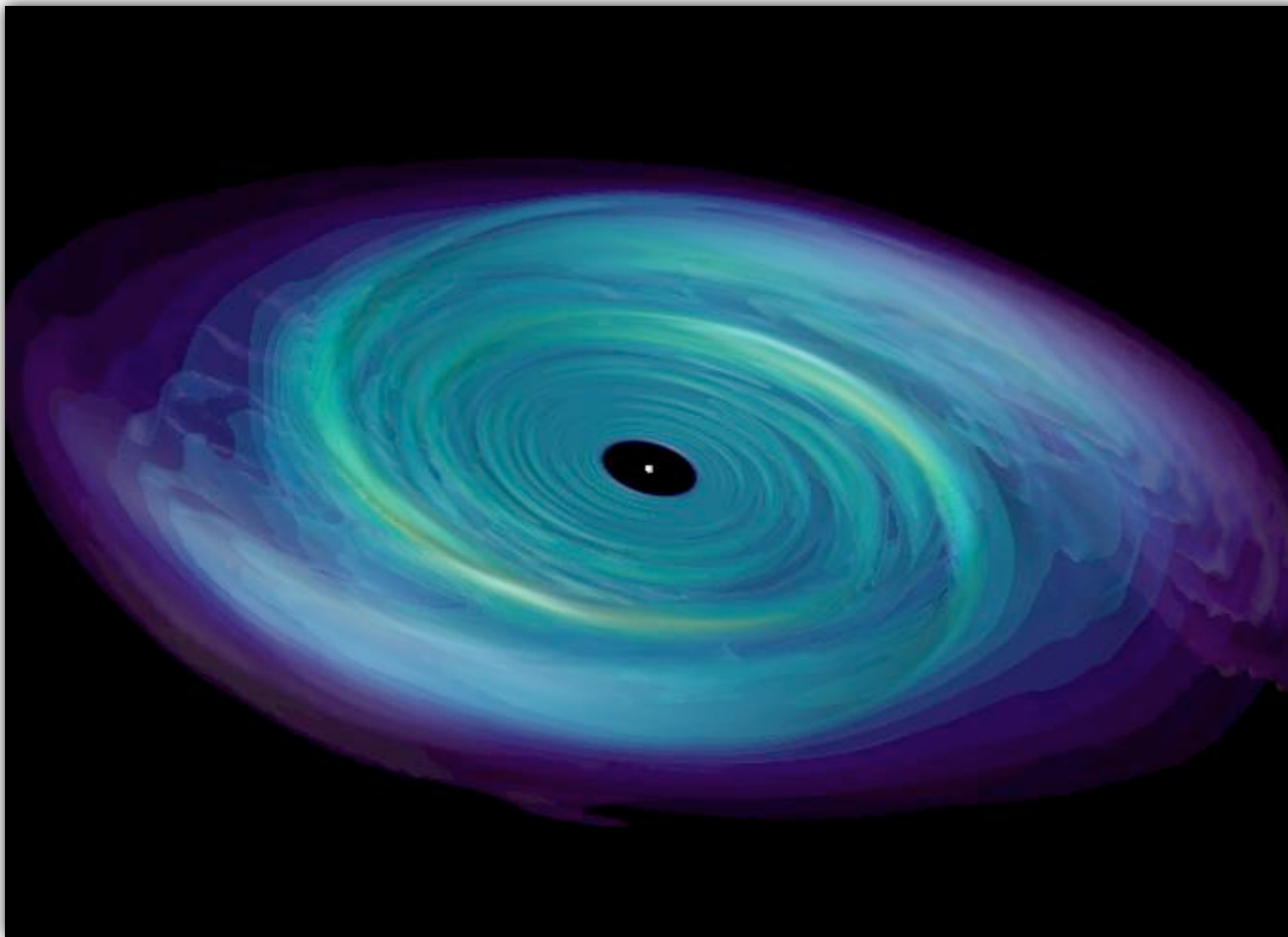Cambridge, CB3 0HA, England

1. INTRODUCTION

If we put a particle in a circular orbit around a central gravitating body, it will stay in that orbit. If we then extract energy and angular momentum from the particle we may allow it to spiral slowly inwards. The amount of energy that can be extracted by such a process is equal to the binding energy of the innermost accessible orbit. For orbits around sufficiently compact objects a reasonable fraction of the particle's rest mass energy can be extracted. For example, of order 10 percent of the rest mass can be obtained from orbits around a neutron star and up to around 40 percent for orbits around a black hole. Thus, the accretion process can be an efficient converter of rest mass to radiation. The problem is to set up the process that can extract the energy and angular momentum.

 If we consider a blob of gas in a circular orbit then we have more flexibility. In particular, if we can find a method of redistributing angular momentum among the gas particles in order to let some of them fall into the potential well, then we are in a position to extract the potential energy so released. The accretion disc provides just such a method. The efficiency with which energy is released and the ubiquity of angular momentum explains why accretion discs are popular in models for some of the most luminous objects—X-ray stars and quasars. However, accretion disc theory predates the discovery of both these, and it is to these initial developments that we now turn our attention.

Disks usually rotate such that each fluid element is moving almost in a circular orbit. As the angular velocity is a function of radius, there is a shearing flow. This means that coupling between adjacent radii exerts a force. Given that the outer parts rotate more slowly, inner try to speed up outer, giving it a higher velocity. This increases the angular momentum of the outer, decreases the angular momentum of the inner, so net result is that angular momentum is transferred outwards and mass flows inwards.

Accretion in a rotating system is only possible if matter looses its angular momentum!

viscous stress tensor: $T_{r\phi}$

mass   ang. mom.

Viscosity transports angular momentum outward, allowing the accretion gas to spiral in toward the BH. Viscosity acts as a source of heat that is radiated away.

3. AM Transport in disk?

o The total energy associated with an orbit is: $E = KE + PE = 1/2\ mv^2 - GMm/r$.

o For a circular orbit, $mv^2/r = GMm/r^2 => v^2 = GM/r$.
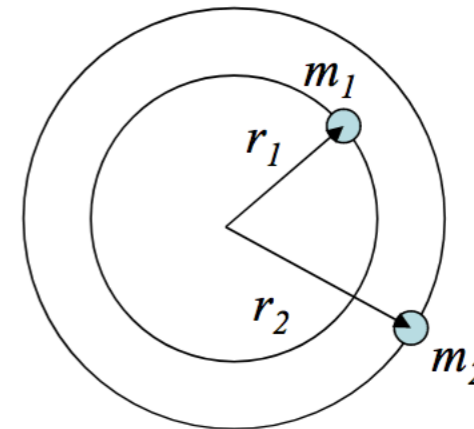
o Therefore
$$E = 1/2m\frac{GM}{r} - \frac{GMm}{r}$$
$$=> E = -\frac{GMm}{2r}$$

o The angular momentum is given by $L = mvr = m\sqrt{\dfrac{GM}{r}}\,r$
$$=> L = m\sqrt{GM}\,\frac{r}{\sqrt{r}}$$

o Lynden-Bell and Pringle (1974) considered how AM could be transported in a disk. Take two bodies in circular orbits with masses m_1 and m_2. The total energy and AM of the system are:

$$E = -\frac{GM}{2}\left(\frac{m_1}{r_1} + \frac{m_2}{r_2}\right) \qquad Eqn.\ 4$$

$$L = \sqrt{GM}\left(m_1\frac{r_1}{\sqrt{r_1}} + m_2\frac{r_2}{\sqrt{r_2}}\right) \qquad Eqn.\ 5$$

3. AM transport in disk

o   Now suppose the orbits are perturbed slightly, while conserving L, $Eqns.4$ and 5 become:

$$\Delta E = \frac{GM}{2}\left(\frac{m_1}{r_1^2}\delta r_1 + \frac{m_2}{r_2^2}\delta r_2\right) \qquad Eqn.6$$

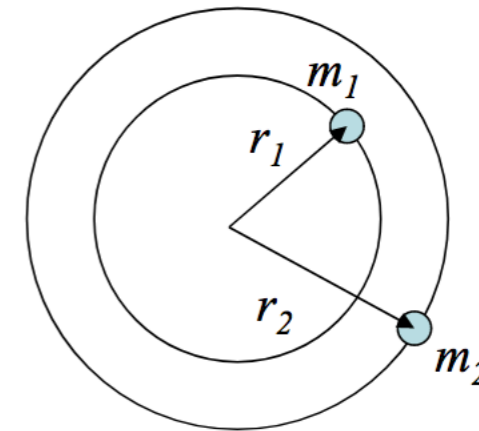$$\Delta L = \sqrt{GM}\,(m_1\sqrt{\delta r_1} + m_2\sqrt{\delta r_2}) = 0 \qquad Eqn.7$$

o   *Eqn. 7* implies that

$$\delta r_2 = -\frac{m_1}{m_2}\sqrt{\frac{r_2}{r_1}}\,\delta r_1$$

o   Substituting this into *Eqn. 6* gives

$$\Delta E = \frac{GM}{2}\left(\frac{m_1}{r_1^2}\delta r_1 + \frac{m_2}{r_2^2}\left(-\frac{m_1}{m_2}\sqrt{\frac{r_2}{r_1}}\,\delta r_1\right)\right)$$

$$= \frac{GMm_1\delta r_1}{2r_1^2}\left(1 - \frac{r_1^2}{r_2^2}\sqrt{\frac{r_2}{r_1}}\right)$$

$$\Rightarrow \Delta E = -\frac{GMm_1\delta r_1}{2r_1^2}\left(\left(\frac{r_1}{r_2}\right)^{3/2} - 1\right)$$

o   If $r_1 < r_2$ we can reduce the energy of the system if $\Delta r_1 < 0$ i.e. moving m_1 closer to the center. Thus the energy can be reduced while conserving AM by moving the initially closer body in and moving the initially outer body further out $\Rightarrow$ *all the mass is concentrated near the inner parts of the solar system, while the AM occupies the outer parts.* See Planetary Science by Cole and Woolfson for further details.

Shakura & Sunyaev thin optically thick disk model (standard model)
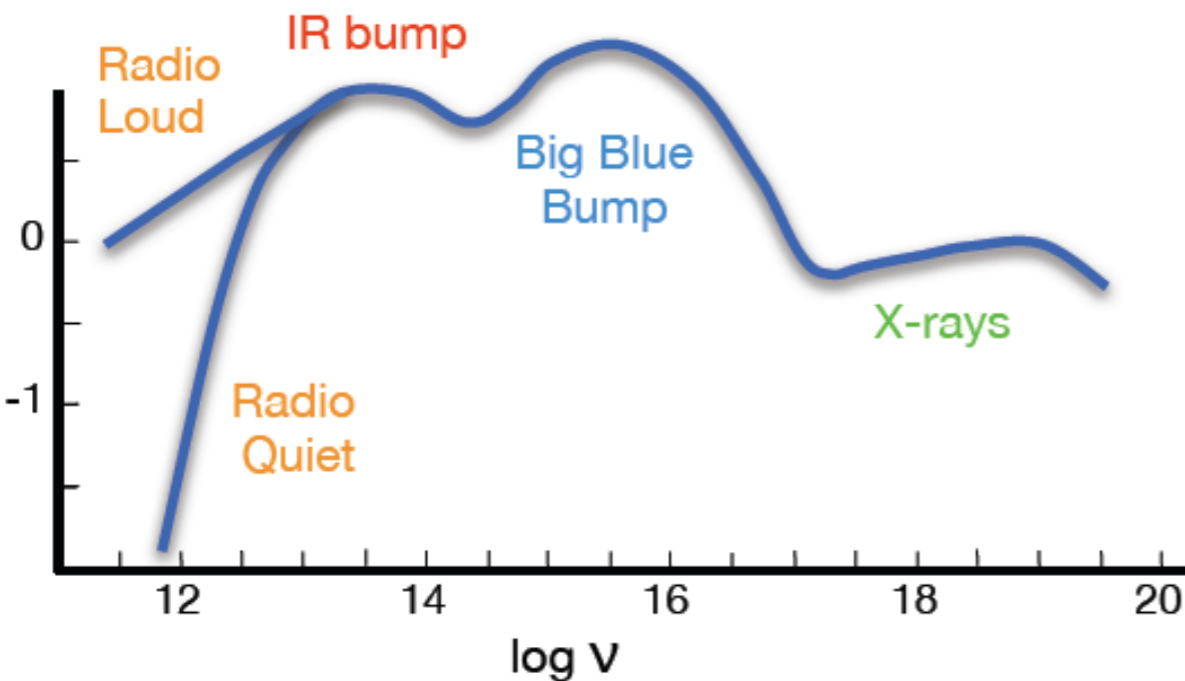

Thin H/R<< 1

R M_{BH}

H
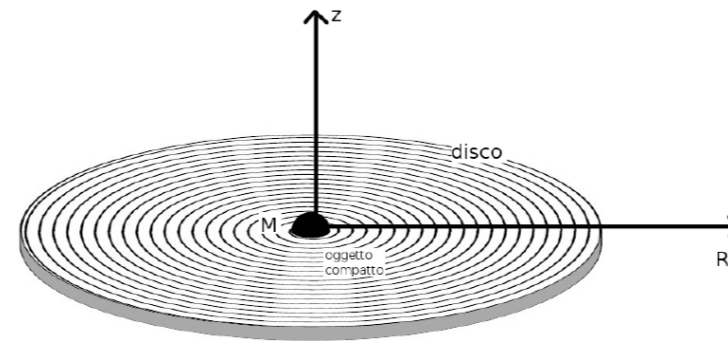
Thick, in the sense that each element of the disk radiates as a black body

If the the disk is optically thick, we can approximate the local emission as blackbody and the effective temperature of the photosphere

$$T(r) \sim 6.3 \times 10^5 \left(\frac{\dot{M}}{\dot{M_E}}\right)^{1/4} M_8^{-1/4} \left(\frac{r}{R_s}\right)^{-3/4} \quad K$$

For AGN with $\quad M_{BH} = 10_8 = 10^8 M_\odot \quad \dot{M} \sim \dot{M_E} = \frac{L_E}{\eta c^2}$
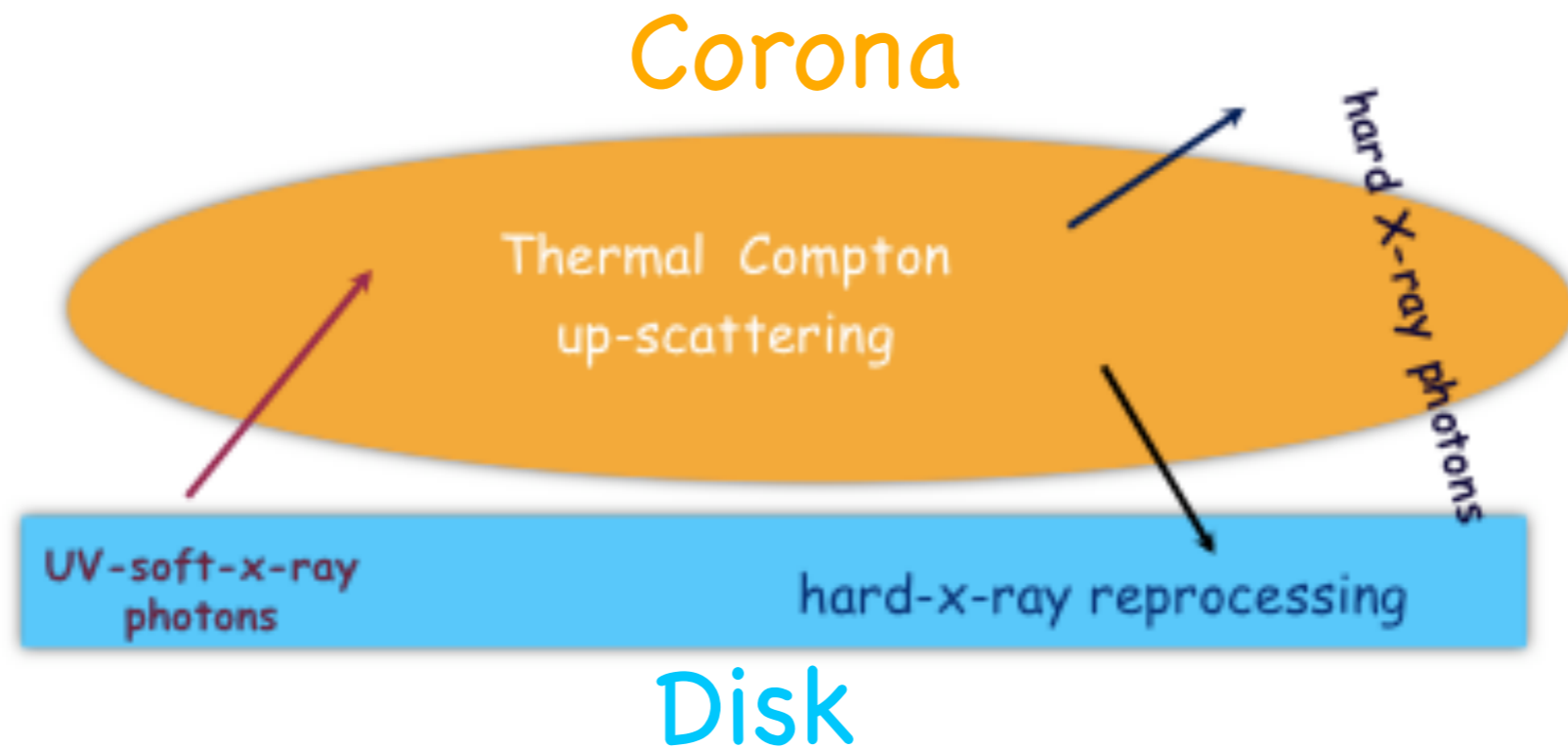

Spectral Energy Distribution (SED)

the peak occurs at UV-soft-X-ray region

$$\frac{\partial B}{\partial \nu} = 0 \quad B(\nu) \propto \nu^3 [e^{\frac{h\nu}{kT}} - 1]^{-1}$$

$$\nu_{max} = 2.8kT/h \sim 10^{16} \quad Hz$$

k = 1.38×10⁻¹⁶ erg/K

h= 6.6 x10⁻²⁶ erg s

Corona

Thermal Compton up-scattering

hard X-ray photons

UV-soft-x-ray photons

hard-x-ray reprocessing

Disk

Thermal Comptonization

With this term we mean the process of multiple scattering of a photon due to a **thermal (Maxwellian)** distribution of electrons.

There is one fundamental parameter measuring the importance of the Inverse Compton process in general, and of multiple scatterings in particular: the Comptonization parameter, usually denoted with the letter **y**.

y = [average # of scatt.] x[average fractional energy gain for scatt.]

Thermal Comptonization

Comptonization on a thermal plasma of electrons characterized by a temp. T and optical depth τ

T_c, τ Hot phase = corona

T_{soft} Cold phase = acc. disc
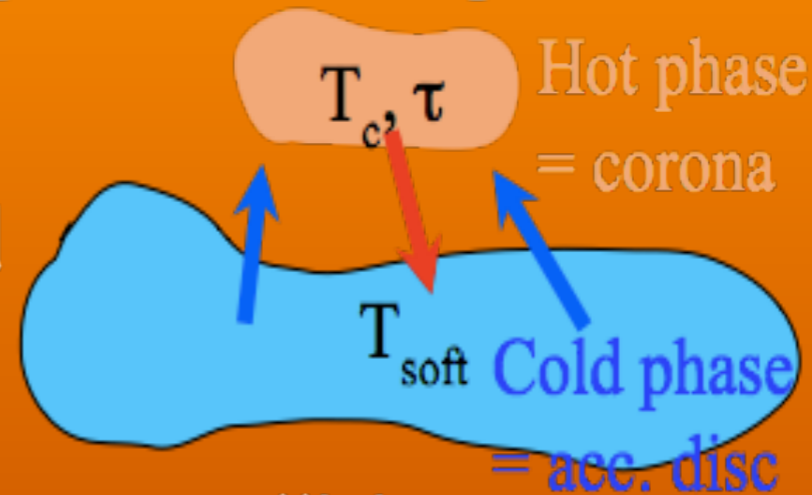
✓ mean relative energy gain per collision

$$\frac{\Delta E}{E} \simeq \left(\frac{4kT}{mc^2} \right) + 16 \left(\frac{kT}{mc^2} \right)^2 \quad \text{for E} \ll \text{kT}$$

$$\leq \quad\quad\quad 0 \quad\quad\quad \text{for E} \gtrsim \text{kT}$$

✓ mean number of scatterings

$$N \simeq (\tau + \tau^2)$$

➡ Compton parameter $y = \frac{\Delta E}{E} N$

$E_f = E_i \, e^y$

Thermal Comptonization Spectrum: the continuum

$$F_E \propto E^{-\Gamma(kT,\tau)} \exp\left(-\frac{E}{E_c(kT,\tau)}\right)$$
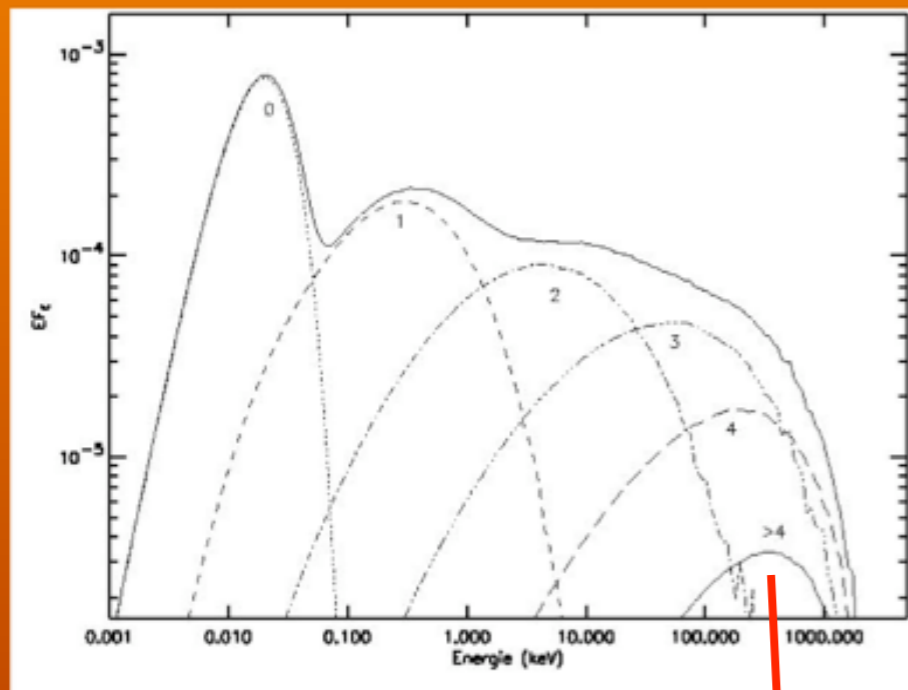
$$\Gamma(\tau, kT)$$

The exact relation between spectral index and optical depth depends on the geometry of the scattering region.
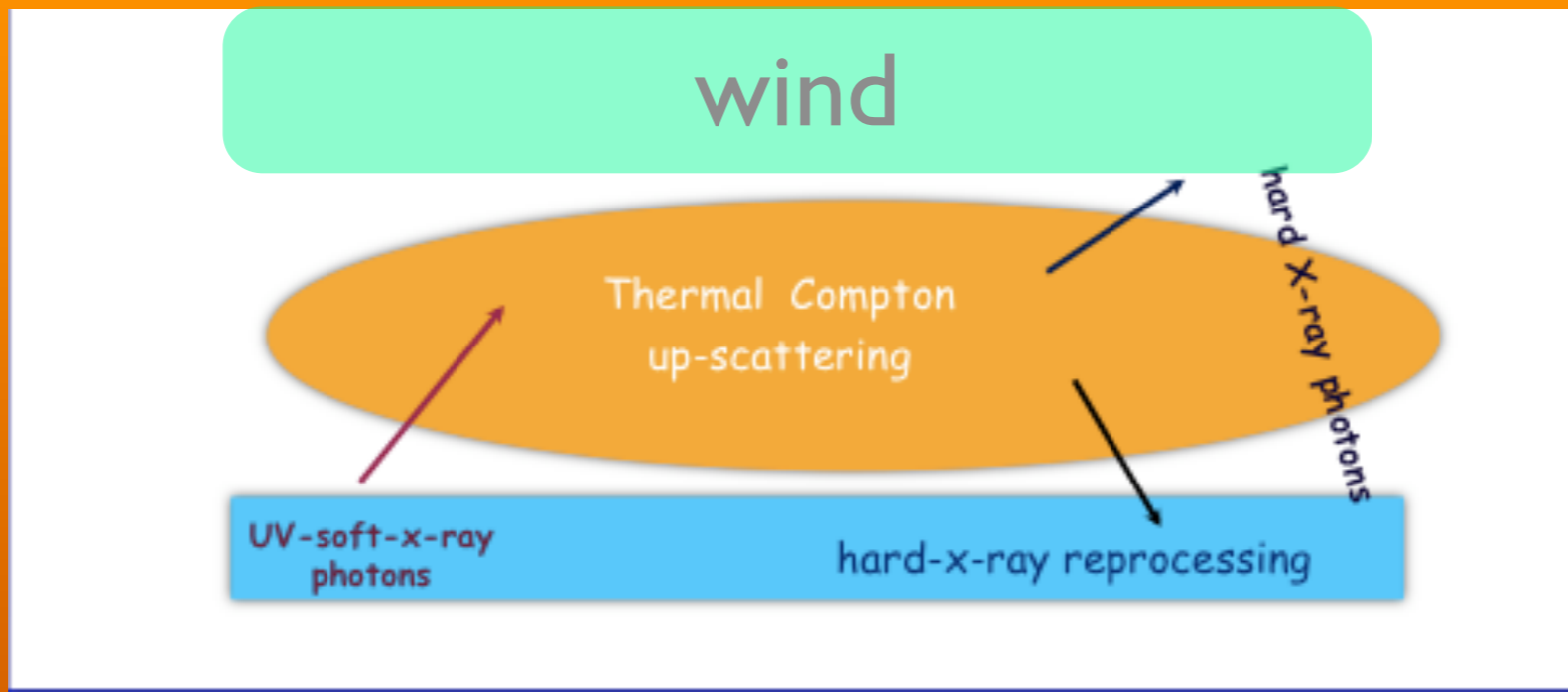
$$E_c \simeq kT$$

As photons approach the electron thermal energy, they no longer gain energy from scattering, and a sharp rollover is expected in the spectrum.

The observed high energy spectral cutoff yields information about the temperature of the underlying electron distribution.
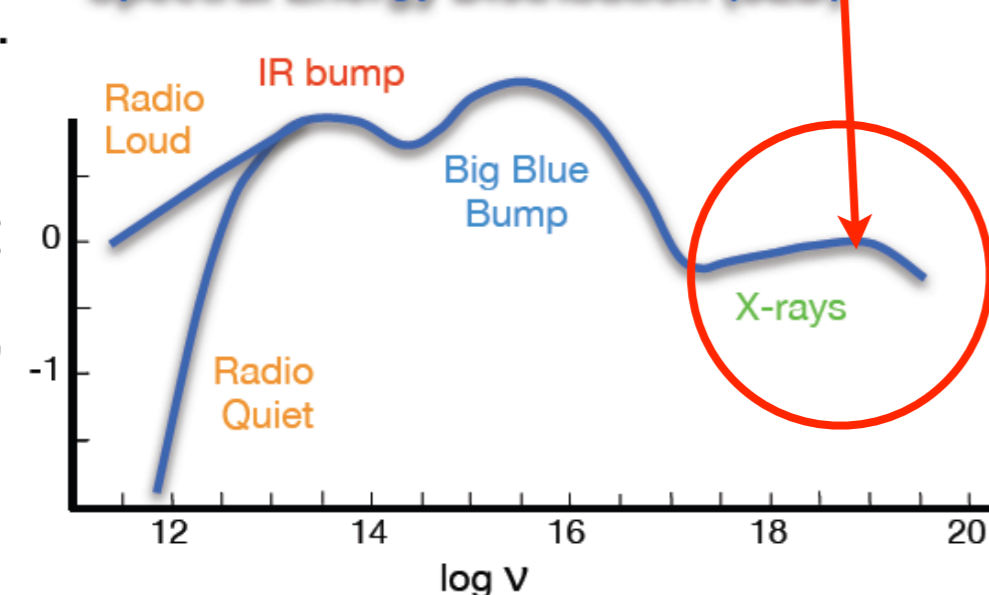
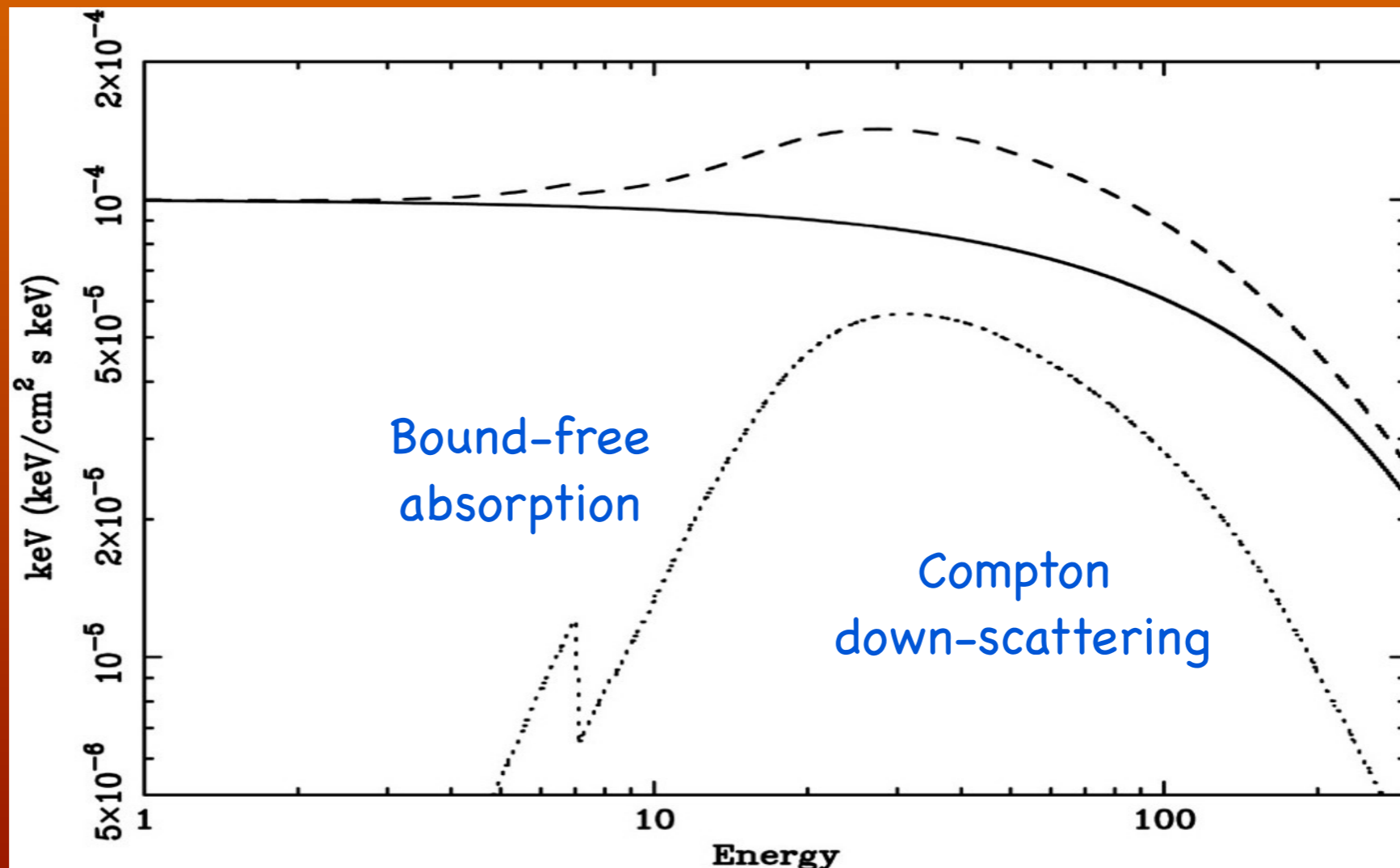- Thermal Comptonization

- Hard X-ray reprocessing

  Iron line   Compton hump
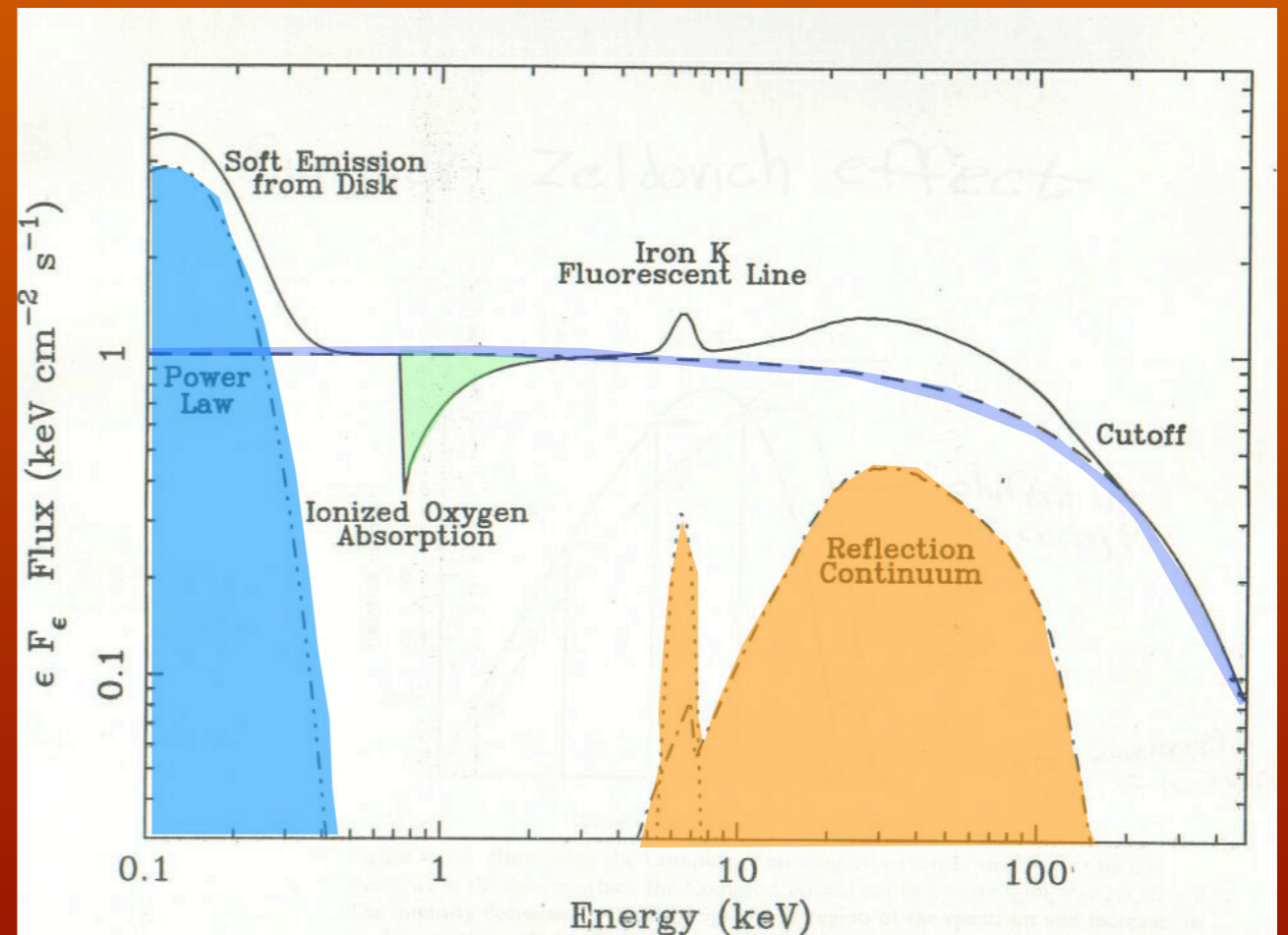
Reflection

At low energies <10 keV the high-Z ions absorb the X-rays. A major part of the opacity above 7 keV is due to Fe K-edge opacity.
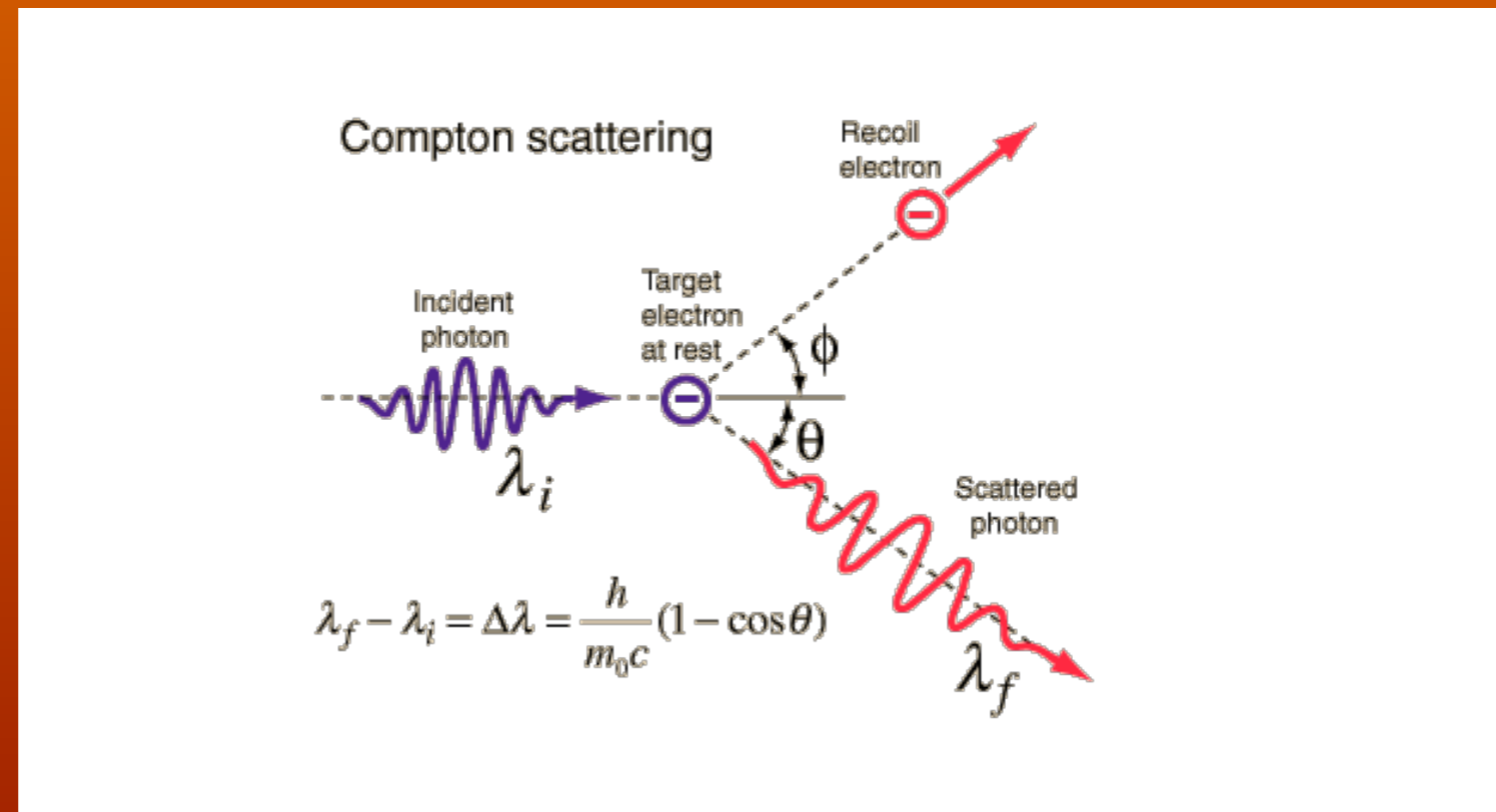
At high energies the Compton shift of the incident photons becomes important.

Photon-electron interaction

Direct Compton Scattering

In this process the photon is absorbed and immediately re-radiated by the electron into a different direction but it looses part of its initial energy. It can be thought as an heating mechanism.
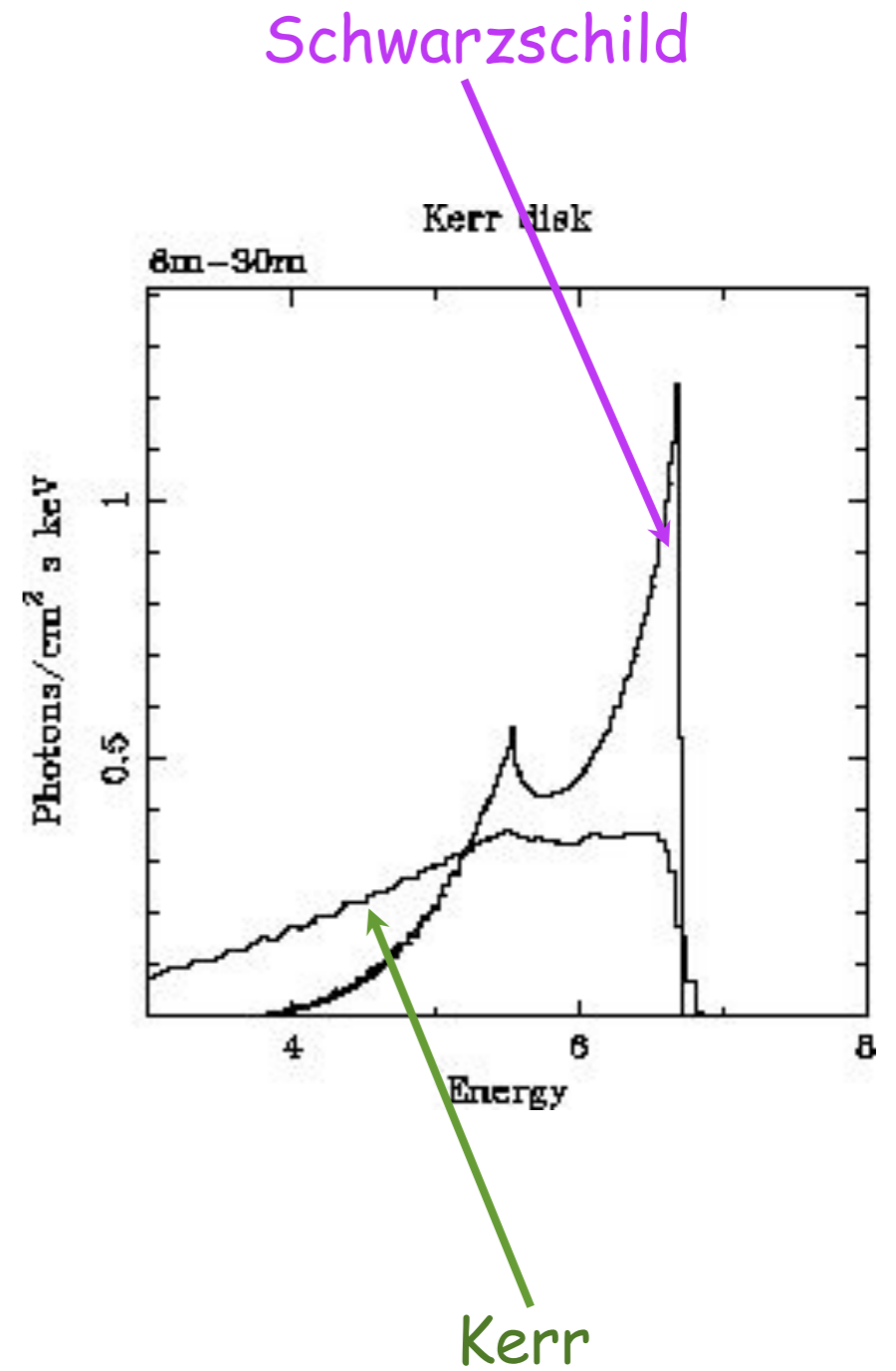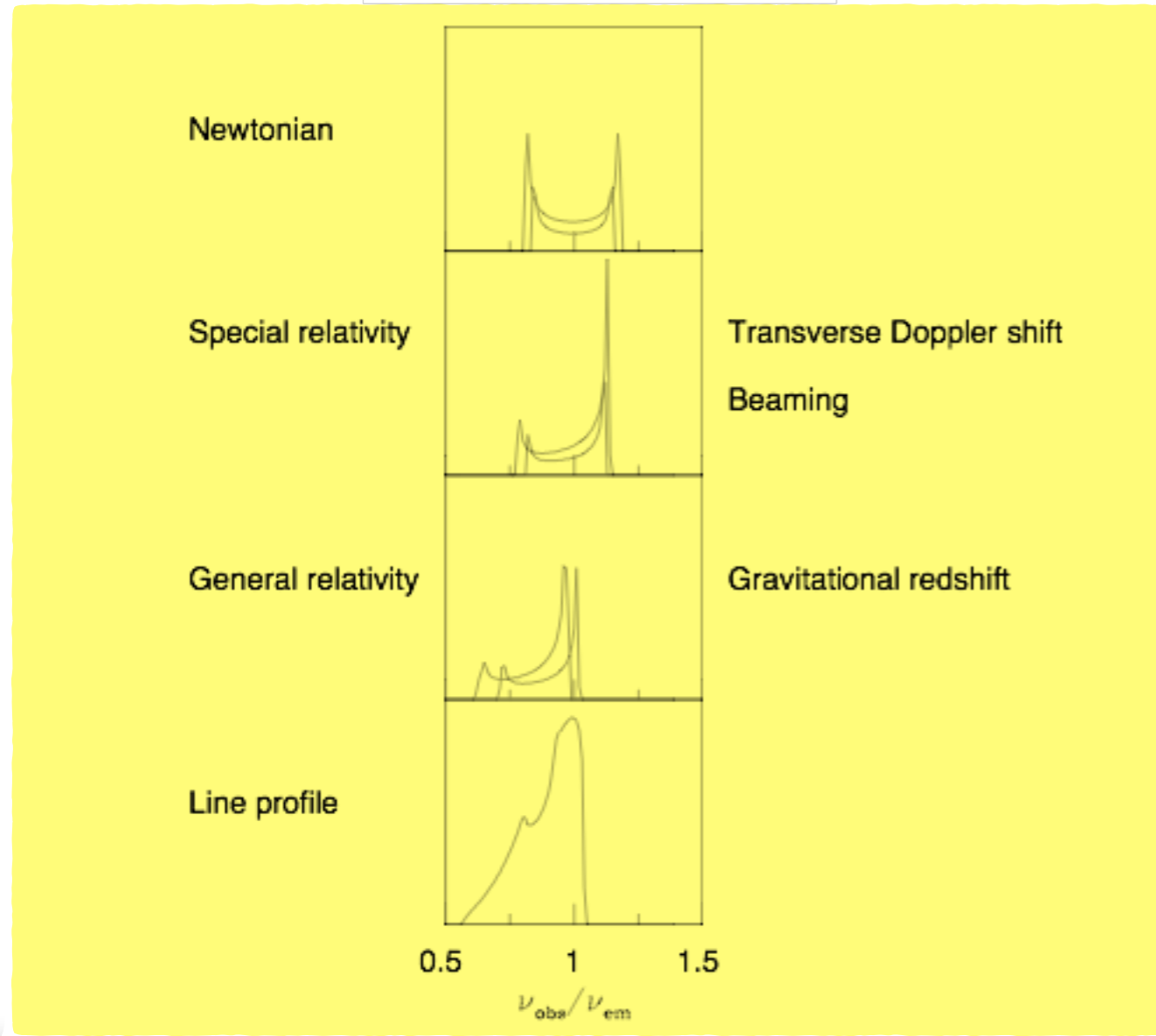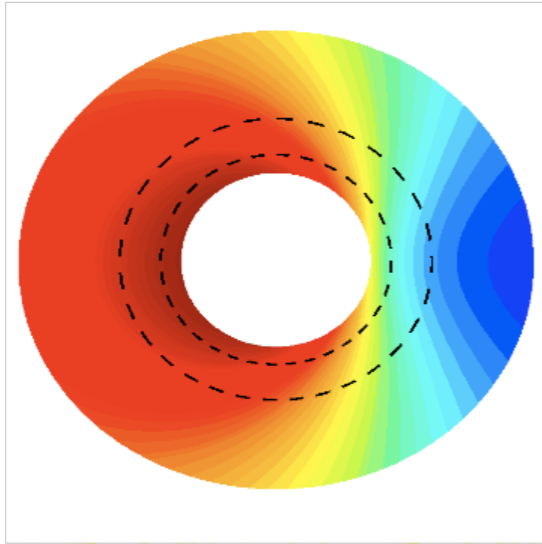
Iron Line

The fluorescent iron line is produced when one of the 2 K-shell (n=1) electrons of an iron atom (or ion) is ejected following photoelectric absorption of an X-ray. Following the photoelectric event, the resulting excited state can decay in one of two ways. An L-shell (n=2) electron can then drop into the K-shell releasing 6.4 keV of energy either as an emission line photon (34 % probability) or an Auger electron (66 % probability).

FLUORESCENCE
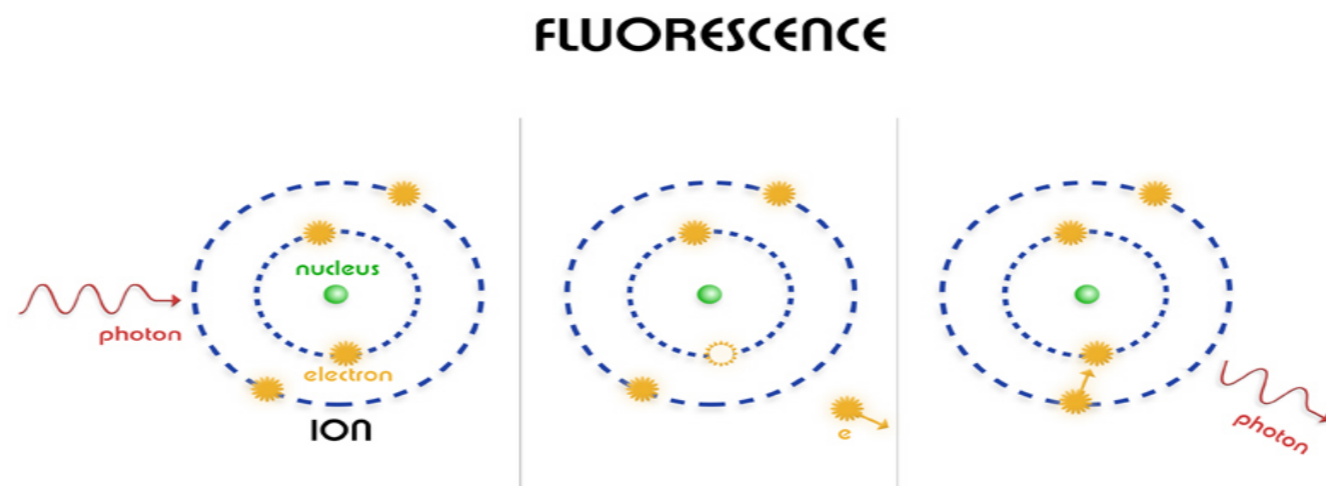
For ionized iron, the outer electrons are less effective at screening the inner K-shell from the nuclear charge and the energy of both the photoelectric threshold and the K line are increased.

BROAD LINE

Newtonian

Special relativity — Transverse Doppler shift / Beaming

General relativity — Gravitational redshift

Line profile

ν_{obs}/ν_{em}

Schwarzschild

Kerr

Kerr disk

8m–30m

Photons/cm^2 s keV

Energy

Energy Equation

$$q^+ = q^- + q^{adv}$$

Thin Accretion Disk

(Shakura & Sunyaev 1973; Novikov & Thorne 1973;...)

Most of the viscous heat energy is radiated

$$q^- \approx q^+ \gg q^{adv}$$

$$L_{rad} : \quad 0.1 \dot{M} c^2$$

Advection-Dominated Accretion Flow (ADAF)

(Ichimaru 1977; Narayan & Yi 1994, 1995; Abramowicz et al. 1995)

Most of the heat energy is retained in the gas

$$q^- \ll q^+ \approx q^{adv}$$

$$L_{rad} \ll 0.1 \dot{M} c^2$$

$$L_{adv} : \quad 0.1 \dot{M} c^2$$

$q+$ is the energy generated by viscosity per unit volume
$q-$ is the radiative cooling per unit volume
q_{adv} represents the advective transport of energy

ADAF

In this solution the accreting gas has a very low density and is unable to cool efficiently. The viscous energy is stored in the gas as thermal energy instead of being radiated and is advected onto the BH. Ions and electrons are thermally decoupled.

• <u>Very Hot:</u> $T_i \sim 10^{12}$K (R_S/R), $T_e \sim 10^{9-11}$K (since ADAF loses very little heat).

• <u>Geometrically thick:</u> $H \sim R$ (most of the viscosity generated energy is stored in the gas as internal energy rather than being radiated, the gas puffes up

• <u>Optically thin</u> (because of low density)
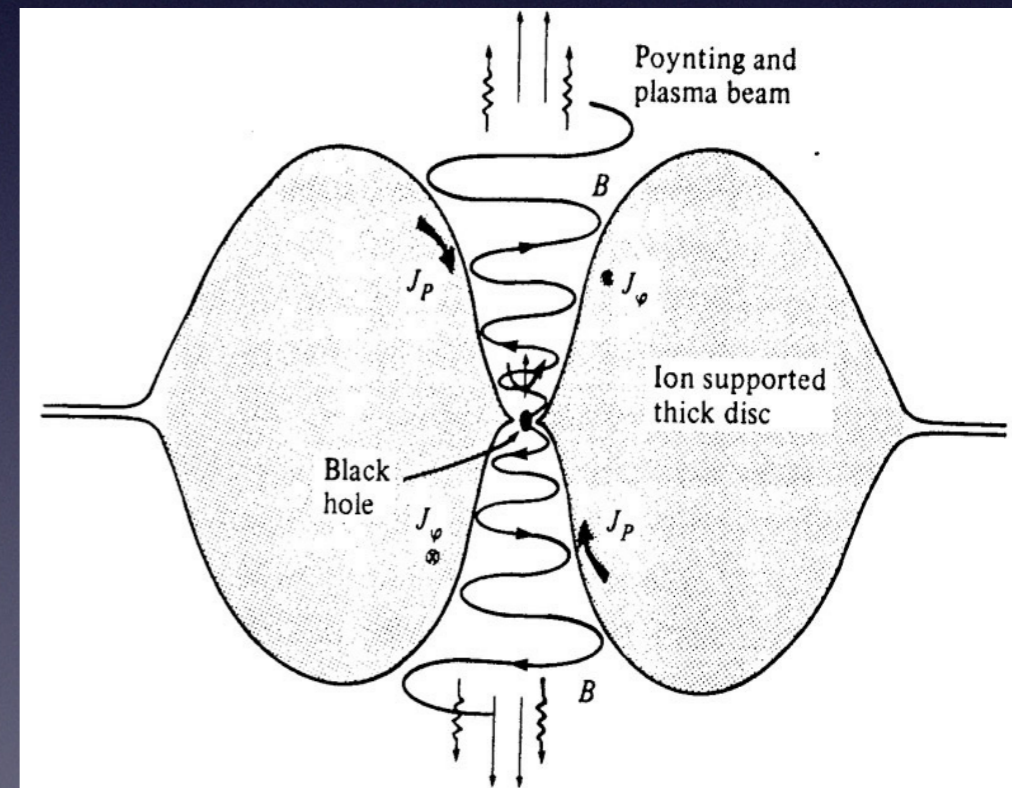
ADAF

The ADAF solution exists only for $\dfrac{\dot{M}}{\dot{M}_E} \leq 0.05 - 0.1$
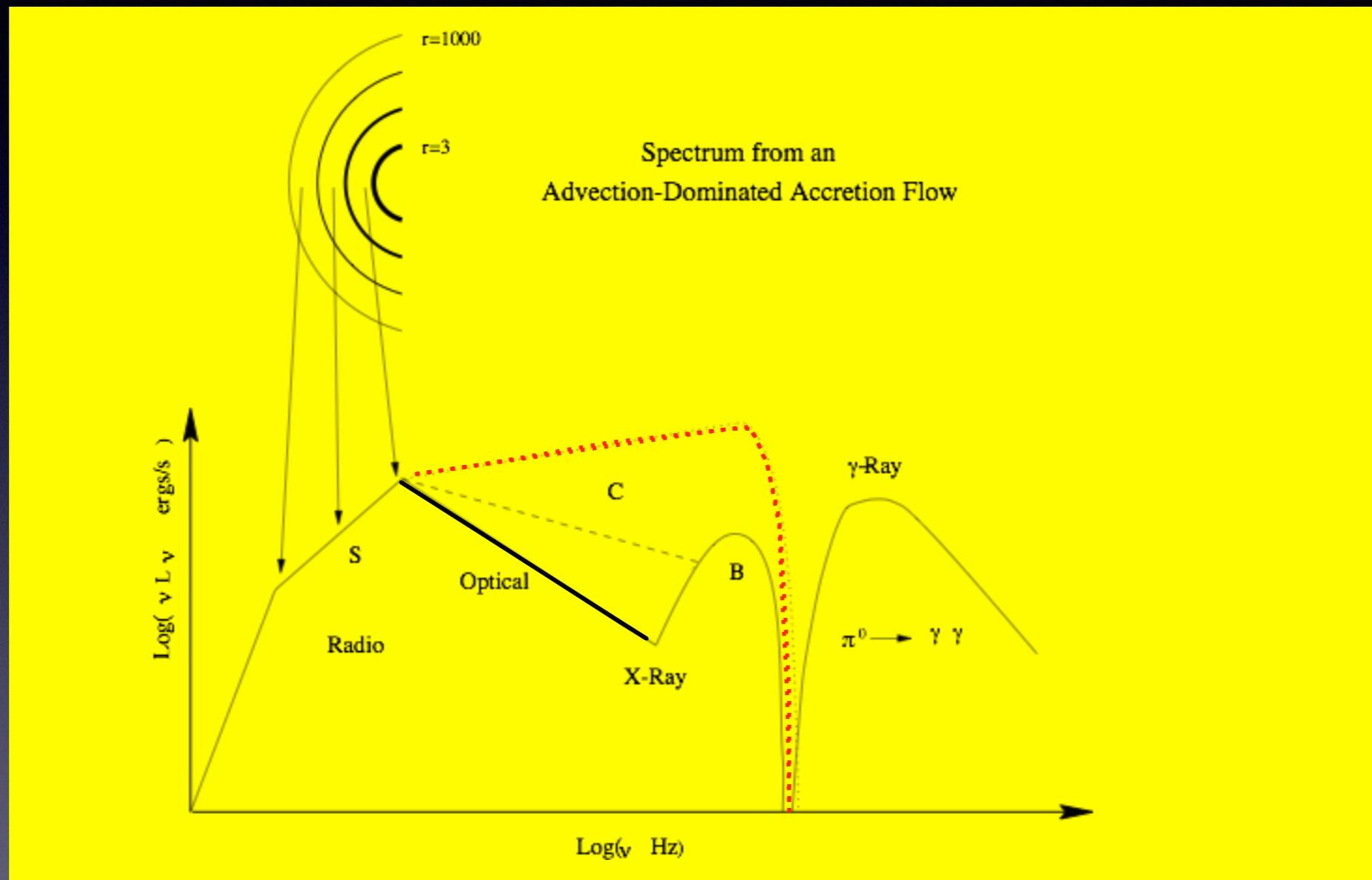
Schematic spectrum of an ADAF around a black hole. S, C, and B refer to electron emission by synchrotron radiation, inverse Compton scattering, and bremsstrahlung, respectively. The solid line corresponds to a low accretion, the dashed line to an intermediate accretion, and the dotted line to the highest (possible) accretion.
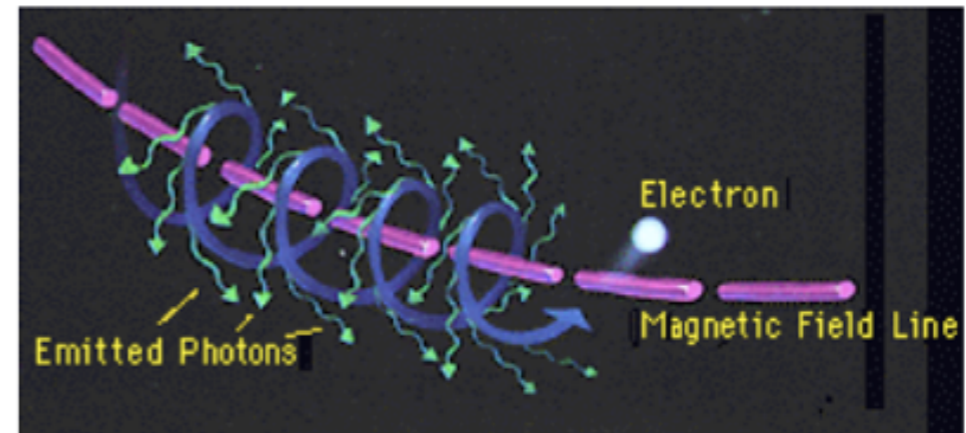
Jets, Lobes

NON-THERMAL PROCESSES

Synchrotron Radiation

Synchrotron radiation is due to the movement of an electron charge in a magnetic field. As a particle gyrates around a magnetic field, it will emit radiation at a frequency proportional to the strength of the magnetic field and its velocity.

Synchrotron radiation is highly polarized and is seen at all wavelengths. At relativistic speeds, the radiation can also be beamed. It is very common in radio spectrum, but can be seen in x-rays. It is usually fit as a power law. For full details, see the review by Ginzburg & Syrovatskii (1969)

The synchrotron radiation of a power law distribution of electron energies

Synchrotron

$$N(\gamma_e) = K\gamma_e^{-p}, \quad \gamma_{min} < \gamma_e < \gamma_{max}, \, p = 1 + 2\alpha$$

$$\epsilon_{sin}(\nu) \propto KB^{\alpha+1}\nu^{-\alpha} \quad \text{erg cm}^{-3}\text{ s}^{-1}\text{ sr}^{-1}$$

Inverse Compton scattering

When the electron is not at rest, but has an energy greater that the typical photon energy, there can be a transfer of energy from the electron to the photon. This process is called Inverse Compton to distinguish it from the direct Compton scattering, in which the electron is at rest, and it is the photon to give part of its energy to the electron.
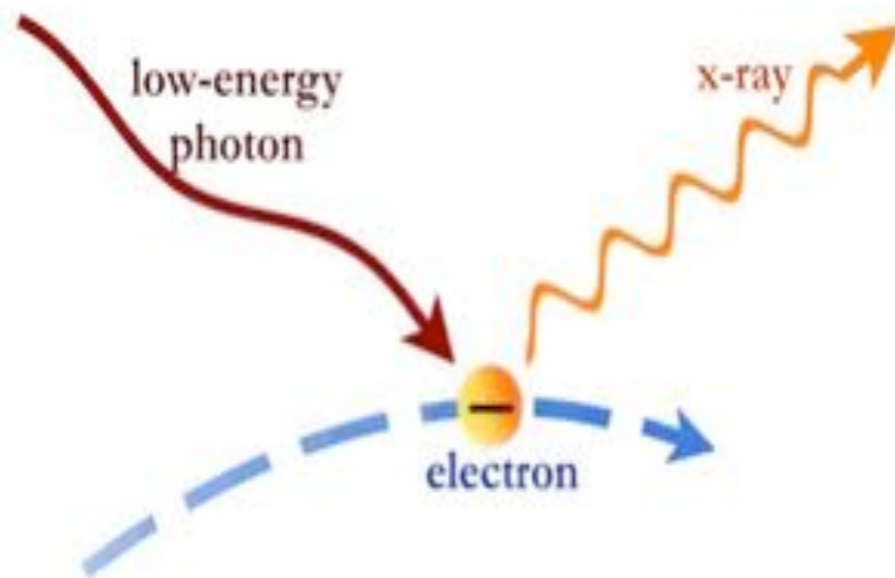
$$< \nu > = \frac{4}{3} \gamma^2 \nu$$

Inverse Compton Radiation

The general result that the frequency of the scattered photons is $\nu \approx \gamma^2 \nu_0$ is of profound importance in high energy astrophysics. We know that there are electrons with Lorentz factors $\gamma \sim 100 - 1000$ in various types of astronomical source and consequently they scatter any low energy photons to very much higher energies. Consider the scattering of radio, infrared and optical photons scattered by electrons with $\gamma = 1000$.

Waveband	Frequency (Hz) ν_0	Scattered Frequency (Hz) and Waveband
Radio	10^9	$10^{15} = $ UV
Far-infrared	3×10^{12}	$3 \times 10^{18} = $ X-rays
Optical	4×10^{14}	$4 \times 10^{21} \equiv 1.6 \text{MeV} = \gamma\text{-rays}$

Thus, inverse Compton scattering is a means of creating very high energy photons indeed. It also becomes an inevitable drain of energy for high energy electrons whenever they pass through a region in which there is a large energy density of photons.

Inverse Compton

For a power law distribution of electrons:

$$N(\gamma_e) = K\gamma_e^{-p}, \quad \gamma_{min} < \gamma_e < \gamma_{max}, p = 1 + 2\alpha$$

Inverse Compton

$$\epsilon_c(\nu_c) \propto K\nu_c^{-\alpha} \int \frac{Ur(\nu)\nu^{\alpha}}{\nu} d\nu \quad \text{erg cm}^{-3}\text{ s}^{-1}\text{ sr}^{-1}$$

U_r is the radiation energy density

$$U_r = \int n(\epsilon)\epsilon d\epsilon$$

- Synchrotron photons in the jet
- Environment photons from Accretion Flow, BLR, NLR, Torus
- Cosmic Microwave Background (CMB) photons

6. Journey along the jet

pc-scale jet

kpc-scale jet

lobes
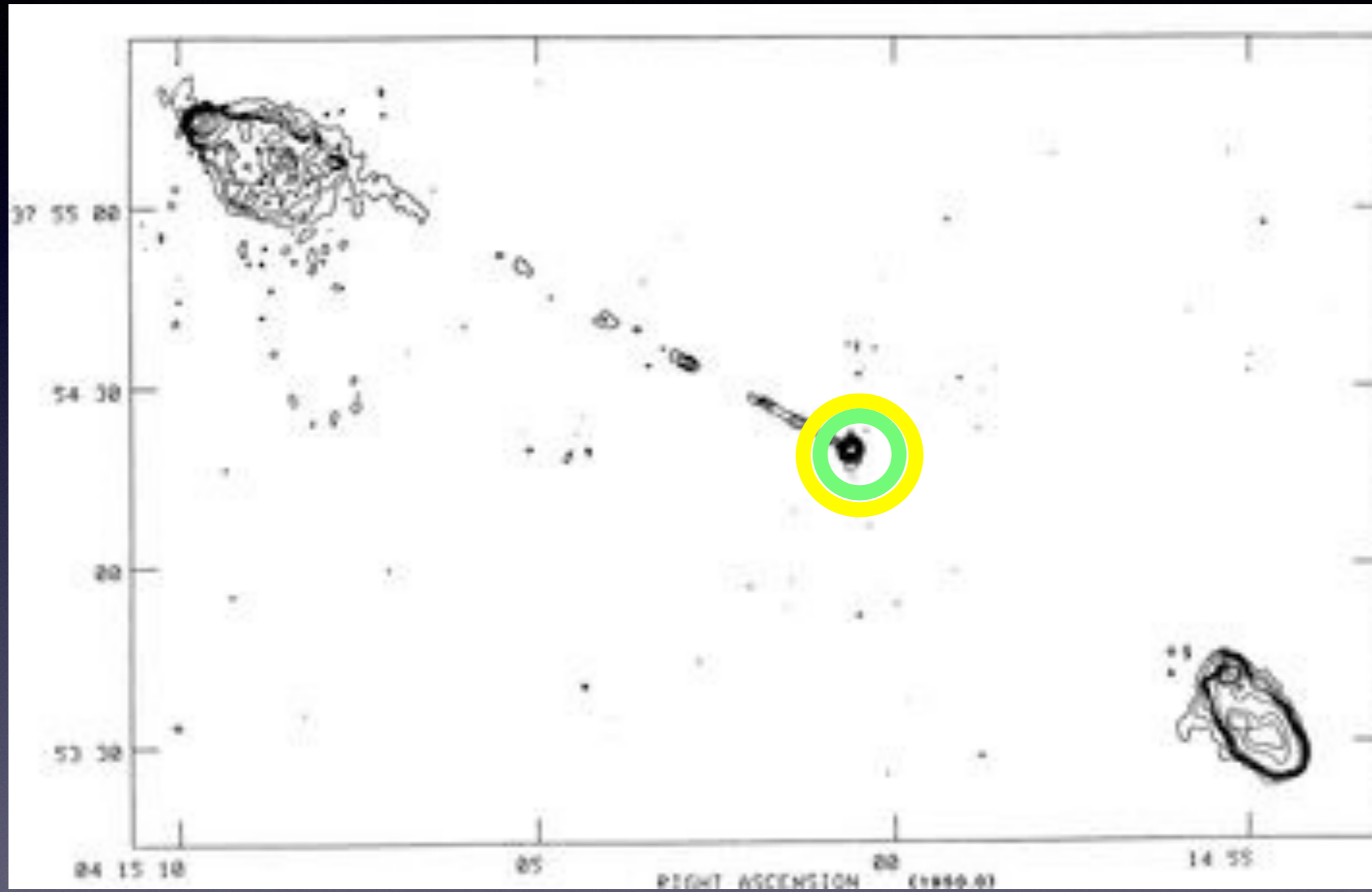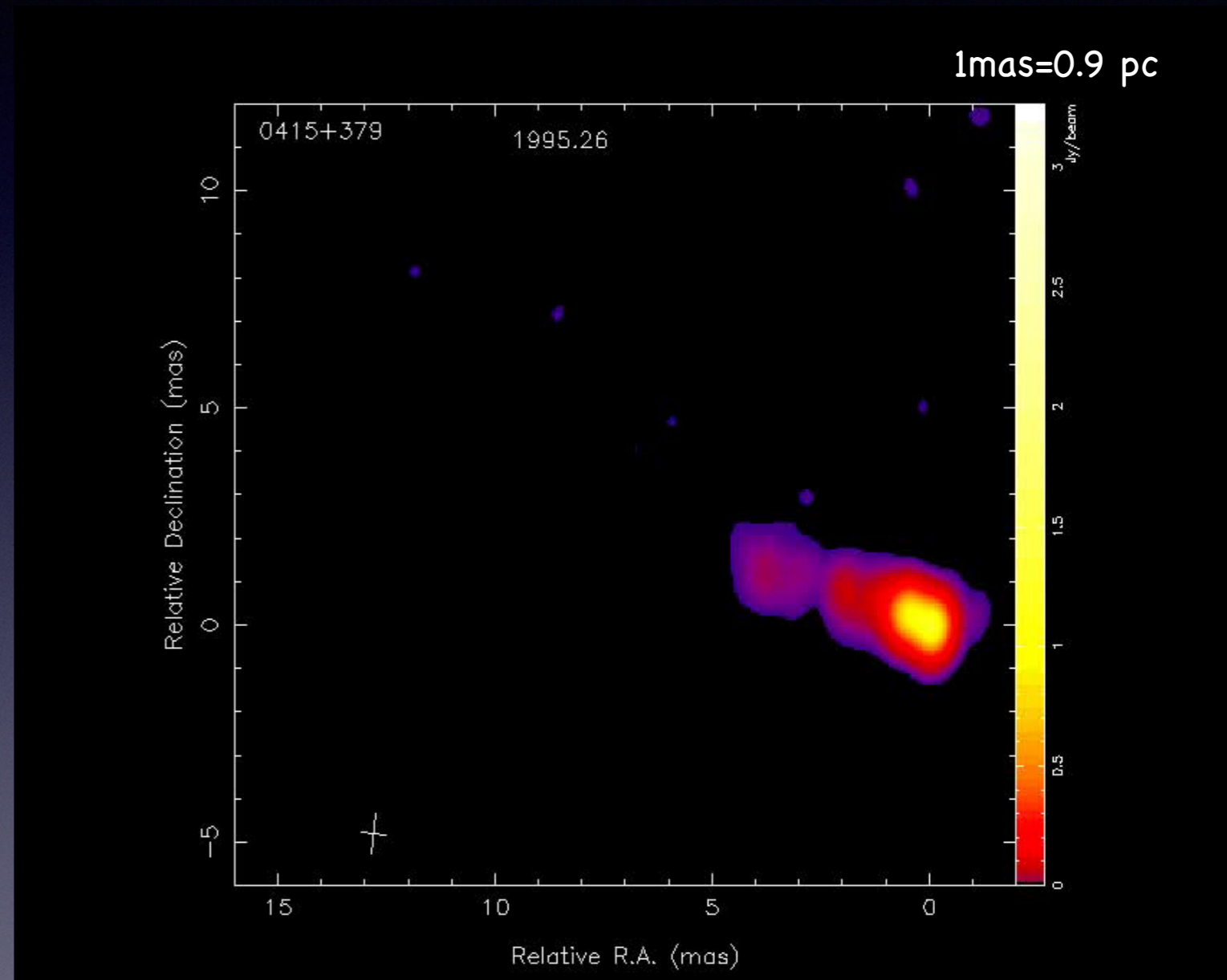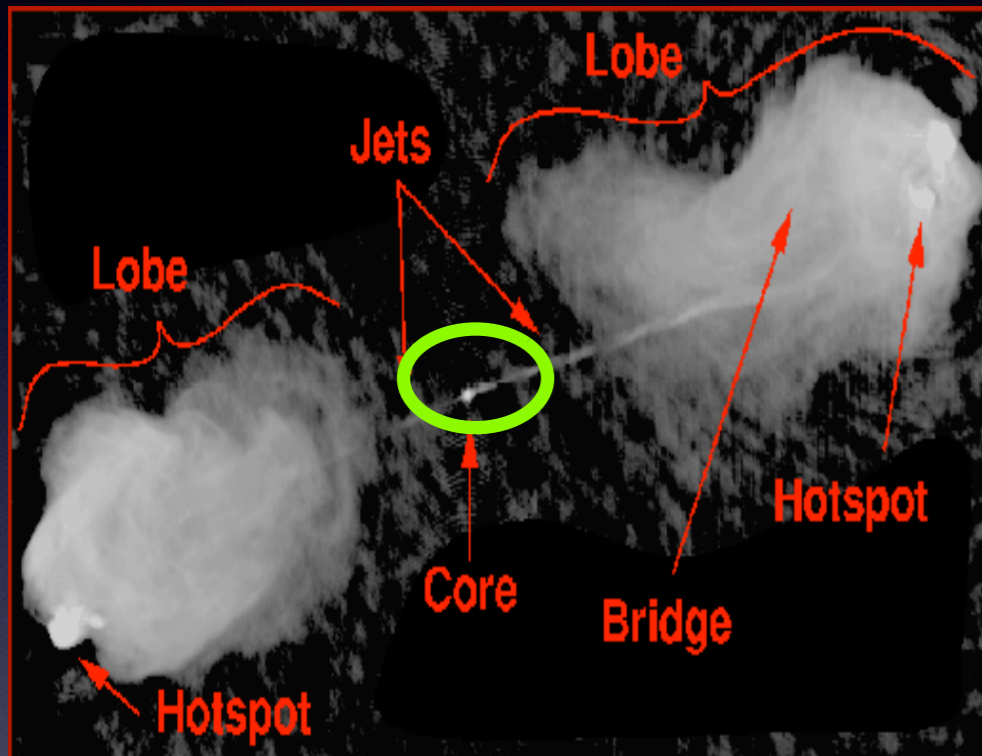
3C 279 Spectral Energy Distribution
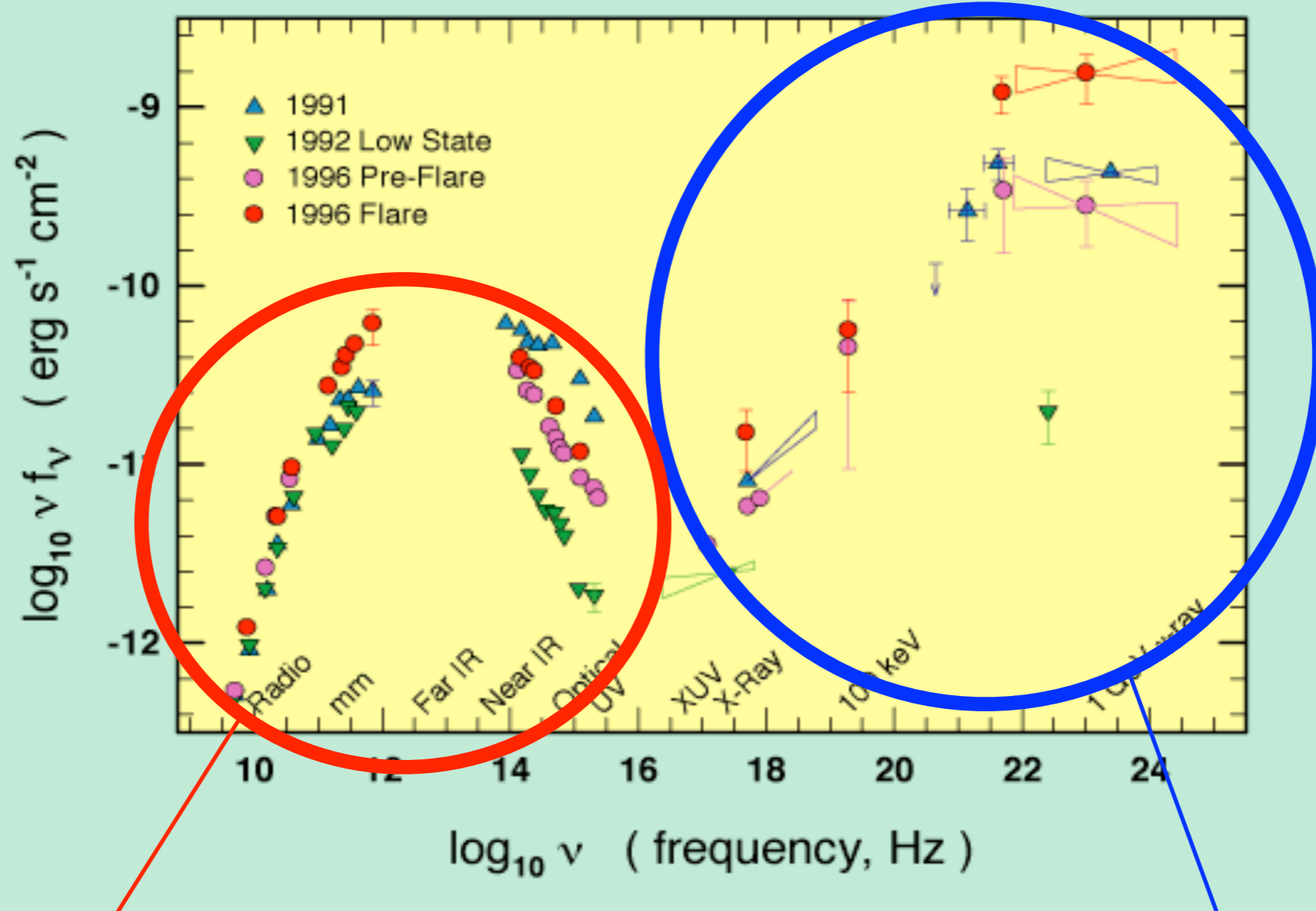
Synchrotron

Inverse Compton

Synchrotron Self–Compton

Consider a population of relativistic electrons in a magnetized region. They will produce synchrotron radiation, and therefore they will fill the region with photons. These synchrotron photons will have some probability to interact again with the electrons, by the Inverse Compton process. Since the electron "work twice" (first making synchrotron radiation, then scattering it at higher energies) this particular kind of process is called synchrotron self–Compton, or SSC for short.

External Compton

The population of relativistic electrons in a magnetized region can also interact with photons externa to the jet produced in the accretion disk, in the broad/narrow line regions in the torus. This particular kind of process is called External Compton, or EC for short.
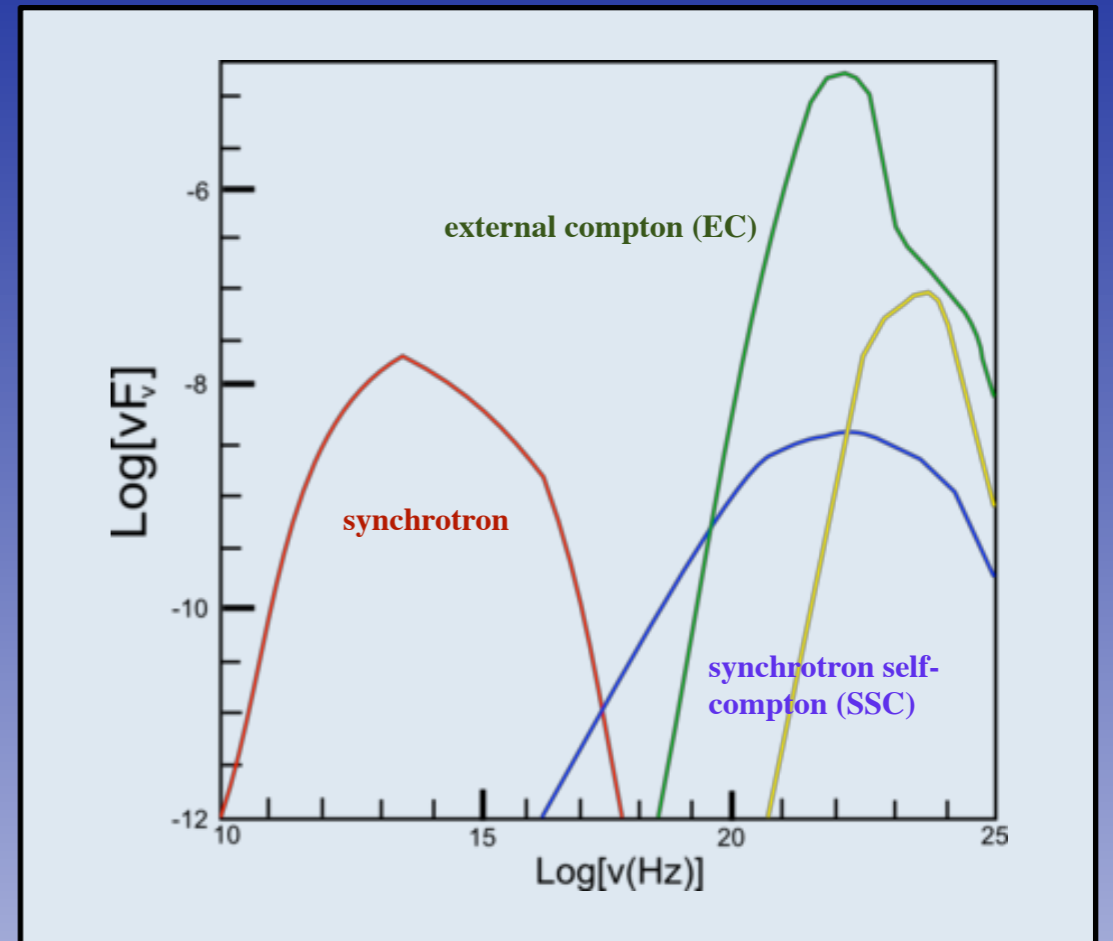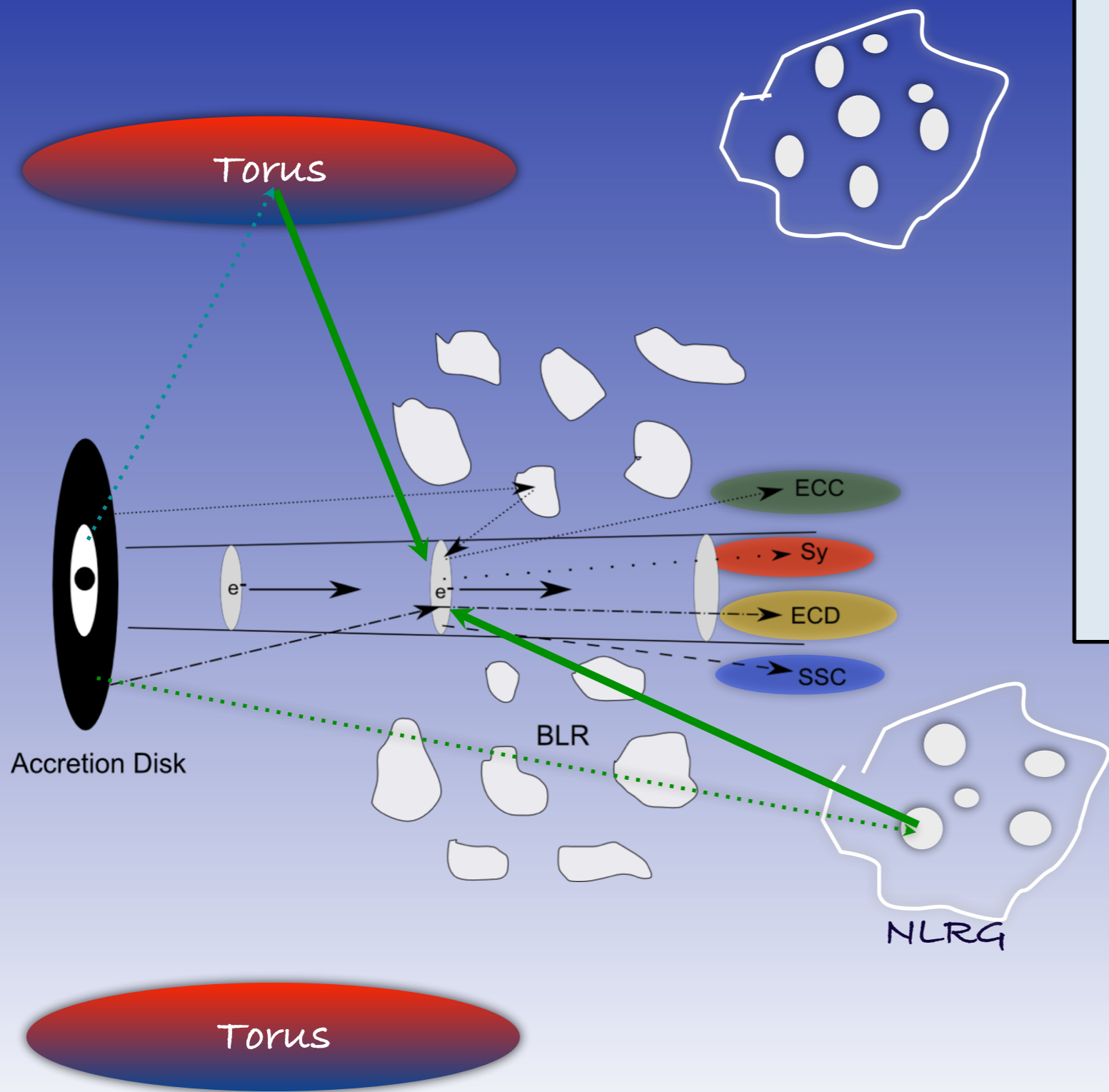
Competition between jet and disk
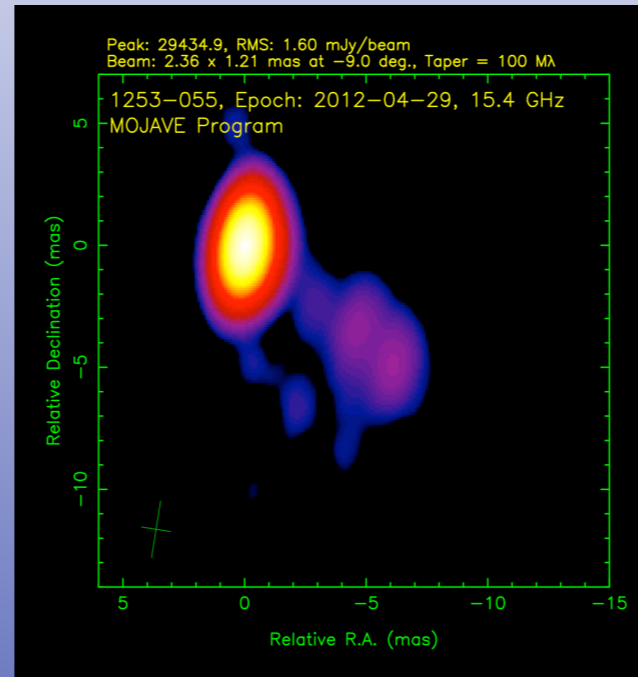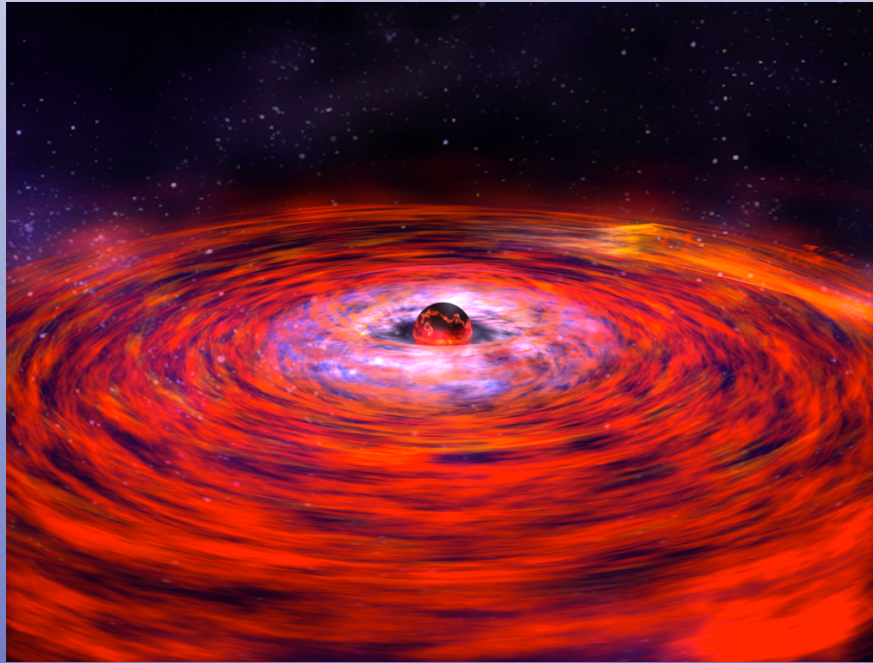
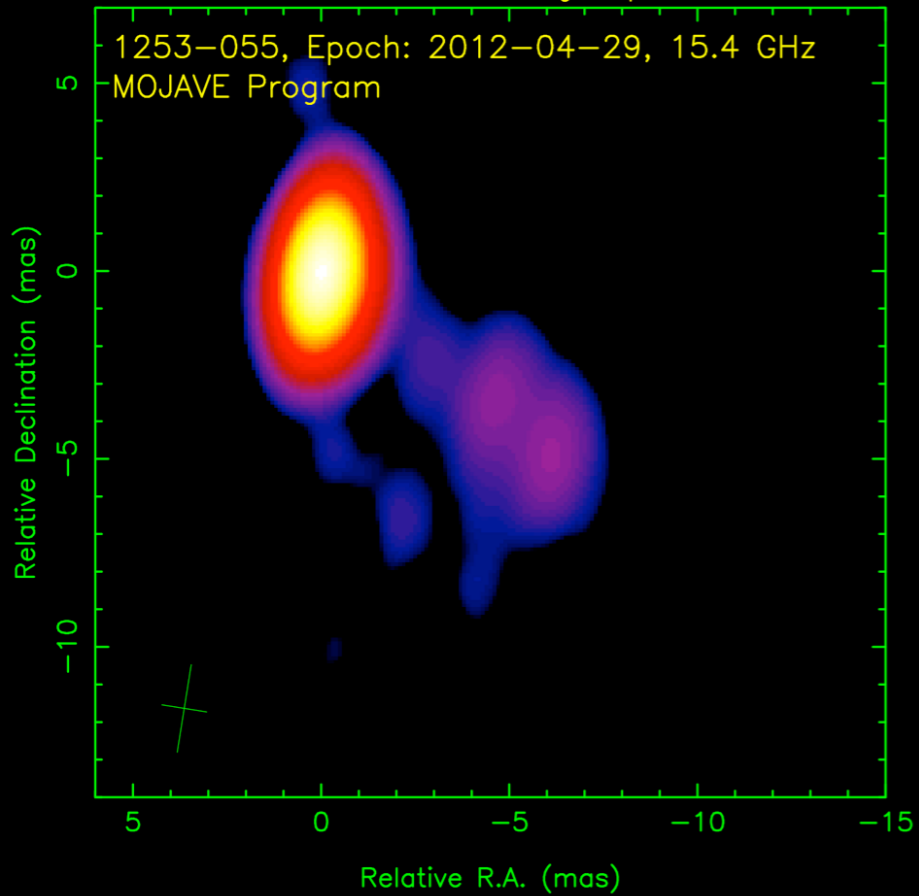**X-ray Spectra:Accretion Disk and pc-scale Jet emission are in competion:**

Angle of sight = 0°   ==>   Jet radiation dominates
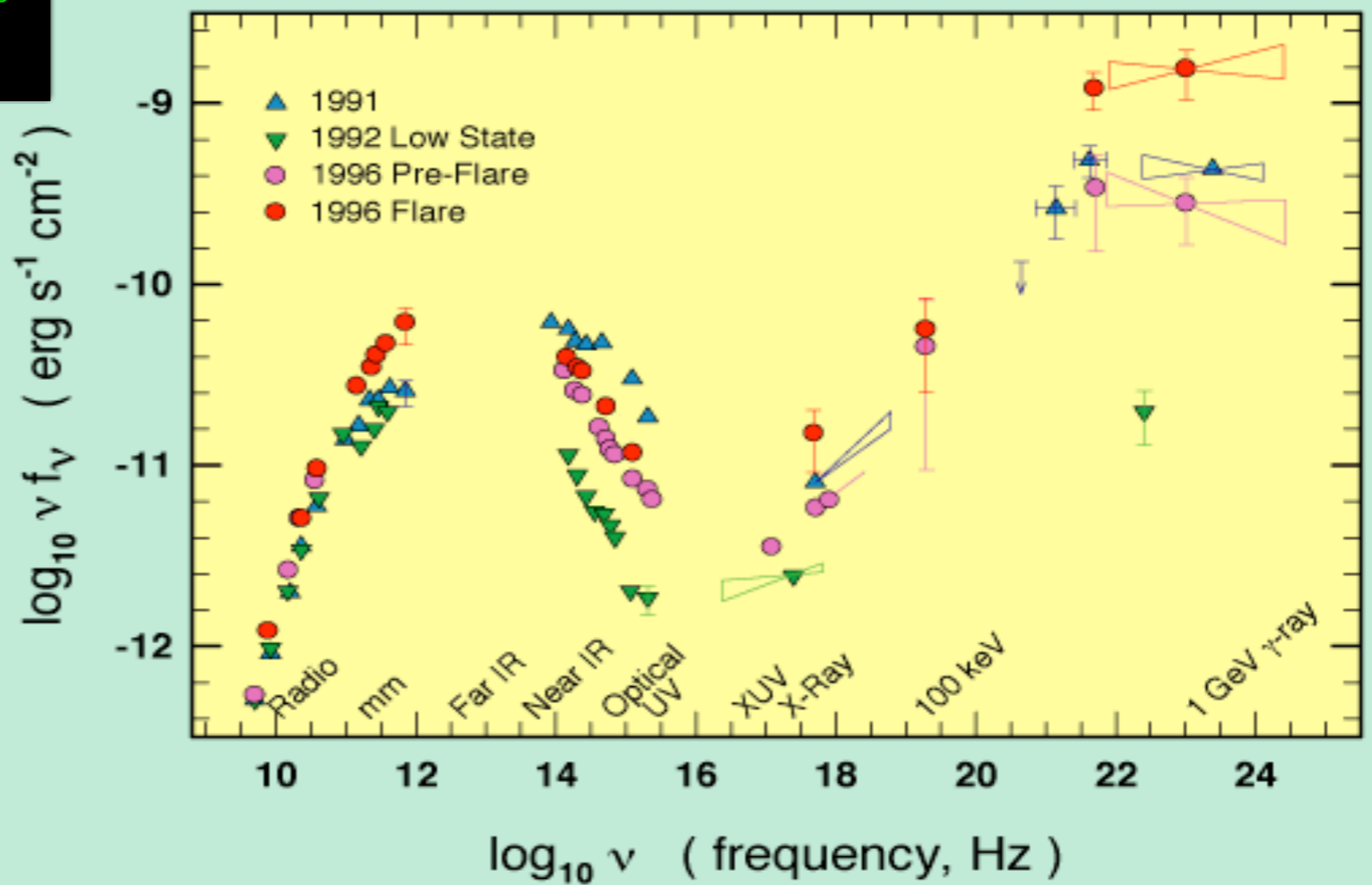
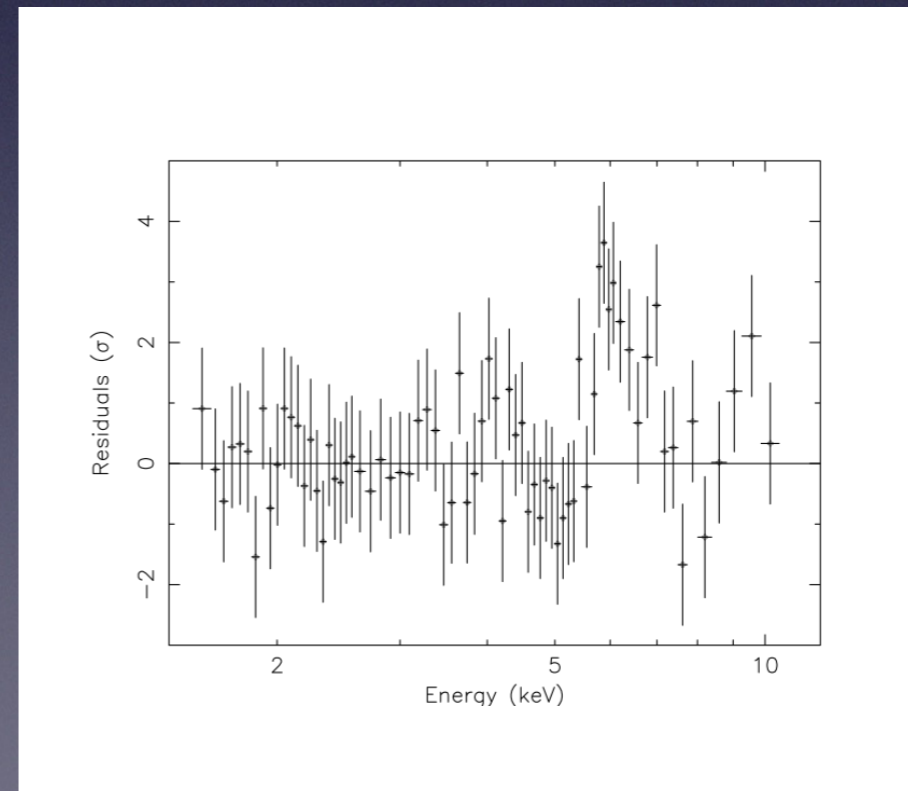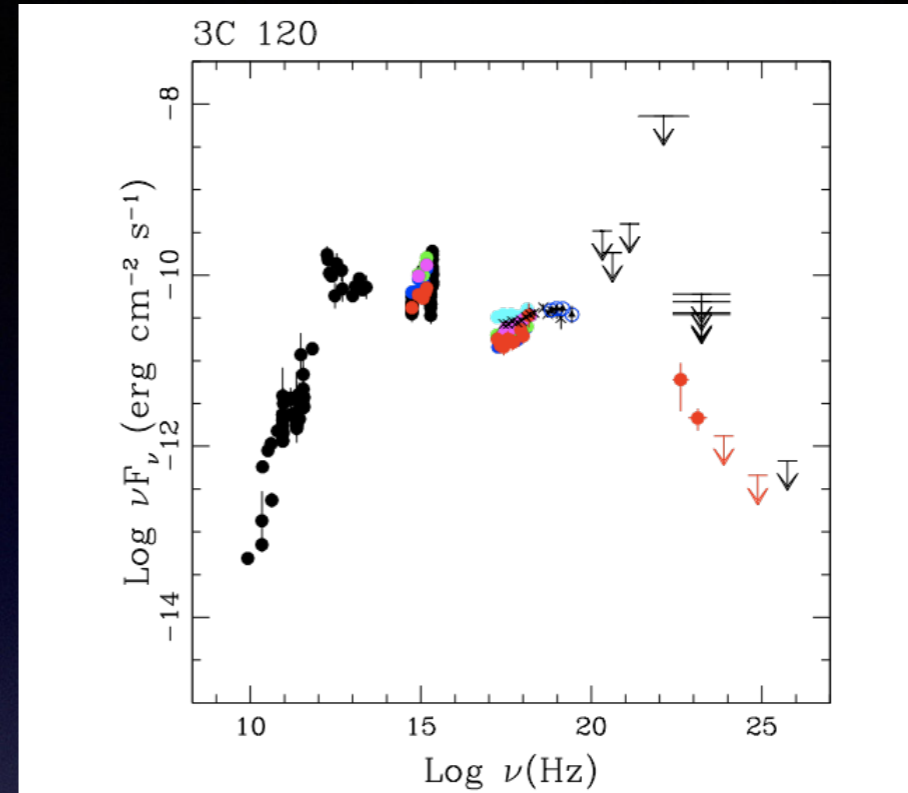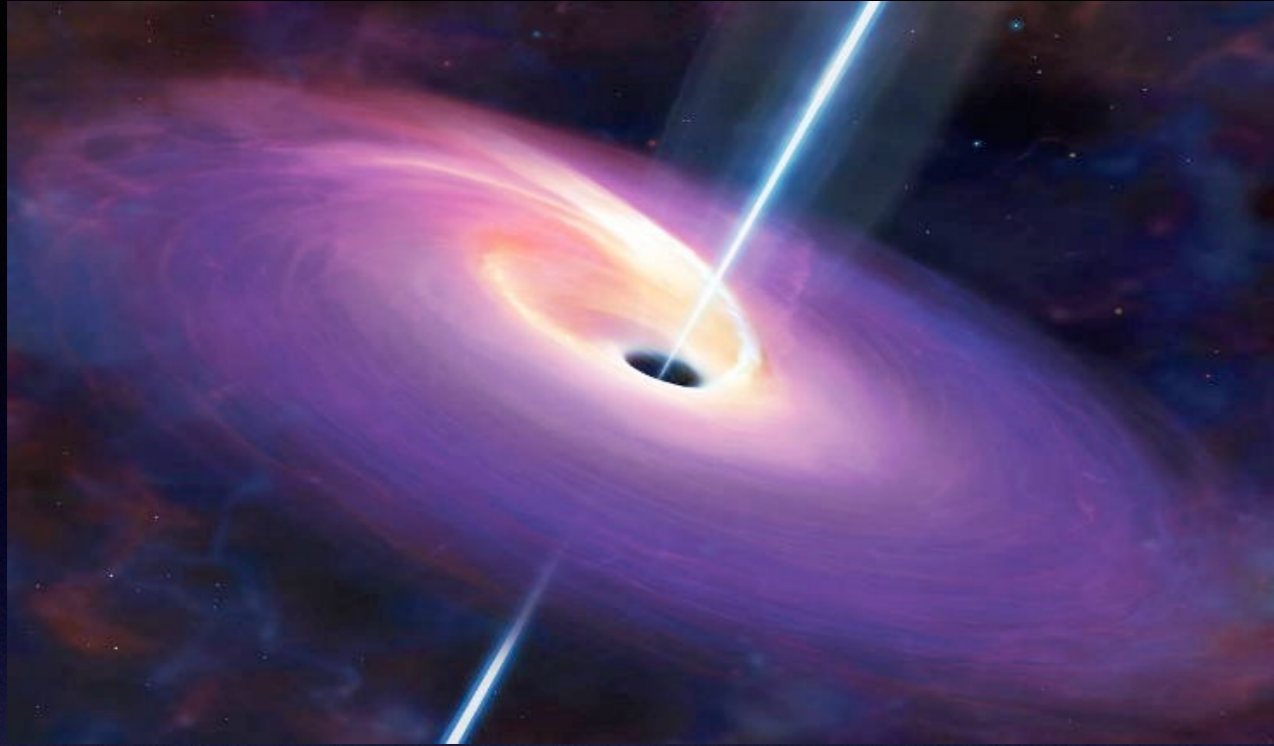**Angle of sight = 90°   ==>   Accretion disk dominates**
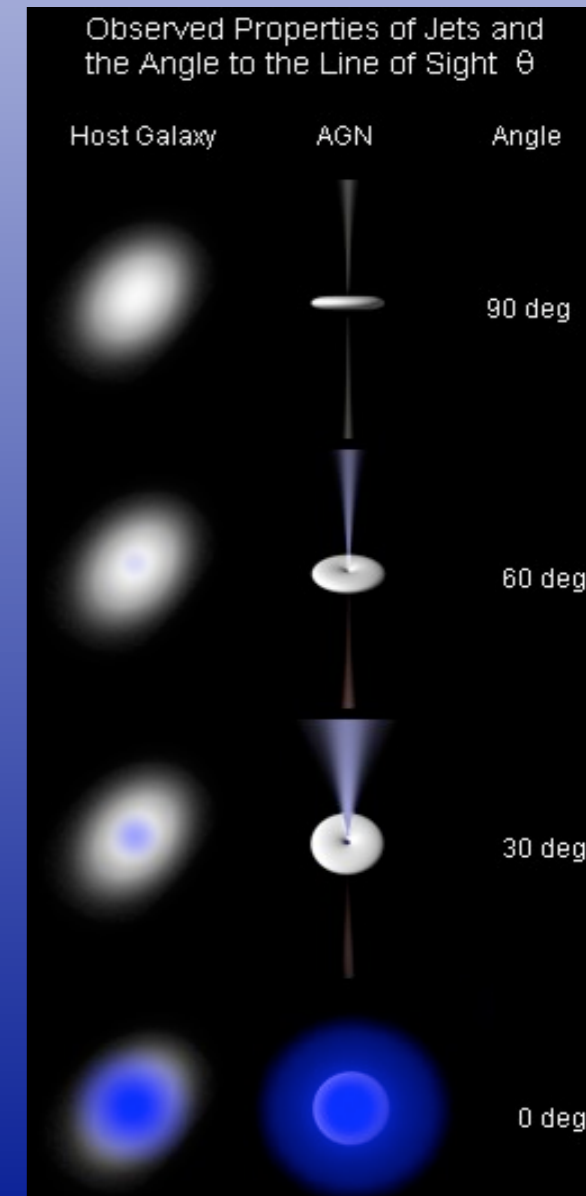
Peak: 29434.9, RMS: 1.60 mJy/beam
Beam: 2.36 x 1.21 mas at −9.0 deg., Taper = 100 Mλ
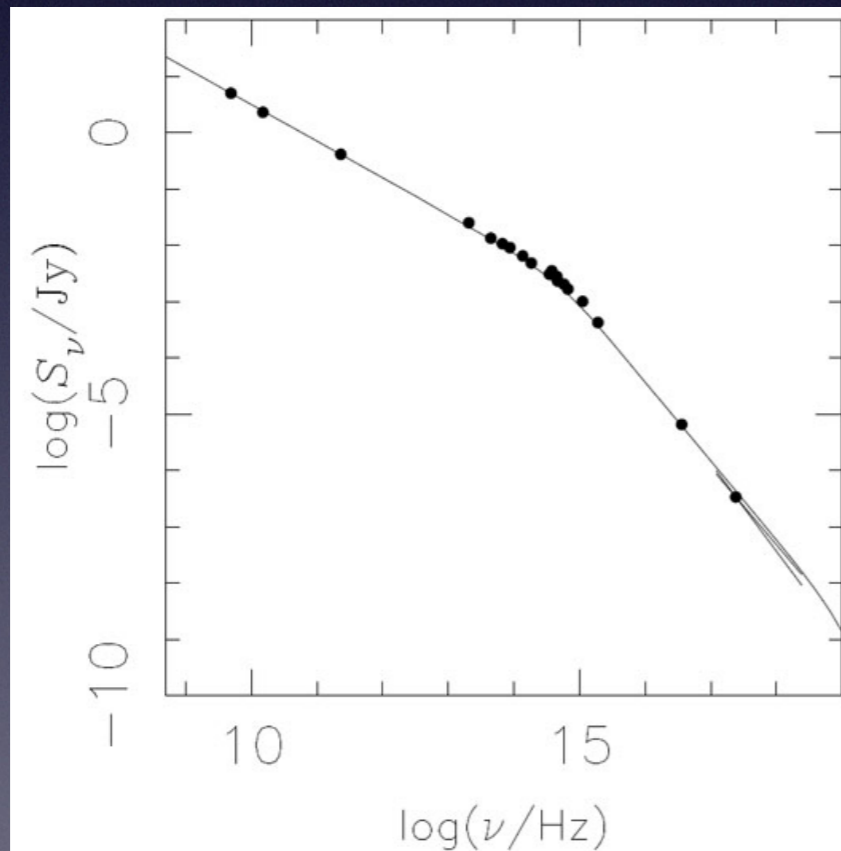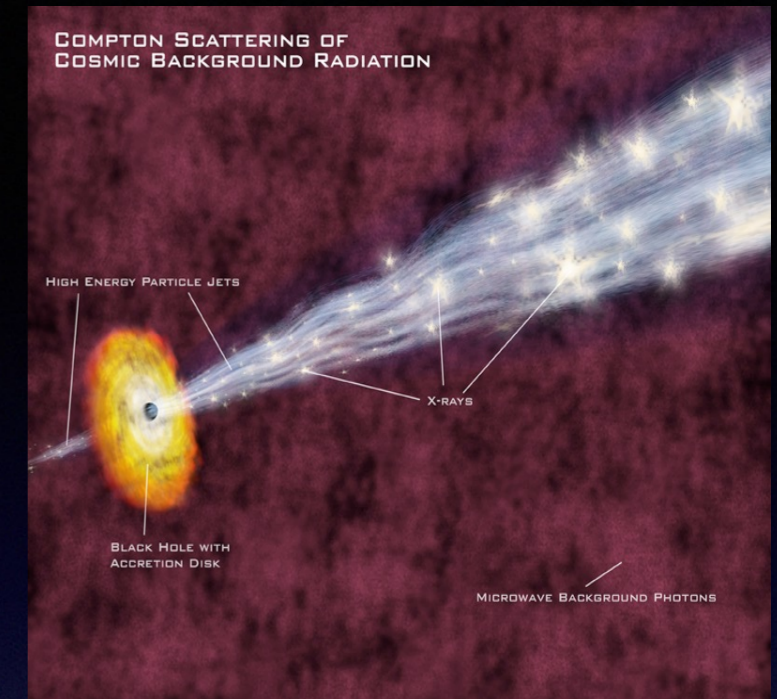
1253−055, Epoch: 2012−04−29, 15.4 GHz
MOJAVE Program

3C 279 Spectral Energy Distribution

- ▲ 1991
- ▼ 1992 Low State
- ⬤ 1996 Pre-Flare
- ⬤ 1996 Flare

3C 120

kpc-scale Jet

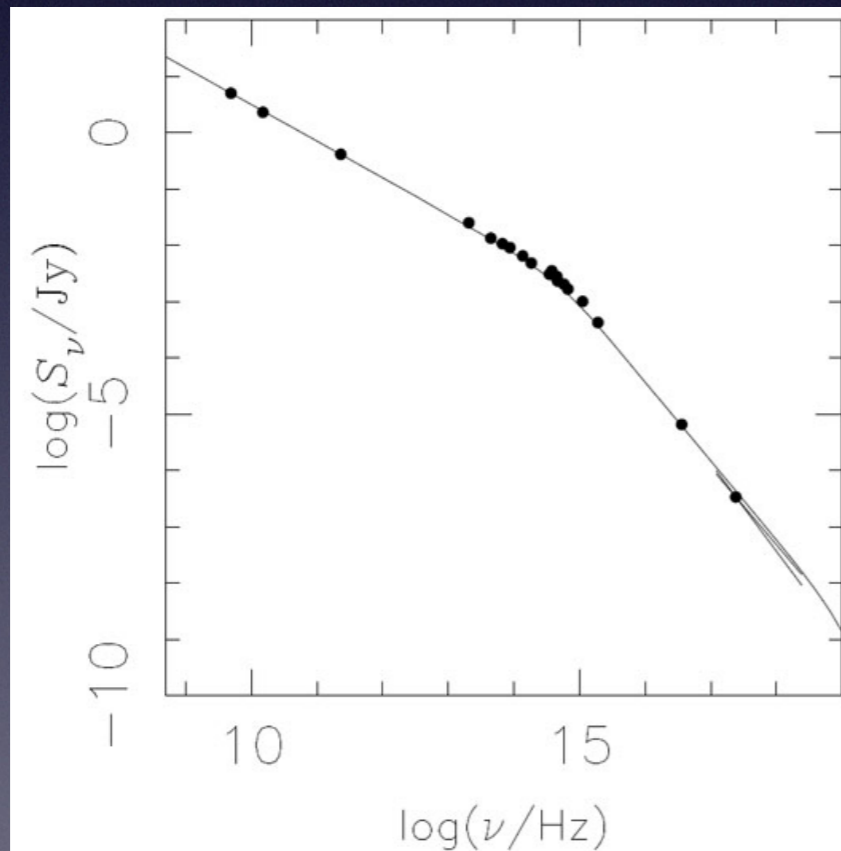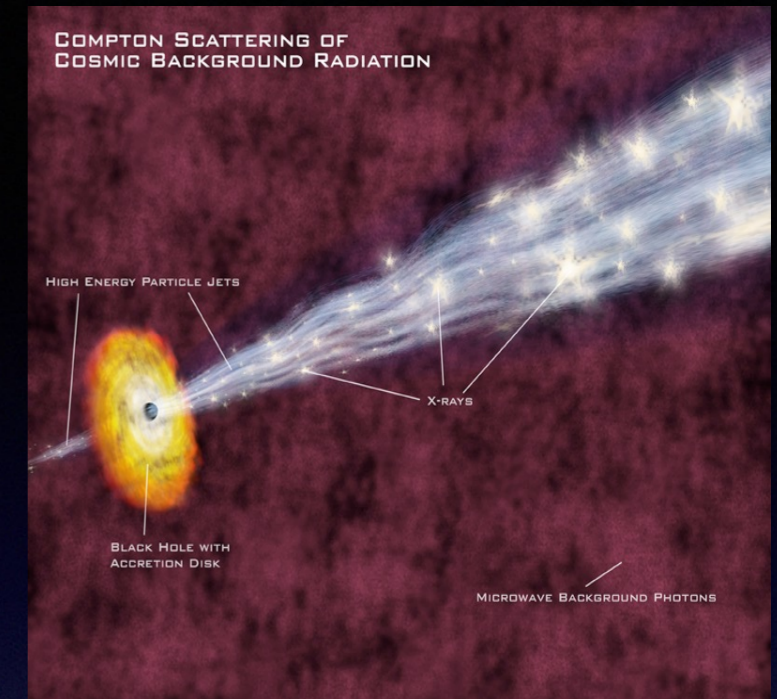COMPTON SCATTERING OF COSMIC BACKGROUND RADIATION

FRI-M87

For low-luminosity (FRI) radio sources, there is strong support for the synchrotron process as the dominant emission mechanism for the X-rays, optical, and radio emissions

Synchrotron process

kpc-scale Jet

COMPTON SCATTERING OF COSMIC BACKGROUND RADIATION

HIGH ENERGY PARTICLE JETS

X-RAYS

BLACK HOLE WITH ACCRETION DISK

MICROWAVE BACKGROUND PHOTONS

FRI-M87

For low-luminosity (FRI) radio sources, there is strong support for the synchrotron process as the dominant emission mechanism for the X-rays, optical, and radio emissions

Synchrotron process

FRII sources require multi-zone synchrotron models, or synchrotron and IC models (seed photons: CMB).
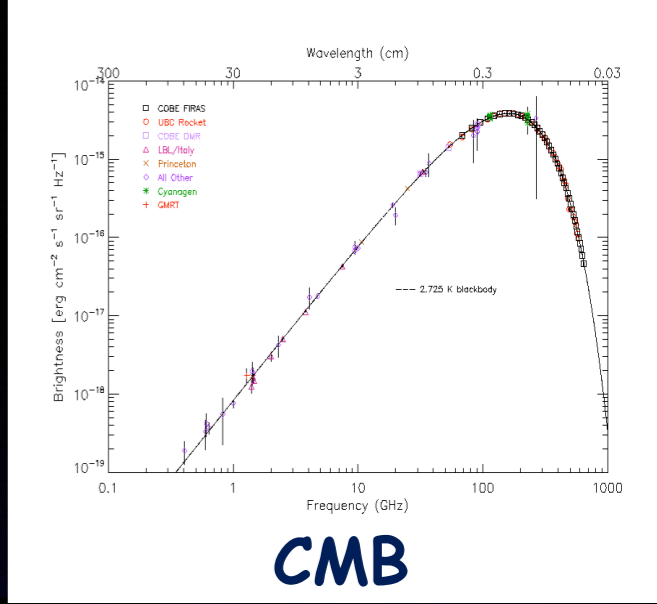The most popular model postulates very fast jets with high bulk Lorentz factors Γ.

FRII-PKS0637-75
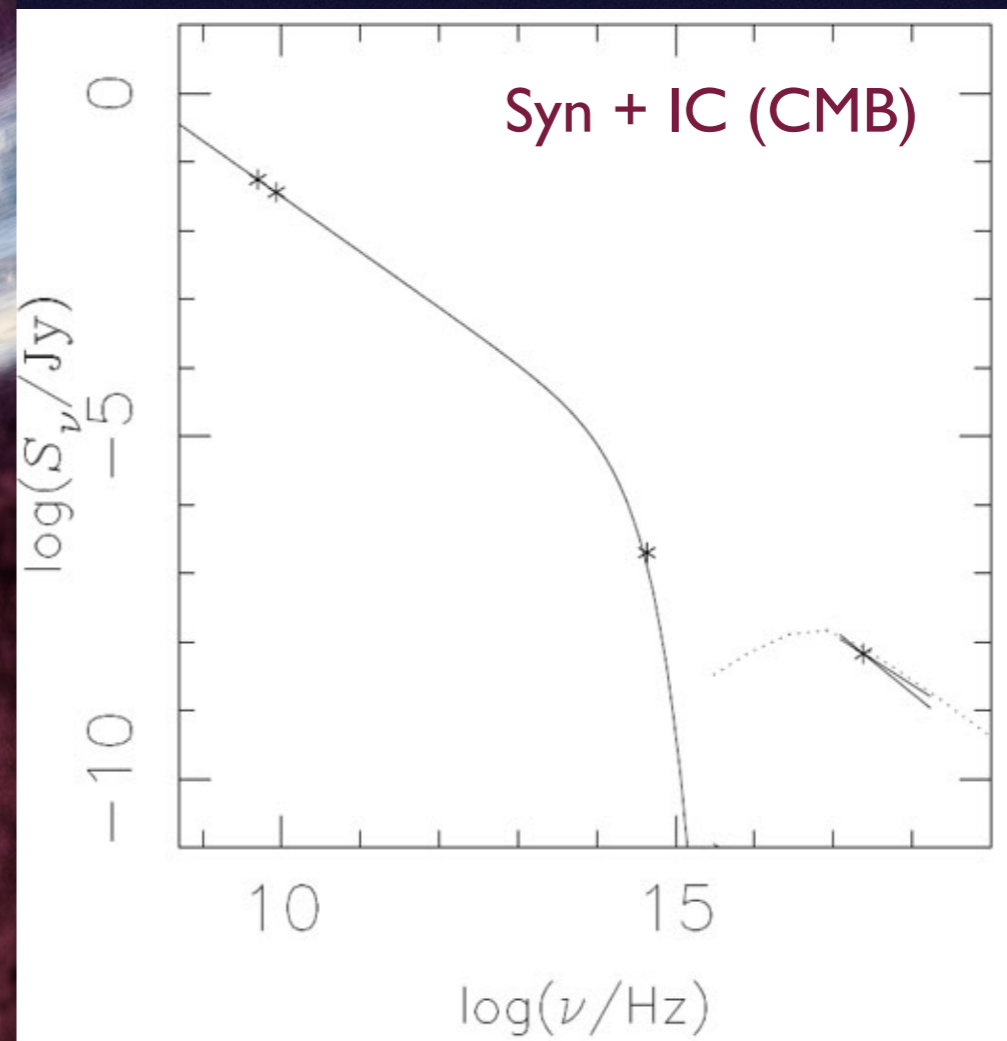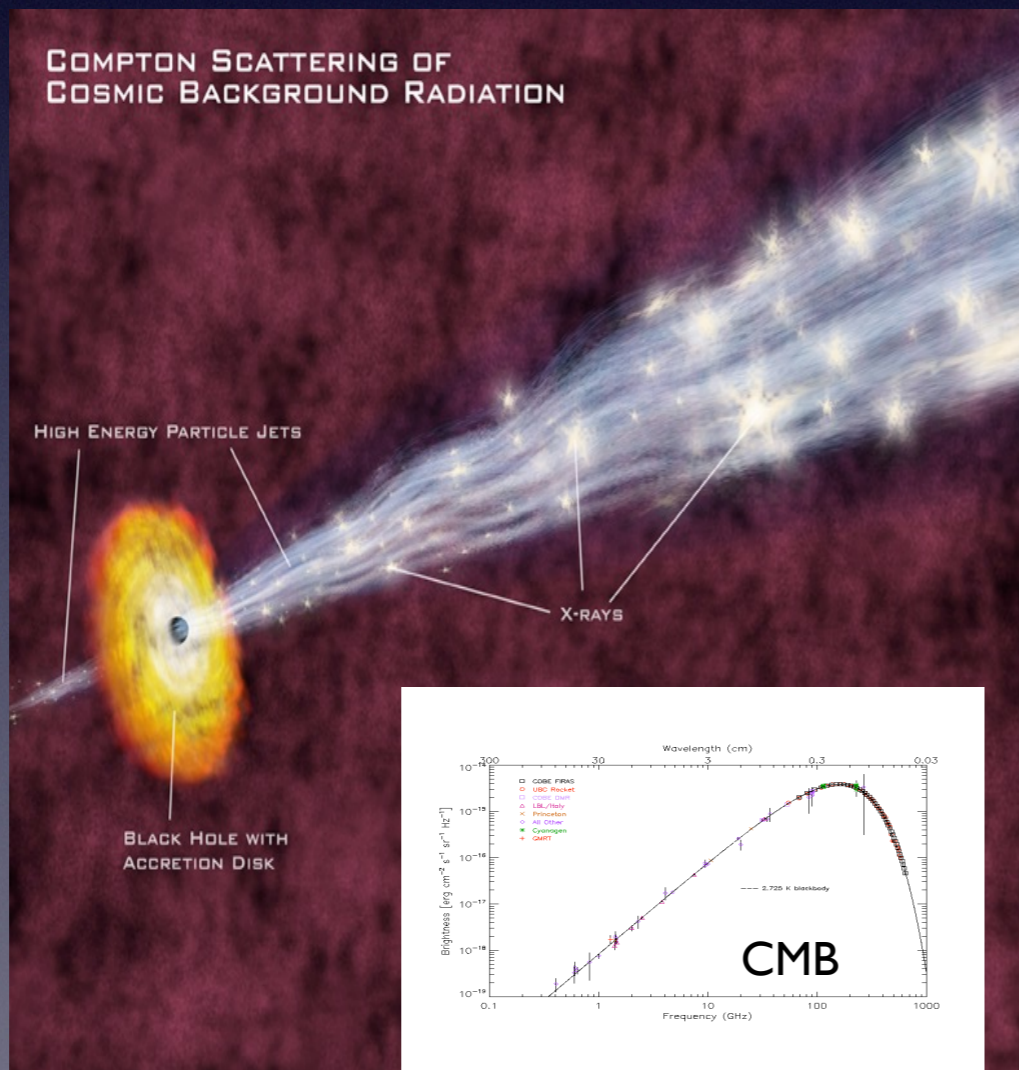
Lobes

relativistic electrons

CMB